TWO-PHASE SOIL STUDY

A. Finite Strain Consolidation

B. Centrifuge Scaling Considerations

Thesis by

Thiam-Soon Tan

In Partial Fulfillment of the Requirements
for the Degree of
Doctor of Philosophy

California Institute of Technology
Pasadena, California

1986

(Submitted 2 August 1985)

ACKNOWLEDGMENTS

First, I would like to thank my advisor, Professor Ronald F. Scott, for the guidance and advice he has given me and for the many stimulating hours he has spent with me discussing issues of importance in both technical and non-technical fields.

The help from Professor John F. Hall is also gratefully acknowledged. His course on the Finite Element Method has taught me to use this versatile method with confidence.

To my friend and former teacher, Dr. R. O. Davis of the University of Canterbury, who first encouraged me to pursue the doctoral degree, I am grateful for the concern and encouragement he has given me all these years.

To all my teachers at the University of Canterbury and California Institute of Technology, thank you. I also would like to thank Gloria Jackson and Sharon Beckenbach for their expert typing of this thesis.

This thesis is the fruit of a lifelong commitment of my father towards my education. To him and all the others in the family, I will always be grateful. To my wife, Giem-Hong, who shares this dream of mine and makes so many sacrifices to ensure that my life is comfortable and that I can concentrate on my work, words cannot express my gratitude.

Finally I would like to thank the National Science Foundation (Grant No. CEE82-19068) for supporting my research.

ABSTRACT

Two different aspects of the behavior of soil as a two-phase medium are studied, namely, the consolidation of soil and scaling relations for soils in centrifuge testing.

PART A

First a consistent approach is presented that unifies all current theories of consolidation of soil. For one-dimensional finite strain consolidation, a Lagrangian finite element scheme is then given and tested against three different experiments and found to give consistent results. For a quick solution to a particular problem, the regular perturbation method applied to the formulation in which the dependent variable is the natural strain is shown to give the most consistent results. For the Eulerian formulation, the material derivative contains a convective term. This convective effect is then analytically studied and found not to be negligible for a final natural strain greater than 10%. A method is then introduced that can account for both the moving boundary and the convective effect. This method is tested in a finite difference scheme and found to give identical results with the Lagrangian finite element scheme for the one-dimensional case. Finally the method is used for the axisymmetric problem of consolidation by vertical drain. The solution to this case suggests that arching and subsequent load redistribution should be considered.

PART B

Conceptually, when a centrifuge is used to test models, the centrifuge is assumed to produce an equivalent ng gravitational field (as on another planet) and the behavior of the model in the ng field is then assumed to be similar to that of the prototype. For most static problems, the centrifuge does model the prototype well but for some dynamic problems, these assumptions can break down. To investigate this, the similarity requirements are examined for the case of a single particle moving in a fluid. It is found that for the post-liquefaction process and for seepage flow, unless the Reynolds number is much less than one in both model and prototype, the centrifuge is not a good simulation of the prototype situation. But, perhaps contrary to expectations, the breakdown is due to the fact that the behavior in the ng planet is not similar to the prototype 1g planet, whereas the centrifuge does simulate the ng planet well. Further, it is shown that the concept of "modeling of models" can lead to misleading results. Lastly, for cratering experiments, it is concluded that the centrifuge will only model the crater shape just after an explosion and not the final crater shape.

TABLE OF CONTENTS

TABLE OF CONTENTS (CONT'D)

TABLE OF CONTENTS (CONT'D)

CHAPTER I

INTRODUCTION

1.1 INTRODUCTION

When a load is applied to a saturated soil, a two-phase medium consisting of a soil phase and a fluid phase, it is borne by both the fluid and the soil skeleton initially in proportion to their stiffnesses. But the increase in the pressure in the fluid and the gradients will cause it to flow through the soil and transfer the excess of its load over hydrostatic pressure to the soil skeleton. Therefore, the occurrence of stress and thus strain in the soil skeleton is a time-dependent process. For a very permeable soil, the time required for fluid flow and the complete transfer of the load borne by the fluid to the soil skeleton is so short that the problem is one of equilibrium; that is, the problem is independent of time. However, for finer grained soil such as clay (k* on the order of 10^{-4} cm/s or less), the time required can be very significant and an analysis that will give the full stress-strain-time relationship is needed (Bowles, 1982). This is the problem known as "consolidation" in soil mechanics.

Consolidation holds a special place in the history of soil mechanics and foundation engineering. To most workers in this field, Terzaghi's one-dimensional formulation of this problem and its success in predicting the general progress of consolidation of soil is usually

---

* A list of symbols is given in Appendix A except for those that are specifically defined in the text.

considered to be the "birth of Soil Mechanics" and Terzaghi is referred to as the "father of Soil Mechanics" (Lambe and Whitman, 1969).

There are two basic types of soil engineering problems in which solutions to the problem of consolidation, that is, stress-strain-time relationships, are needed. The first type involves prediction of displacements or settlements and the second when there is danger of the shearing stresses exceeding the shearing strength of the soil (Taylor, 1948), which is dependent on the time-varying pore water pressure. For the first type, surface displacements, which result from integration of the strains developed in the soil skeleton, are averaged quantities and thus are insensitive to assumptions regarding the components of the soil response. For the second type of problem, a more refined model may be needed to give an accurate prediction of the local behavior.

To solve the problem of consolidation in soil completely, that is, to solve a three-dimensional finite strain dynamic case, is very difficult even with today's knowledge of numerical methods and the availability of computers. This problem requires a knowledge of the constitutive behavior of the soil skeleton and the fluid-soil interrelationship, both under dynamic conditions. Each of these items is still a much researched topic. To obtain some approximate solutions, many assumptions have to be made so that a highly idealized but amenable situation results.

Terzaghi's one-dimensional infinitesimal strain formulation which required many idealized and restrictive assumptions was first published in 1923 (Terzaghi, 1923). Since then it has been extensively used in

practice and is described in all soil mechanics texts (Terzaghi, 1943, Taylor, 1948, Scott, 1963 and Lambe & Whitman, 1969) as the basis for consolidation problems. As a result of this extensive usage, a lot of engineering experience has been accumulated on methods of linearizing the various parameters. Thus, despite its idealizations, acceptable results often can be achieved in practice. Many efforts have been made to extend this work to three dimensions and to relax some of the more restrictive assumptions. But none has achieved the generality of use of Terzaghi's highly idealized model. The reason is that most of the models are complicated; even the linear two- or three-dimensional models are complex mathematically. Thus, only numerical solutions are available for these models in contrast with the simplicity and availability of closed-form solutions for Terzaghi's formulation. An account of these efforts will be given in Section 1.2 of this chapter.

Terzaghi's one-dimensional solution has least applicability to soft soils which exhibit large strains or compressions. The reason is clear, since Terzaghi's solution assumes infinitesimal strain. Another reason for the breakdown of Terzaghi's solution is that in soft soil, often consolidation due to its own weight is very significant and may be the only load to cause consolidation. An example is consolidation of land reclaimed using marine clay. However, this is neglected in Terzaghi's formulation.

Thus, in recent years the main effort has been to formulate and solve the consolidation problem when the strains involved are very substantial (of order of 30% or more) and to account for the self-weight

if necessary. Because of the complexity of the problem, most of the efforts have been concentrated on the one-dimensional case (Mikasa, 1965, Gibson et al., 1967, Lee & Sills, 1979). Naturally, this problem can be formulated in either the Lagrangian or the Eulerian frame (Fung, 1965). It is a simple matter to transform from one formulation to the other in the one-dimensional case. However, it is important to have a clear idea of what each formulation encompasses. For example, in the Eulerian formulation, the material derivative contains a convective term which may not be negligible.

A much more difficult problem is the extension of large strain effects to three dimensions. For the three-dimensional problem, the governing equations obtained in an Eulerian formulation are simpler than those obtained in a Lagrangian formulation. But in an Eulerian formulation, one has to contend with moving boundaries and the existence of a convective term in the material derivative. Another problem is that some of the one-dimensional work cannot be straightforwardly generalized to three dimensions. The reason for this is that the constitutive relation used for the one-dimensional problem has been specialized; for example, only a void ratio versus effective stress relation is needed. But for three-dimensional problems, a general constitutive relation is needed in most instances.

Clearly, there is a need to have a consistent formulation that is applicable to both one- and three-dimensional problems. Furthermore, the effect of neglecting the convective term in the material derivative needs to be studied. A method must be found that can account for the

convective term in any numerical schemes that are used to solve the problem in an Eulerian formulation. Also, to make the results attractive to practising geotechnical engineers, some closed-form solutions should be provided for the simpler problems. These are the objectives of this study.

In Chapter II, the problem of consolidation will be formulated without restriction to one dimension, infinitesimal strain or constant material properties. Many of the special current theories will be derived from this formulation and, where necessary, inconsistencies will be pointed out. In Chapter III, a closed-form analytical solution will be given for the nonlinear problem of one-dimensional finite strain consolidation of a semi-infinite layer. A perturbation method is also suggested that will be shown to give good agreement with finite element results generated for the one-dimensional finite strain consolidation of a finite layer. As a separate consideration the finite element program is developed specifically for the one-dimensional problem and allows variable material properties and self-weight consolidation. The effect of neglecting the convective term is analytically studied for the problem of consolidation of a semi-infinite layer and shown to be significant for this case when the natural strain exceeds ten percent. A concept that has the capability to include the convective term in the Eulerian formulation will be introduced and its workability demonstrated for the one-dimensional case using a finite difference scheme. The attractiveness of this concept is that it can be applied to three-dimensional problems. Since the general three-dimensional problem is

still a very difficult problem, this concept, incorporated in a finite element scheme, is applied to a special case of consolidation using a vertical drain. This is an axisymmetric three-dimensional problem.

Having described the objectives of this study and given an outline of the presentation of this report, in the next section an account of the efforts made in the last sixty years towards solving the problem of consolidation will be given.

1.2 HISTORICAL PERSPECTIVE

Terzaghi was the first to realize that, for a saturated soil, the applied loads were borne by both the soil skeleton and fluid and that the strain developed in the soil skeleton was a result of the stress in the soil skeleton only. Thus the concept of effective stress was born. This concept, for one dimension, is given by:

$$\sigma = \sigma' + p = \sigma' + (u + u_s) \quad . \tag{1.1}$$

He then applied this concept to establish the equation of one-dimensional consolidation (Figure 1.1)*; he recognized the analogy to the transient heat conduction problem and for constant applied total pressure obtained an equation similar to the one-dimensional diffusion or heat-conduction equation:

$$c_v \frac{\partial^2 u}{\partial z^2} = \frac{\partial u}{\partial t} \tag{1.2}$$

* Figures are presented at the end of each chapter.

where the diffusion constant or "coefficient of consolidation" is given by

$$c_v = \frac{k}{\gamma_f m_v} \quad . \tag{1.3}$$

Equation (1.1) and (1.2) together describe the problem of one-dimensional consolidation. This work was presented in his classic text Erdbaumechanik (Terzaghi, 1925). In his formulation, the following assumptions were made:

(i) The soil layer thickness before and after consolidation remains unchanged. He made reference to the problem of heat conduction where the conducting medium was assumed to remain undeformed, too. This implied that the deformation that occurred had to be small and the strain infinitesimal.

(ii) The voids of the soil are completely filled with water.

(iii) Both the water and solid constituents of the soil are perfectly incompressible.

(iv) Darcy's law is strictly valid.

(v) The coefficient of permeability k is a constant.

(vi) The time lag of consolidation is due entirely to the low permeability of the soil.

(vii) For the range of pressure considered, the strain is infinitesimal and the constitutive relation of the soil structure linear and time-independent.

(viii) Both the compression and the flow are one-dimensional.

Again following practice in heat conduction problems, the one-dimensional consolidation equation that was derived by Terzaghi was generalized to three dimensions (Rendulic, 1936 and Carrillo, 1942). The isotropic equation obtained was of the form:

$$c_v\left(\frac{\partial^2 u}{\partial x^2} + \frac{\partial^2 u}{\partial y^2} + \frac{\partial^2 u}{\partial z^2}\right) = \frac{\partial u}{\partial t} \qquad (1.4)$$

and for axisymmetrical problems in polar coordinates,

$$c_v\left(\frac{\partial^2 u}{\partial r^2} + \frac{1}{r}\frac{\partial u}{\partial r} + \frac{\partial^2 u}{\partial z^2}\right) = \frac{\partial u}{\partial t} \quad . \qquad (1.5)$$

Equation (1.5) was used to solve problems with radial flow (Carrillo, 1942 and Terzaghi, 1943). Because of the linearity of this equation, Carrillo was able to show that three-dimensional radial flow as described by equation (1.5) could be resolved into plane radial flow and rectilinear one-dimensional vertical flow.

In equations (1.2), (1.4) and (1.5), the interaction between the fluid and soil skeleton and the stress-strain relation of the soil skeleton are combined into one coefficient c_v (equation 1.3). This coefficient is normally determined experimentally. Also in these equations, the excess pore pressure of the fluid is the only dependent variable. This arises if the total stress in equation (1.1) is a constant with time and space. If the boundary conditions can be specified in terms of the excess pore pressure also, then the problem becomes uncoupled. This is indeed the case for the one-dimensional problem (Figure

1) and thus equation (1.2) is correct. But analogous to thermo-elastic problems, the total stress is not a constant in general. This is easily understood since during the process of consolidation, the soil deforms and its properties change continuously. Thus equations (1.4) and (1.5) are not strictly correct since in their derivation the total stress is assumed to be constant.

Biot took a different approach. He assumed that the soil skeleton was isotropic and linearly elastic and from the equations of continuity and equations of equilibrium formulated a rigorous general theory of three-dimensional consolidation (Biot, 1941a). The anisotropic problem was considered by him in a later paper (Biot, 1955). He used all of Terzaghi's assumptions except for relaxing the requirement of an incompressible fluid. For the isotropic case, he obtained a set of coupled partial differential equations with two dependent variables, namely, the excess pore water pressure and the volumetric strain:

$$c\nabla^2\theta = \frac{\partial\theta}{\partial t} \tag{1.6}$$

$$(\lambda+2G)\nabla^2\theta + \nabla^2 p = 0 \tag{1.7}$$

where the coefficient of consolidation, c, is now defined

$$c = (\lambda+2G)\frac{k}{\gamma_f} \quad . \tag{1.8}$$

Yoshikuni and Nakanodo (1974) have shown that equations (1.6) and (1.7) can be reduced to a form similar to equations (1.4) and (1.5) in the special case where the consolidation potential is a constant with time

and space. They defined the consolidation potential, ϕ, as:

$$\phi = (\lambda+2G)\theta + p \quad . \tag{1.9}$$

For an irrotational problem, they showed that ϕ is a function of time only.

Biot used equations (1.6) and (1.7) to solve a couple of two-dimensional problems (Biot, 1941b; and Biot and Clingan, 1941). In these, the surface settlement was the only quantity computed. Because of this, it was left to Mandel to find that even if the applied load was constant with time, the total stress at all points could change with time (Mandel, 1953). This has become known as the "Cryer-Mandel" effect in the literature (Lambe and Whitman, 1969) though Cryer found the variable total stress effect at a much later date (Cryer, 1963). Mandel found that for a finite layer of soil subjected to a constant load and allowed to drain radially only, the total pore pressure at the center of the layer first increased and then decreased. This physically very logical phenomenon could not be predicted by Terzaghi's work.

Cryer used both Terzaghi's and Biot's theories to predict the behavior of a saturated sphere of soil subjected to a uniform hydrostatic load and allowed to drain at the surface. He found that the settlement behaviors as predicted by the two theories were similar. But, he too found that, according to Biot's theory, the pore pressure at the center of the sphere would first increase and then decrease whereas the pore pressure would decrease right from the start according to Terzaghi's theory. The existence of the "Cryer-Mandel" effect implies

that equations (1.6) and (1.7) should be used instead of equation (1.4) or (1.5). However, because of its simplicity, equations (1.4) or (1.5) continue to be used in the geotechnical profession and are the basis of many studies (Barron, 1948; Richart, 1959; Davis & Raymond, 1965 and Atkinson & Eldred, 1981).

As described, both Terzaghi's and Biot's work assumes that Darcy's law is valid and the effective stress-strain relationship for the soil is linear. However, there is evidence that flow through some clay may be non-Darcian [see (Mitchell, 1976) for a brief survey]. Also for soil, a linear stress-strain relation is valid only if the strain is very small. For the one-dimensional case, many efforts have been made to extend the classical Terzaghi's formulation to include more realistic assumptions. For examples, Barden and Berry (1965) used a power law and Elnaggar et al. (1973) used a four-parameter relation in place of Darcy's law; Davis and Raymond (1965) used an exponential rule for the effective stress-void ratio relation. These researches were based on Terzaghi's concept which, as was explained, was valid only for infinitesimal strain.

Mikasa (1965) and Gibson, et al. (1967) were the first to realize that the investigation of the effect of non-linear soil behavior must be done in the context of large strain since these non-linearities are likely to be important only if the void changes and strains are appreciable [see Schiffman et al. (1984) for some examples]. They realized the need to have a formulation that removed the limitation of infinitesimal strain. Accordingly, they established the problem of "one-dimensional

finite strain consolidation" and obtained:

Mikasa

in Eulerian frame

$$\frac{\partial}{\partial \xi}\left(c_v \frac{\partial \varepsilon}{\partial \xi}\right) - \frac{\partial}{\partial \xi}\left[\frac{k}{1+e} \cdot \left(\frac{\gamma_s}{\gamma_f} - 1\right)\right] = \frac{\partial \varepsilon}{\partial t} \quad ; \qquad (1.10)$$

in Lagrangian frame

$$\zeta^2 \frac{\partial}{\partial a}\left(c_v \frac{\partial \zeta}{\partial a}\right) - \frac{\partial}{\partial a}\left[\frac{k}{1+e}\left(\frac{\gamma_s}{\gamma_f} - 1\right)\right] = \frac{\partial \zeta}{\partial t} \quad ; \qquad (1.11)$$

Gibson

in Lagrangian frame

$$\frac{\partial}{\partial z}\left(\frac{1}{\gamma_f} \cdot \frac{k}{1+e} \cdot \frac{d\sigma'}{de} \cdot \frac{\partial e}{\partial z}\right) - \left(\frac{\gamma_s}{\gamma_f} - 1\right)\frac{\partial}{\partial z}\left(\frac{k}{1+e}\right) + \frac{\partial e}{\partial t} = 0 \quad . \qquad (1.12)$$

Consolidation processes governed by equations (1.10)-(1.12) include the effects of self-weight which are neglected in both Terzaghi's and Biot's work. Another point to be noted is that Mikasa's formulation in the Eulerian frame [equation (1.10)] omits the convective term for the material derivative of the dependent variable, the natural strain. This has not been noted previously. Also, as noted by Pane and Schiffman (1981), Mikasa's formulations are valid for uniform initial conditions only; that is, all the dependent variables are constant spatially at time t = 0. Such a restriction does not exist for Gibson's work.

In the Eulerian formulation, the problem involves moving boundaries. For example, in the one-dimensional problem (Figure 1.1)

when a load is applied to the top surface, the soil skeleton begins to deform with time. Thus the surface will settle continuously and its settlement is the summation of the strain at each point. In an Eulerian formulation, the surface at each instant is the boundary for that instant and thus the problem involves a moving boundary. Further, because every single point is moving with time, for the Eulerian formulation, the material derivative involves a convective term. This differs from the classical moving boundary heat conduction problem known as Stefan's problem (Crank, 1975). Thus many of the numerical schemes that were developed for the heat conduction problems (Crank, 1975) are inapplicable. Also, moving boundaries are difficult to handle. For these reasons, most workers have used the Lagrangian formulation (Gibson, et al., 1967; Monte & Krizek, 1976; Mikasa & Ohnishi, 1981 and Gibson, et al., 1981). An exception to this was Lee & Sills (1979) who were able to formulate the problem in an Eulerian frame and eliminate the convective term in the material derivative. Their formulation was thus similar to the classical Stefan's problem and they were able to use the Crank-Gupta method (Crank, 1975) to solve this one-dimensional case numerically. But Lee and Sill's one-dimensional formulation cannot be extended to three dimensions without introducing some convective effect.

In recent years, efforts have been made to extend the finite strain theory to three dimensions (Carter et al., 1977 and 1979). This work was formulated in the Eulerian frame since the governing equations are simpler in this formulation. The finite element method was then used for the spatial discretization and the difference method in the time

domain. However, the use of the difference method does not account for the convective term in the material derivative unless special procedures not employed by Carter are introduced.

From the account just presented, it is clear that many different models have been developed to solve the problem of consolidation. These models are derived in different ways and based on different idealizations. In the next chapter, a consistent formulation is presented that will unify all these models.

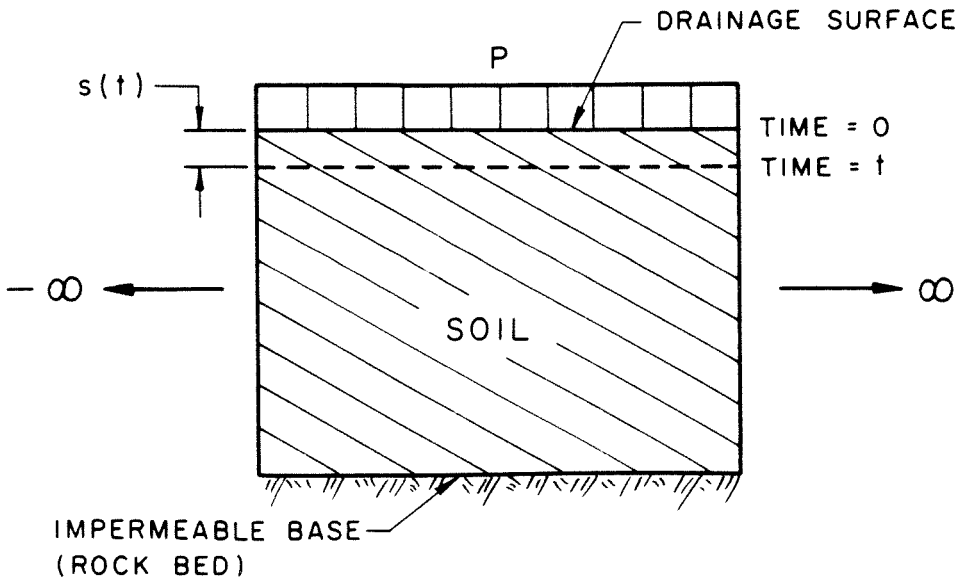

(a)

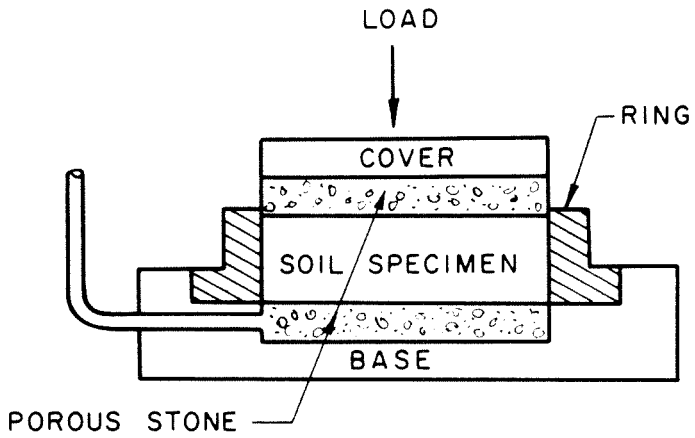

(b)

Figure 1.1 One-dimensional Consolidation
a. Field condition
b. Laboratory condition

CHAPTER II

THEORY OF CONSOLIDATION

2.1 INTRODUCTION

To derive the governing equations for the process of consolidation requires a knowledge of the constitutive relation for the soil skeleton and a relation governing the flow of fluid through the soil medium. Also, since the consolidation process is time dependent, it is in reality a dynamic problem. Clearly, this is an extremely difficult situation.

In all the studies to date, the consolidation problem has been treated as quasi-static. That is, instead of the equations of motion, the equations of equilibrium are used. The time variable is then introduced through the equation of continuity. In the subsequent derivation, the problem will be treated dynamically and formulated accordingly; that is, the equations of motion are used. This provides a basis for future research where the dynamics of the problem may need to be considered. However, in the current study solutions are developed for the quasi-static case only.

Constitutive relations for soil are still a much debated and researched topic (Bardet, 1983). For consolidation, there are two ways to deal with it. The first is to assume a constitutive model and formulate the problem rigorously. Examples of such an approach are to be found in Biot's formulation (Biot, 1941a and 1955) and Carter et al.'s work (Carter et al., 1979). The second approach, which is more

popular, is to lump all the material properties into the coefficient of consolidation and this coefficient is then determined experimentally. However, this approach is feasible for certain types of problems only such as one-dimensional consolidation and consolidation using a vertical drain with no lateral strain. Terzaghi's formulation is a good example of such an approach. Others who use this approach include Mikasa (1965), Gibson et al. (1967) and Lee & Sills (1979). In this study, when feasible, the second approach is preferred for two reasons. First, the individual material property is difficult to determine whereas a large amount of experience has been accumulated on the determination of the coefficient of consolidation. Second, the variations of this coefficient are less marked than are the changes of the individual component of the material properties (Gibson et al., 1967; and Lee and Sills, 1981). Thus, the determination of this coefficient is less sensitive to error.

In most studies to date, Darcy's law is assumed to govern the flow of fluid through the porous medium. This will be assumed too in this study. However while formulating the problem, we will show how any variant of Darcy's law can be incorporated into the governing equations. Even if Darcy's law is assumed, the determination of the coefficient of permeability is difficult for soft clay (Pane et al., 1983). This is another reason why the approach that lumps all the material properties into a coefficient that is determined experimentally is preferred by geotechnical engineers.

In the current study, the soil skeleton will be thought of as a fluid. In this way, the formulation is similar in many ways to that for two-phase flow (Wallis, 1969). The three-dimensional case will be formulated in the Eulerian frame as the governing equations are simpler in this frame. For one-dimensional consolidation, it will be shown how to transform this Eulerian formulation to the Lagrangian formulation.

2.2 GOVERNING EQUATIONS

Conservation of Mass

In this study, "soil" will be considered as a two-phase medium; the "solid phase" refers to the soil grains and the "fluid phase" to the fluid (usually water).

Let the porosity of the saturated soil be n. Then, the fluid will occupy a fraction n of the volume of soil and the solid particles (1-n) of the soil. Thus, if the equations of continuity are written for the whole flow field in a manner analogous to two-phase flow (Wallis, 1969), we can write:

conservation of the solid phase:

$$\frac{\partial}{\partial t}\left[\rho_s(1-n)\right] + \nabla\cdot\left[\rho_s(1-n)\underset{\sim}{v}_s\right] = 0 \quad ; \tag{2.1}$$

conservation of the fluid phase:

$$\frac{\partial}{\partial t}(\rho_f n) + \nabla.(\rho_f n \underset{\sim f}{v}) = 0 \quad . \tag{2.2}$$*

In equations (2.1) and (2.2), the $\nabla.$ is the divergence operator.

If both the solid phase and the fluid phase are assumed to be incompressible, then equations (2.1) and (2.2) become:

conservation of the solid phase

$$-\frac{\partial n}{\partial t} + \nabla.\,[(1-n)\underset{\sim s}{v}] = 0 \quad ; \tag{2.3}$$

conservation of the fluid phase

$$\frac{\partial n}{\partial t} + \nabla.\,(n\underset{\sim f}{v}) = 0 \quad . \tag{2.4}$$

Eliminating $\frac{\partial n}{\partial t}$ from equations (2.3) and (2.4) gives:

$$\nabla.\,[n(\underset{\sim f}{v} - \underset{\sim s}{v})] + \nabla.\,\underset{\sim s}{v} = 0 \quad . \tag{2.5}$$

Let

$$\underset{\sim}{v} = n(\underset{\sim f}{v} - \underset{\sim s}{v}) \quad . \tag{2.6}$$

In soil mechanics, v is normally referred to as the approach velocity or superficial velocity. Using equations (2.5) and (2.6) in equation (2.3) gives:

---

* The subscripts s and f represent the solid and fluid phases, respectively.

$$\frac{Dn}{Dt} + (1-n)\nabla . \underset{\sim}{v} = 0 \qquad (2.7)$$

where

$$\frac{Dn}{Dt} = \frac{\partial n}{\partial t} + \underset{\sim s}{v} . \nabla n \quad . \qquad (2.8)$$

Observe that in equation (2.8) the velocity in the convective term of the material derivative is the velocity of the solid phase. This fact will be made use of at a later stage.

Conservation of Momentum

The momentum equations or the equations of motion can be written in vectorial form as:

for the solid phase,

$$\rho_s \left(\frac{\partial \underset{\sim s}{v}}{\partial t} + \underset{\sim s}{v} . \nabla \underset{\sim s}{v} \right) = \underset{\sim s}{b} + \underset{\sim s}{f} + \nabla p \qquad \text{(three equations)} \quad ; \qquad (2.9)^*$$

for the fluid phase,

$$\rho_f \left(\frac{\partial \underset{\sim f}{v_f}}{\partial t} + \underset{\sim f}{v} . \nabla \underset{\sim f}{v} \right) = \underset{\sim f}{b} + \underset{\sim f}{f} + \nabla p \qquad \text{(three equations)} \quad . \qquad (2.10)$$

In deriving equations (2.9) and (2.10), the following points are to be noted:

(i) $\underset{\sim s}{b}$ and $\underset{\sim f}{b}$ are the body forces per unit volume of that component, which act on each component.

* In accordance with soil mechanics convention, compressive stresses are positive and tensile stresses negative.

(ii) ∇p is an averaged gradient of pressure and is usually the thermodynamic pressure of the fluid phase.

(iii) $\underset{\sim}{f}_s$ and $\underset{\sim}{f}_f$ are, to quote Wallis (1969), "what is left over" to balance the equations. The $\underset{\sim}{f}$'s contain components due to hydrodynamic drag, apparent mass effects during relative acceleration, particle-particle forces (effective stresses), and so on. In subsequent developments, $\underset{\sim}{f}_f$, the "balancing force" in the fluid phase is assumed to be due to hydrodynamic drag only and $\underset{\sim}{f}_s$, the "balancing force" in the solid phase, will comprise hydrodynamic drag and the particle-particle forces (effective stress). If the effective stress is $\underset{\sim}{\sigma}'$, then the contribution of particle-particle forces to $\underset{\sim}{f}_s$ in a unit volume of soil is $\nabla.\underset{\sim}{\sigma}'$. Further, let $\underset{\sim}{F}_s$ and $\underset{\sim}{F}_f$ be defined as the hydrodynamic drag per unit volume of soil acting on the solid and fluid phase, respectively. Since in a unit volume of soil the fluid phase occupies a fraction n of the volume, and the solid phase, (1-n), and the $\underset{\sim}{f}$'s are defined as force per unit volume of the respective component, the following is obtained:

$$\underset{\sim}{f}_s = \frac{\underset{\sim}{F}_s}{(1-n)} - \frac{\nabla.\underset{\sim}{\sigma}'}{1-n} \qquad (2.11)$$

$$\underset{\sim}{f}_f = \frac{\overset{F}{\sim}_f}{n} \tag{2.12}$$

and since hydrodynamic drag action and reaction are equal and opposite, the following equality holds:

$$\underset{\sim}{F}_f = -\underset{\sim}{F}_s \quad . \tag{2.13}$$

(iv) In equation (2.11), the effective stress principle is employed. This principle in its original form (Terzaghi, 1925) is a one-dimensional expression [equation (1.1)]. However, this has been generalized to three dimensions (Biot, 1941a; Schiffman, 1970 and Garg and Nur, 1973). In three dimensions, the principle is:

$$\underset{\sim}{\sigma} = \underset{\sim}{\sigma}' + p\underset{\sim}{1} \quad . \tag{2.14}$$

Using equations (2.11)-(2.13) to eliminate f_s and f_f, the following equation of motion for the composite medium is obtained:

$$(1-n)\rho_s\left(\frac{\partial \underset{\sim}{v}_s}{\partial t} + \underset{\sim}{v}_s \cdot \nabla \underset{\sim}{v}_s\right) + n\rho_f\left(\frac{\partial \underset{\sim}{v}_f}{\partial t} + \underset{\sim}{v}_f \cdot \nabla \underset{\sim}{v}_f\right) = \underset{\sim}{b}_s(1-n) + \underset{\sim}{b}_f n + \nabla \cdot \underset{\sim}{\sigma}' + \nabla p \quad . \tag{2.15}$$

Observe that if the inertia terms are neglected (the left-hand side equals zero), then equations (2.15) are the equations of equilibrium in terms of effective stresses and pore pressure (Scott, 1963).

Flow Relation: Darcy's Law

In equation (2.10), if the inertia terms are neglected and the following relation is assumed for the hydrodynamic term:

$$\underset{\sim f}{f} = (\gamma_f \underset{\sim}{k}^{-1}) \underset{\sim}{v} \quad , \tag{2.16}$$

then the following relation is obtained:

$$\underset{\sim}{v} = -\frac{\underset{\sim}{k}}{\gamma_f} (\nabla p + \underset{\sim f}{b}) \quad . \tag{2.17}$$

This is Darcy's law as it is understood in soil mechanics. It was originally obtained experimentally for the one-dimensional case by Darcy in 1856. The use of equation (2.16) shows that Darcy's law is based on a linear viscous phenomenon. For soft clay there is evidence that flow through a porous medium may not be Darcian (Scheidegger, 1974 and Mitchell, 1976). Any variant of Darcy's law, for example a power law or an exponential law, can be easily substituted in equation (2.16) instead of the linear relation used presently.

Consolidation Equations

In terms of the void ratio e, equation (2.7) can be rewritten as:

$$\frac{De}{Dt} + (1+e)\nabla . \underset{\sim}{v} = 0 \tag{2.18}$$

where

$$e = \frac{n}{1-n} \quad . \tag{2.19}$$

Using Darcy's law [equation (2.17)] in equation (2.18), the following is obtained:

$$(1+e)\nabla . \frac{\underset{\sim}{k}}{\gamma_f} (\nabla p + \underset{\sim f}{b}) = \frac{De}{Dt} \quad . \tag{2.20}$$

If the inertia term is neglected, the equation of equilibrium is obtained from equation (2.15):

$$\nabla . \underset{\sim}{\sigma'} + \nabla p + \underset{\sim s}{b} (1-n) + \underset{\sim f}{b} n = 0 \quad . \tag{2.21}$$

Equations (2.20) and (2.21) with an appropriate constitutive model govern the process of consolidation. The two equations have been derived without assuming infinitesimal strain.

2.3 SPECIFIC CONSOLIDATION THEORIES

Terzaghi's and Biot's Theories: Infinitesimal Theories

If we assume that the soil skeleton is isotropic and linearly elastic, then the stress-strain relation is given by (Fung, 1965):

$$\underset{\sim}{\sigma'} = \lambda\theta \underset{\sim}{1} + 2G\underset{\sim}{\delta} \tag{2.22}$$

where $\underset{\sim}{\delta}$ is the infinitesimal strain tensor and θ, the volumetric strain, is the trace of the strain tensor and is related to the void ratio as follows:

$$\theta = \frac{e_o - e}{1+e_o} \quad . \tag{2.23}$$

Next we will assume that the coefficient of permeability is isotropic. This implies that $\underset{\sim}{k}$ in equation (2.20) is given by:

$$\underset{\sim}{k} = k\underset{\sim}{1} \quad . \tag{2.24}$$

If the strain developed is assumed to be infinitesimal, then the distinction between the Eulerian and Lagrangian formulation disappears (Fung, 1965). With the assumption of infinitesimal strain, the following approximations are also true:

$$\frac{De}{Dt} \simeq \frac{\partial e}{\partial t} \tag{2.25}$$

$$(1+e) \simeq (1+e_o) \quad . \tag{2.26}$$

Using equations (2.22)-(2.26) in equations (2.20) and (2.21) and neglecting the body forces, the following is obtained:

$$\frac{k}{\gamma_f} (\lambda+2g)\nabla^2\theta = \frac{\partial \theta}{\partial t} \quad . \tag{2.27}$$

Equation (2.27) together with the equilibrium equation (2.21) [neglecting body forces] is Biot's formulation (Biot, 1941a). If the problem is specialized to the one-dimensional case and use is made of the fact that, in this special case, the total stress is a constant in time and space if the applied load is constant with time, Terzaghi's formulation [equation (1.2)] is obtained.

One-dimensional Finite Strain Consolidation

Equations (2.20) and (2.21) will now be specialized for the case of one-dimensional finite strain consolidation. The concept of the natural strain ε is very useful in the Eulerian formulation and is defined in differential form as:

$$d\varepsilon = -\frac{d\ell}{\ell} \tag{2.28}$$

where ℓ is the current length of an element that has compressed by $d\ell$. Integration of equation (2.28) from time t = 0 to time t gives:

$$\varepsilon = \ln\left(\frac{1+e_o}{1+e}\right) \quad . \tag{2.29}$$

If e_o is a constant, then using this definition in equation (2.18), the relative velocity of the fluid with respect to the soil skeleton is obtained:

$$\frac{\partial v}{\partial \xi} = \frac{D\varepsilon}{Dt} \quad . \tag{2.30}$$

In Mikasa's formulation, it is here that the convective effect in the material derivative is omitted (Mikasa, 1965; Mikasa and Ohnishi, 1981).

For the special case of constant e_o, that is, uniform initial condition and using the natural strain as the dependent variable, the following equation is obtained from equations (2.20) and (2.21):

$$\frac{\partial}{\partial \xi}\left[\frac{k(\varepsilon)}{\gamma_f}\left(\frac{\partial \sigma'}{\partial \xi} - \frac{\gamma_s - \gamma_f}{1+e}\right)\right] = \frac{D\varepsilon}{Dt} \quad . \tag{2.31}$$

A relation is now needed to relate the effective stress with the natural strain. In soil mechanics, it is generally accepted that the effective stress is uniquely related to the void ratio if the loading is monotonic (Schofield and Wroth, 1968). This is assumed throughout this study. With this assumption and for constant e_o, it is clear from equation (2.29) that the effective stress is uniquely related to the natural strain. Thus, the following definition can be made:

$$\frac{d\sigma'}{d\varepsilon} = \frac{1}{m_v(\varepsilon)} \tag{2.32}$$

and

$$c_v = \frac{k(\varepsilon)}{\gamma_f m_v(\varepsilon)} \quad . \tag{2.33}$$

Using equations (2.32)-(2.33) in equations (2.31), the following is obtained for the one-dimensional case:

$$\frac{\partial}{\partial \xi}\left(c_v \frac{\partial \varepsilon}{\partial \xi}\right) - \frac{\partial}{\partial \xi}\left[\frac{k(\varepsilon)}{\gamma_f} \cdot \frac{\gamma_s - \gamma_f}{(1-e)}\right] = \frac{D\varepsilon}{Dt} \tag{2.34}$$

This is the same as Mikasa's formulation except for the fact that the material derivative is used and not the local derivative with respect to time.

For the one-dimensional problem, often it is easier to formulate the problem in the Lagrangian formulation. Some workers (Gibson et al., 1967; Lee and Sills, 1979; and Gibson et al., 1981) have introduced a new independent variable z which identifies the volume of solids in a prism of soil of unit cross sectional area (sometimes referred to as the

"equivalent height" of solid content) (see Figure 2.1). The relation between the three different coordinates (the Lagrangian coordinate a, the Eulerian coordinate ξ, and the new coordinate z that is referenced in a Lagrangian frame) for the one-dimensional case in differential form is as follows:

$$dz = \frac{da}{1+e_o} = \frac{d\xi}{1+e} \quad . \tag{2.35}$$

Using equation (2.35) in equations (2.20) and (2.21), and assuming monotonic loading, the following is obtained:

$$\frac{\partial}{\partial z}\left[\frac{k(e)}{\gamma_f(1+e)}\frac{d\sigma'}{de}\frac{\partial e}{\partial z}\right] - \left(\frac{\gamma_s}{\gamma_f} - 1\right)\frac{\partial}{\partial z}\left[\frac{k(e)}{1+e}\right]\frac{\partial e}{\partial z} + \frac{\partial e}{\partial t} = 0 \quad . \tag{2.36}$$

This is Gibson's equation (Gibson et al. 1967). This formulation, which uses the void ratio as the dependent variable, is no longer restricted to the problem of uniform initial conditions.

Consolidation with Vertical Drain: Finite Strain

In practice, often the time required for the completion of the natural consolidation process is too long. This can be costly as construction normally cannot begin until the soil has consolidated. A way to accelerate this process is to install vertical drains at equal spacing in the area needed. This, in effect, reduces the drainage path of the fluid and thus increases the rate of settlement. This case is now presented for later study.

The problem considered is illustrated in Figure 2.2. This is an axisymmetric problem. In general, a full constitutive model is required and equations (2.20) and (2.21) cannot be uncoupled. A general solution would thus require a solution to the "equilibrium problem" at each instant, a difficult problem on its own. In this study, the special case where the vertical wall of the drain and the outer diameter of the region are fixed in space and the applied load constant with time is studied. For this special problem, if the strain is infinitesimal, it has been shown that the Cryer-Mandel effect disappears (Yoshikuni and Nakanodo, 1974); that is to say, the total stress is constant with time. With this consideration equations (2.20) and (2.21) can be combined to give:

$$\nabla \cdot \left(\frac{k}{\gamma_f} \nabla p \right) = m_v \frac{Dp}{Dt} \quad . \tag{2.37}$$

This equation was also obtained by Mikasa and Ohnishi (1981) except that again the convective term in the material derivative was neglected in their formulation.

With the derivation of the governing equation for consolidation using vertical drains, Chapter II is concluded. Thus far, a consistent approach to formulating consolidation theory is presented. In Chapter III, solutions and methods of solution will be given for various consolidation problems governed by the equations just presented.

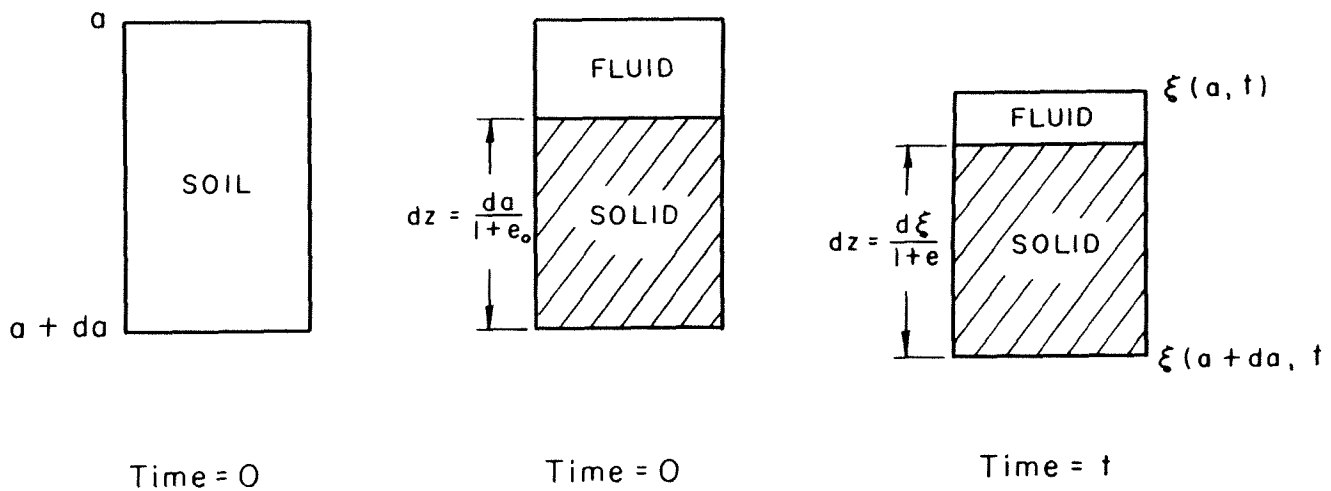

Figure 2.1 Schematic representation of the three coordinates: a, the Lagrangian coordinate, ξ, the Eulerian coordinate and z the "equivalent height" of solid content

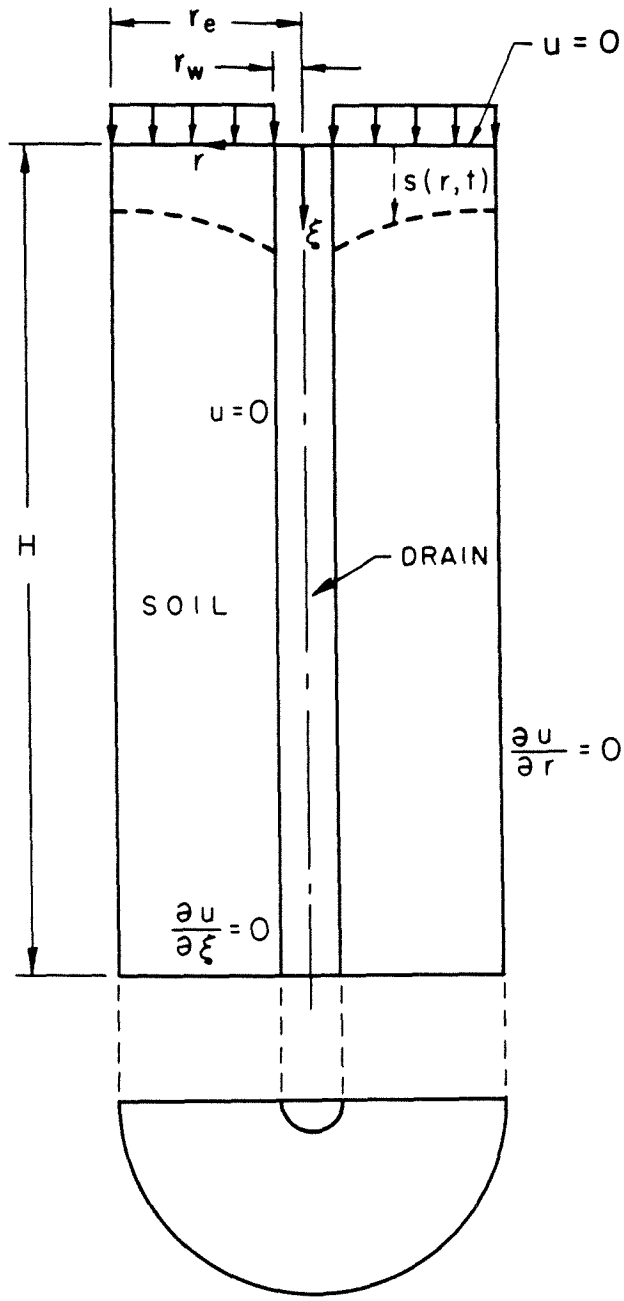

Figure 2.2 Consolidation by vertical drain .... an axisymmetric problem

CHAPTER III

SOLUTIONS AND RESULTS

3.1 INTRODUCTION

In Chapter II, the theory of consolidation was presented and the governing equations derived. In this chapter, various solutions and methods of solution will be given.

Since the one-dimensional case has been used most extensively in practice, it will be studied in detail. First, an analytical solution will be derived for the exact formulation of finite strain consolidation of a semi-infinite layer (see Figure 3.1) including convection but neglecting self-weight. Then an analytical solution is derived for the same problem with the exception that the convective term is neglected. The comparison of these two solutions will illustrate the significance of the convective term.

Next, the finite element method is applied to the more realistic case of consolidation of a finite layer. The governing equations are formulated in the Lagrangian frame, and the finite element method is used for the spatial discretization while the explicit forward difference method is used for the temporal discretization. As the Lagrangian formulation is used, the finite element mesh does not need to be updated each time step. Furthermore, the use of the explicit forward difference method will yield a simple matrix equation. The elements used are three-node linear elements. In this formulation, all properties are allowed to be non-linear and the effect of self-weight is included.

To make the results of this study more attractive to geotechnical engineers, some closed-form approximate solutions will be derived for the consolidation of a finite layer neglecting self-weight. This is achieved by applying the perturbation method to a particular formulation. These approximate closed-form results will be compared with the results generated by the finite element method.

In the multi-dimensional case, the governing equations are simpler in the Eulerian formulation. However, this formulation involves moving boundaries and a material derivative. The latter fact separates it from the classical moving boundary heat conduction problem known as Stefan's problem (Crank, 1975) in which the boundary moves, but the material inside it does not deform. Thus, numerical methods developed for Stefan's problem cannot be used here.

A method is thus introduced that can be incorporated in a numerical scheme to account for the convective effect and the moving boundary in an Eulerian formulation for the finite strain consolidation problem. This method, which in essence is similar to the updated Lagrangian scheme (Bathe, 1982), is demonstrated for the one-dimensional case and its validity verified. The attractiveness of this is that it can be extended to multi-dimensional cases.

The method is then applied to the three-dimensional problem of consolidation using a vertical drain subjected to the restriction of zero lateral strain (Barron, 1948; Yoshikuni and Nakanodo, 1974).

3.2 ONE-DIMENSIONAL FINITE STRAIN CONSOLIDATION

3.2.1 Analytical Solutions

Consolidation of a Semi-infinite Layer (see Figure 3.1)

Neglecting self-weight, the following equation with the void ratio as the dependent variable and z the equivalent "height of solid content" as the independent variable is obtained from equation (2.36):

$$\frac{\partial}{\partial z}\left[\frac{c_v}{(1+e)^2}\frac{\partial e}{\partial z}\right] = \frac{\partial e}{\partial t} \qquad (3.1a)$$

where

$$c_v = -\frac{k(1+e)}{\gamma_f}\frac{1}{\frac{de}{d\sigma'}} \qquad (3.1b)$$

and together with the effective stress equation (equation (1.1)) govern the consolidation process. Note that since z is referenced to a Lagrangian frame, the material derivative is the same as the time derivative. The definition of c_v given by equation (3.1b) is exactly equivalent to that given by equation (2.33). c_v will be assumed to be a constant. Equation (3.1a) is a Lagrangian formulation of the problem. The boundary and initial conditions for this case are:

at z = 0

$$e(0,t) = e_f \quad ; \qquad (3.1c)$$

at $z = \infty$

$$e(\infty,t) = e_o \quad ; \tag{3.1d}$$

at $t = 0$

$$e(z,0) = e_o \quad . \tag{3.1e}$$

Equations (3.1) describe a non-linear diffusion-type problem. This particular formulation has been chosen because nonlinear equations of this form are analytically solvable (Crank, 1975).

Using the following definitions:

$$e^* = \frac{e_o - e}{e_o - e_f} \tag{3.2a}$$

$$\beta = \frac{e_o - e_f}{1+e_o} \tag{3.2b}$$

$$z^* = \frac{z}{2} \frac{1+e_o}{\sqrt{c_v t}} \tag{3.2c}$$

equation (3.1a) can be reduced to an ordinary non-linear differential equation:

$$\frac{d}{dz^*} \left[\frac{1}{(1-\beta e^*)^2} \frac{de^*}{dz^*} \right] = -2z^* \frac{de^*}{dz^*} \quad . \tag{3.3}$$

If the following definition is now made:

$$f = \frac{e_o - e}{1+e} \tag{3.4a}$$

and a new dimensionless variable w and an arbitrary parameter b are introduced through the following specially defined relation:

$$\frac{dz^*}{dw} = b(1+f) \quad , \tag{3.4b}$$

then equation (3.3) becomes:

$$\frac{d^2f}{dw^2} = \left[\frac{df}{dw} - 2z^*b \right] \frac{\frac{df}{dw}}{(1+f)} \tag{3.5a}$$

where f = f(w). From equations (3.1c)-(3.1e), the following boundary conditions are obtained:

at $w = \infty$

$$f = 0 \quad ; \tag{3.5b}$$

at $w = \infty$

$$\frac{df}{dw} = 0 \quad ; \tag{3.5c}$$

at $w = 1$

$$f = \frac{\beta}{1-\beta} \quad . \tag{3.5d}$$

The solution to this problem is given by:

$$f(w) = \frac{\sqrt{\pi}\, b}{1-\beta} \exp(b^2) \left[1-\text{erf}(bw)\right] \tag{3.6a}$$

and w is related to z as follows:

$$z^* = \frac{-b}{1-\beta} \exp\,[b^2(1-w^2)] + bw(1+f) \qquad (3.6b)$$

where the parameter b is given by:

$$\sqrt{\pi} b \exp\,(b^2)[1-\text{erf}\,(b)] = \frac{e_o - e_f}{1+e_o} \quad . \qquad (3.6c)$$

Equations (3.18)-(3.20) provide the solution to the problem described by equations (3.1)-(3.5). The settlement of the top surface is given by:

$$s(t) = \int_0^\infty (e_o - e)dz \quad . \qquad (3.7a)$$

Using equations (3.6) and the definitions (3.2), and (3.4) in equation (3.7a) gives:

$$s(t) = 2b\sqrt{c_v t} \quad . \qquad (3.7b)$$

The solution as represented by equations (3.6) is shown in Figure 3.2 for typical values of e_f.

Consolidation of a Semi-infinite Layer Neglecting Convective Effect

To solve this case, the Eulerian formulation is chosen since, with the neglect of convection, this formulation resembles the classical Stefan's moving boundary problem in heat conduction. The governing equation comes from equation (2.34) with the body force and convective term neglected and is given by:

$$c_v \frac{\partial^2 \varepsilon}{\partial \xi^2} = \frac{\partial \varepsilon}{\partial t} \quad . \tag{3.8a}$$

The boundary and initial conditions are:

at the top surface $\xi = s(t)$

$$\varepsilon(s(t),t) = \varepsilon_f \quad ; \tag{3.8b}$$

at $\xi = \infty$

$$\varepsilon(\infty,t) = 0 \quad ; \tag{3.8c}$$

at $t = 0$

$$\varepsilon(\xi,0) = 0 \quad . \tag{3.8d}$$

With the way the problem is set up (see Figure 3.1), the coordinate of the top surface is the same as the settlement of the surface s(t) and thus is an unknown a priori. It is the existence of this unknown boundary (to be determined from the solution), exemplified by equation (3.8b) that causes the system to be non-linear despite the fact that the governing equation (3.8a) is linear. For a prism of soil of unit cross-sectional area, the settlement of the surface is the same as the amount of fluid flowing out of the surface. Thus s(t) is given by:

$$s(t) = \int_0^t v|_{\xi=s(t)} \, dt \tag{3.9a}$$

where v is the approach velocity of the fluid. Differentiating equation (3.9a) with respect to time and using Darcy's law [equation (2.17)] with equations (2.32) and (2.33) to replace v, the following is obtained:

$$\frac{ds(t)}{dt} = - c_v \frac{\partial \varepsilon}{\partial \xi}\Big|_{\xi=s(t)} \tag{3.9b}$$

and the initial condition for s(t) is:

at t = 0

$$s = 0 \quad . \tag{3.9c}$$

Equations (3.8) with s(t) as defined in equations (3.9) describe a problem that is mathematically similar to the classical moving boundary heat conduction or Stefan's problem (Crank, 1975). This problem is solvable by using the method of similarity group which is akin to a method suggested by Neumann to solve the Stefan's problem (Carslaw and Jaeger, 1959). Using this method, the solution is given by:

$$\varepsilon(\xi,t) = \frac{\sqrt{\pi}}{2} \alpha \exp\left(\frac{\alpha^2}{4}\right)\left[\operatorname{erf}(\alpha/2) - \operatorname{erf}\left(\frac{\xi}{2\sqrt{c_v t}}\right)\right] + \varepsilon_f \tag{3.10a}$$

where α is the solution to the following equation:

$$\alpha \exp\left(\frac{\alpha^2}{4}\right)\left[1-\operatorname{erf}\ (\alpha/2)\right] = \frac{2\varepsilon_f}{\sqrt{\pi}} \tag{3.10b}$$

and the settlement s(t) is given by:

$$s(t) = \alpha \sqrt{c_v t} \quad . \tag{3.10c}$$

Equations (3.10) represent the solution to the finite strain consolidation of a semi-infinite layer, neglecting the convective effect. The comparison of this solution to that given by equations (3.6) to (3.7) will illustrate the significance of neglecting the convective effect. This comparison in terms of the settlement/$\sqrt{c_v t}$ is shown in Figure 3.3 and in terms of the natural strain in Figure 3.4. As expected, when the strain is small (approaches infinitesimal strain), there is little difference between the two solutions; that is, the convective effect is negligible when the strain is small (final natural strain of order of 0.10 or less). However, as the strain becomes larger, the difference also becomes significant. For example, when the final natural strain is 0.8, the difference between the two rates of settlement is 130 percent.

This has serious implications. In some of the studies for multi-dimensional finite strain consolidation problems, for example, Mikasa and Ohnishi (1981), the problem is formulated in the Eulerian frame neglecting the convective effect, while in other studies, for example, Carter et al. (1977), a difference method is used for the temporal discretization without any special procedure to account for the convective term. This assumes implicitly that the convective effect is negligible. For the one-dimensional case, it has been demonstrated that for finite strain (the natural strain of order 0.1 or larger), the convective effect is very significant. Clearly, it is to be expected

that the same conclusion holds for multi-dimensional problems. Later on, a method will be introduced to account for the convective effect in a numerical scheme.

3.2.2 Finite Element Solutions

The more practical case of the finite strain consolidation of a finite layer including self-weight is now considered. The governing equation to be used, in a Lagrangian formulation, is obtained from equation (2.36):

$$[1+e_o(a)]\,\frac{\partial}{\partial a}\left[c_v(e)\,\frac{(1+e_o(a))}{(1+e)^2}\,\frac{\partial e}{\partial a}\right] + [1+e_o(a)]\,\frac{d}{de}\left[\frac{k(e)}{1+e}\left(\frac{\gamma_s}{\gamma_f}-1\right)\right]\frac{\partial e}{\partial a} = \frac{\partial e}{\partial t}\ . \qquad (3.11)$$

Introducing the following dimensionless variables:

$$x = \frac{a}{H} \qquad (3.12a)$$

and

$$T = \frac{c_v(e(0,0))t}{H^2} = \frac{c_{vo}t}{H^2}\ \text{(say)} \qquad (3.12b)$$

equation (3.11) becomes:

$$(1+e_o(x))\,\frac{\partial}{\partial x}\left[\frac{c_v(e)}{c_{vo}}\,\frac{1+e_o(x)}{(1+e)^2}\,\frac{\partial e}{\partial x}\right] + (1+e_o(x))\,\frac{d}{de}\left(\bar{k}\right)\frac{\partial e}{\partial x} = \frac{de}{dT} \qquad (3.13a)$$

where

$$\bar{k} = \frac{k(e)}{1+e} \cdot H \cdot \frac{1}{c_{vo}} \left(\frac{\gamma_s}{\gamma_f} - 1 \right) . \qquad (3.13b)$$

The boundary and initial conditions are given by:

at $x = 0$

$$e(0,t) = f(t) \quad ; \qquad (3.13c)$$

at $x = 1$, the boundary forms an impervious base, so that

$$v = 0 \quad ; \qquad (3.13d)$$

and, at $t = 0$

$$e(x,0) = e_o(x) \quad . \qquad (3.13e)$$

Using Darcy's law [equation (2.17)] and the equilibrium equation (2.21), the impervious condition at $x = 1$ [equation (3.13d)] becomes:

$$\frac{\partial e}{\partial x}\Big|_{x=1} = \frac{H(\gamma_s - \gamma_f)}{1+e_o(1)} \frac{de}{d\sigma'} \quad . \qquad (3.13f)$$

Equations (3.13) will now be solved by the finite element method. In essence, the method involves the discretization of the entire region (where the problem is defined) into elements and the dependent variable is then assumed to behave in a certain specified manner within each element (linearly, if two nodes are used to define an element and quadratically if three nodes are used).

Using the Galerkin method and following standard procedures in finite element formulation (Zienkiewicz, 1977), the following matrix

equation is obtained:

$$\underset{\sim}{C}\,\frac{d\underset{\sim}{\phi}}{dt} + \underset{\sim\sim}{K}\underset{\sim}{\phi} = \underset{\sim}{F} \quad . \tag{3.14}$$

In equation (3.14), ϕ is the vector of the nodal values of e; $\underset{\sim}{K}$ is like a stiffness matrix, $\underset{\sim}{C}$ a damping matrix and $\underset{\sim}{F}$ a loading matrix. The two global matrices, $\underset{\sim}{K}$ and $\underset{\sim}{C}$, are assembled from the element matrices. The element matrices are given by:

$$k_{ij}^{e\ell} = \int_{ve} \frac{c_v^{e\ell}(e)}{c_{vo}} \cdot \frac{1+e_o(x)}{(1+e)^2} \cdot \left[(1+e_o)\, \frac{\partial N_i^{e\ell}}{\partial x} + N_i^{e\ell}\, \frac{\partial e_o}{\partial x} \right] \frac{\partial N_j^{e\ell}}{\partial x}\, dx - \int_{ve} N_i^{e\ell}\, (1+e_o)\, \frac{\overline{dk}^{e\ell}}{de}\, \frac{\partial N_j^{e\ell}}{\partial x}\, dx \tag{3.15a*}$$

and

$$C_{ij}^{e\ell} = \int_{ve} N_i^{e\ell}\, N_j^{e\ell}\, dx \tag{3.15b}$$

where N are the shape functions (Zienkiewicz, 1977). In this study, a three-node linear element is used and the shape functions are quadratic. $\underset{\sim}{F}$ comes from the boundary conditions and for the case under study, the only contribution is from the impervious condition at x = 1 [equation (3.13f)]. Note that conceptually every internal element has two boundary conditions, which cancel each other out. The boundary condi-

* The superscript eℓ indicates value in an element.

tion at the top surface (x = 0) is specified and will be included in the assembly later on. However, conceptually, with the way the finite element is formulated, it does not contribute to F as in equation (3.42). Thus for F , the only value is:

$$F_{\text{last node}} = \left[\frac{1+e_o(1)}{1+e(1)}\right]^2 \frac{c_v(e(1))}{c_{vo}} \frac{\partial e}{\partial x}\Big|_{x=1} \quad . \qquad (3.15c)$$

Using the explicit forward difference scheme to solve equation (3.14), the following equation is obtained:

$$\underset{\sim}{C}\ \underset{\sim}{\phi}(t+\Delta t) = \underset{\sim}{F}\ \Delta t + \left[\underset{\sim}{C} - \underset{\sim}{K}\ \Delta t\right]\underset{\sim}{\phi}(t) \qquad (3.16)$$

If the solution at time t, that is, $\underset{\sim}{\phi}(t)$ is known, then the solution at time (t+Δt) is obtained from equations (3.16). With the way the problem has been formulated, it may be observed from equation (3.15b) that the matrix C is <u>symmetric</u> and <u>constant</u> with time. This makes equation (3.16) easy and cheap to solve.

As a check on the validity of this finite element formulation of one-dimensional finite strain consolidation, the method is used to compute the results of tests done by Croce, et al. (1984) and Mikasa and Takada (1984).

The tests done by Croce et al. were conducted in the centrifuge at the University of Colorado and were intended to simulate the self-weight consolidation of a prototype layer of initial thickness of 5.0 meter with an initial void ratio of 2.86. The layer thickness was reduced

from 5.0 meters to 3.3 meters during the process of consolidation.

Both the effective stress versus void ratio and permeability versus void ratio relations of the soil used are highly nonlinear. These relations were experimentally determined by Croce et al. (1984) and are shown in Figure 3.5. However, in their report no mathematical functions to describe these relations were given.

Hence, in this study two trials were made to fit mathematical functions to the given data. The functions used are:

Trial 1

for k versus e, (polynomial fit for $\ln k$)

$$k = \exp\left[-21.12 + 21.15e - 12.94e^2 + 3.94e^3 - 0.457e^4\right]$$

(k in m/day) ; (3.17a)

for e versus σ',

$$e = 2.14 - 0.409\ln\sigma' + 0.117(\ln\sigma')^2 - 0.0455(\ln\sigma')^3 + 0.00772(\ln\sigma')^4 \quad (\sigma' \text{ in } kN/m^2) \; ; \quad (3.17b)$$

Trial 2

for k versus e,

$$k = \exp\left[-14.41 + 5.72e - 0.837e^2\right] \quad (k \text{ in m/day}) \; ; \quad (3.17c)$$

for e versus σ',

$$e = 2.13 - 0.278 \ln \sigma' \qquad (\sigma' \text{ in } kN/m^2) \quad . \qquad (3.17d)$$

The coefficients necessary for the evaluation of the matrices $\underset{\sim}{K}$ and $\underset{\sim}{C}$ in equations (3.15a) and (3.15b) are then deduced from these fitted functions.

The comparison of the dimensionless settlement (degree of settlement) versus time calculated by the finite element method with the experimental data is shown in Figure 3.6.

As can be seen from Figure 3.6, the computed results for both trials give almost identical solutions. However, the fitting functions for the second trial are simpler than that for the first trial. Of particular interest is the fact that the relation used for e versus σ' in the second trial (equation (3.17d)) is in a form generally suggested for soils (Schofield and Wroth, 1968). Another interesting observation is that the calculated results at long (prototype) time (over 500 days) still agree with the experimental data. In a field situation, the result from a consolidation theory incorporating time-independent soil behavior is unable to predict the settlement after a long time since over long intervals, creep (viscous flow) and not consolidation dominates the prototype settlement behavior. However, creep is not simulated in a centrifuge experiment, and therefore viscous flow of the soil, which does occur in the model, develops only over the short model time (minutes) rather than over a time corresponding to the prototype situation.

In the study by Croce et al., the experimental data were also compared to the results predicted by Terzaghi's theory. They concluded that Terzaghi's theory was inadequate to predict the consolidation of a thick layer and a finite strain theory was needed.

In the study by Mikasa and Takada (1984), tests were conducted in the centrifuge at Osaka City University. Two sets of self-weight consolidation tests were carried out; the first test was done on a soil with an initial void ratio of 3.20 and the second with a void ratio of 3.98. The initial prototype thickness of layer these tests were intended to model is 10 m. For the first test, the final settlement was equivalent to 2.45 m in the prototype and for the second test, the final settlement was 3.45 m. The e versus σ' but not the k-e relation was given by the authors. For the purpose of this study, a trial function for the k-e relation is constructed from data given by Mikasa and Takada as follows:

For $e_o = 3.2$

k versus e relation

$$k = \exp(-26.90 + 5.96e - 0.628e^2) \quad ; \qquad (3.18a)$$

e versus σ' relation (as given by Mikasa and Takada)

$$e = 2.22 - 0.31 \ln \sigma' \quad . \qquad (3.18b)$$

For $e_o = 3.98$, the k versus e relation is the same as (3.18a). The e versus σ' relation is:

$$e = 2.31 - 0.334 \ln \sigma' \quad . \qquad (3.18c)$$

The finite element results based on these relations are compared with the experimental results and shown in Figures (3.7) and (3.8). In Figure (3.9), the void ratio versus depth behaviors for different times is shown. Also shown in the figure is the measured void ratio distribution when the consolidation process has ended. The computed results in both cases agree very well with the experimental data. Note too that the observations made earlier on the Croce et al. study with regard to the functional form for the e versus σ' relation and the behavior after a long time are evident here too.

Clearly, the very good agreement of the predicted results as compared to the experimental results gives confidence both in the consolidation theory and the use of the finite element method for such a theory. This study also suggests that a linear e versus ($\ln \sigma'$) relation [basis of many constitutive laws (see Bardet, 1983), for example] will indeed describe one-dimensional soil behavior well.

3.2.3 Approximate Closed-form Solutions-Perturbation Method

In this section, approximate closed-form solutions are derived for the finite strain condition using the perturbation technique. These solutions are derived for the consolidation of a thin layer (that is, for cases where the self-weight is significantly less than the applied load) and will be useful to geotechnical engineers who may need a quick and relatively accurate consolidation solution.

The perturbation method will be applied to the Lagrangian formulation in which the dependent variable is the natural strain ε. Before the perturbation method is actually carried out, it will be demonstrated that this particular choice of formulation should produce the best results. To do this, three different infinitesimal theories will be used to predict the consolidation of a semi-infinite layer neglecting self-weight and the results will be compared to the analytical solution obtained in Section (3.2.1). The reason the infinitesimal theories are used is that the first-order perturbation is actually the linearization of the non-linear problem. This linearization is equivalent to assuming the strain is infinitesimal. The three theories to be used are:

(i) Terzaghi's theory

The governing equation is given by:

$$c_v \frac{\partial^2 u}{\partial a^2} = \frac{\partial u}{\partial t} \qquad (3.19a)$$

where u is the excess pore pressure.

(ii) Infinitesimal theory from Lee and Sills's formulation (Lee and Sills, 1979)

The following equation governs:

$$c_v \frac{\partial^2 n}{\partial a^2} = \frac{\partial n}{\partial t} \qquad (3.19b)$$

where n is the porosity.

(iii) Infinitesimal theory from Mikasa's formulation (the formulation which is used in this study)

This is given by:

$$c_v \frac{\partial^2 \varepsilon}{\partial a^2} = \frac{\partial \varepsilon}{\partial t} \qquad (3.19c)$$

where ε is the natural strain.

The rate of settlement as predicted by the three infinitesimal theories is compared to an analytical solution of the finite strain theory (obtained from section 3.2.1). As can be seen in Figure 3.10, the results as predicted by the infinitesimal theory based on Mikasa's formulation gives the best result.

A reason is postulated to explain why this particular formulation would give such a good result. It is seen from the study in Section 3.2.1 that Mikasa's formulation, neglecting the convective effect, gives a rate of settlement that is greater than if the effect is not neglected (Figure 3.3). This is obvious since the strain gradient [left-hand side of equation (3.8a)] has to "drive" a smaller material derivative (since the convective part is neglected). However, the "Eulerian strain gradient" in equation (3.8a) becomes a "Lagrangian strain gradient" [equation (3.19)] after linearization and thus is reduced in value. This seems to suggest that the errors involved in the linearization process [neglecting the convective effect on the right-hand side of equation (3.8a) and using a smaller strain gradient on the left-hand side] tend to cancel each other out.

The perturbation technique is powerful and can be applied to many different nonlinear problems (including both geometrical and material nonlinearities). To illustrate the procedure and to show the viability of this method, it is now applied to the consolidation of a finite layer neglecting self-weight and having a constant coefficient of consolidation. The governing equation is equation (2.34) with the natural strain as a dependent variable. It is then transformed to a Lagrangian form using equation (2.35). The equation to be used is:

$$\exp(\varepsilon)\,\frac{\partial}{\partial x}\left[\exp(\varepsilon)\,\frac{\partial \varepsilon}{\partial x}\right] = \frac{\partial \varepsilon}{\partial T} \tag{3.20a}$$

where the dimensionless variables $x = \frac{a}{H}$ and $T = \frac{c_v t}{H^2}$ are used. The initial and boundary conditions are given by:

at $x = 0$

$$\varepsilon(0,T) = \varepsilon_f \; ; \tag{3.20b}$$

at $x = 1$

$$\frac{\partial \varepsilon}{\partial x} = 0 \; ; \tag{3.20c}$$

at $t = 0$

$$\varepsilon(x,0) = 0 \; . \tag{3.20d}$$

The settlement of the top surface is given by:

$$s(t) = H \cdot \int_0^1 \left[1 - \exp(-\varepsilon)\right] dx \quad . \tag{3.21}$$

Since in equations (3.20), the final natural strain ε_f is the only specified value, it is used to form the following approximation:

$$\varepsilon = \varepsilon_f \varepsilon_1(x,t) + \varepsilon_f^2 \varepsilon_2(x,t) + \ldots \tag{3.22}$$

In most practical problems, it is rare for ε_f to exceed one and thus we can consider ε_f to be "small." Following the standard procedure for regular perturbation (Ames, 1972), equation (3.22) is substituted into equations (3.20), and, equating like powers of ε_f, the following systems of equations are obtained:

<u>order of ε_f</u>

$$\frac{\partial^2 \varepsilon_1}{\partial x^2} = \frac{\partial \varepsilon_1}{\partial T} \tag{3.23a}$$

with the following initial and boundary conditions:

at $x = 0$

$$\varepsilon_1(0,T) = 1 \quad ; \tag{3.23b}$$

at $x = 1$

$$\frac{\partial \varepsilon_1}{\partial x}(1,T) = 0 \quad ; \tag{3.23c}$$

at t = 1

$$\varepsilon_1(x,0) = 0 \quad . \tag{3.23d}$$

The settlement, to order of ε_f, is given by:

$$s(t) = H \int_0^1 [1 - \exp(-\varepsilon_f \varepsilon_1)]dx + 0(\varepsilon_f^2) \quad . \tag{3.24}$$

(order of ε_f^2)

The governing equation is:

$$\frac{\partial^2 \varepsilon_2}{\partial x} = \frac{\partial \varepsilon_2}{2T} - 2\varepsilon_1 \frac{\partial^2 \varepsilon_1}{\partial x^2} - \left(\frac{\partial \varepsilon_1}{\partial x}\right)^2 \tag{3.25a}$$

and the initial and boundary conditions are:

at x = 0

$$\varepsilon_2(0,T) = 0 \quad ; \tag{3.25b}$$

at x = 1

$$\frac{\partial \varepsilon_2}{\partial x} = 0 \quad ; \tag{3.25c}$$

at t = 1

$$\varepsilon_2(x,0) = 0 \quad . \tag{3.25d}$$

The settlement is now given by:

$$s(t) = H \cdot \int_0^1 [1 - \exp(-\varepsilon_f \varepsilon_1 - \varepsilon_f^2 \varepsilon_2)]dx + 0(\varepsilon_f^3) \quad . \qquad (3.26)$$

If a more accurate solution is needed, this method can be followed through for as many orders as required, though the effort required to solve the higher-order systems increases very significantly. Equations (3.23) are mathematically similar to the classical one- dimensional heat conduction or diffusion problem (see Crank, 1975 or Carslaw and Jaeger, 1959). The solution to equations (3.23) is as follows:

$$\varepsilon_1(x,T) = 1 - \sum_{n=0}^{\infty} \frac{2}{\lambda_n} \exp(-\lambda_n^2 T) \sin(\lambda_n x) \qquad (3.27a)$$

where

$$\lambda_n = \left(\frac{2n+1}{2}\right)\pi \quad . \qquad (3.27b)$$

Using equations (3.27) for ε_1 in equation (3.25a), the following equation is obtained:

$$\begin{aligned} \frac{\partial^2 \varepsilon}{\partial x^2} = \frac{\partial \varepsilon_2}{\partial T} &- 4\sum_{m=0}^{\infty} \lambda_m \exp(-\lambda_m^2 T) \sin(\lambda_m x) \\ &+ \sum_{n=0}^{\infty} \sum_{m=0}^{\infty} 2 \exp(-a_1 T) \cos[(\lambda_m - \lambda_n)x](2a_2 - 1) \\ &- \sum_{n=0}^{\infty} \sum_{m=0}^{\infty} 2 \exp(-a_1 T) \cos[(\lambda_m + \lambda_n)x](2a_2 + 1) \end{aligned} \qquad (3.28a)$$

where a_1 and a_2 are defined as follows:

$$a_1 = \lambda_n^2 + \lambda_m^2 \tag{3.28b}$$

and

$$a_2 = \frac{\lambda_m}{\lambda_n} \quad . \tag{3.28c}$$

Using the eigenfunction expansion method (Hildebrand, 1976), the following solution to equations (3.28) is obtained:

$$\varepsilon_2 = 4\sum_{n=0}^{\infty} \lambda_n T \exp(-\lambda_n^2 T) \sin(\lambda_n x) + \sum_{\ell=0}^{\infty}\sum_{m=0}^{\infty}\sum_{n=0}^{\infty} (2a_2-1)\frac{4}{a_1-\lambda_\ell^2}\left[\exp(-a_1 T) - \exp(-\lambda_\ell^2 T)\right] \quad .$$

$$\left[\frac{\lambda_\ell}{\lambda_\ell^2-a_3^2}\right]\sin(\lambda_\ell x) \tag{3.29a}$$

$$+ \sum_{\ell=0}^{\infty}\sum_{m=0}^{\infty}\sum_{n=0}^{\infty} -(2a_2+1)\frac{4}{a_1-\lambda_\ell^2}\left[\exp(-a_1 T) - \exp(-\lambda_\ell^2 T)\right] \quad .$$

$$\left[\frac{\lambda_\ell}{\lambda_\ell^2-a_4^2}\right]\sin(\lambda_\ell x)$$

where

$$a_3 = \lambda_m - \lambda_n \tag{3.29b}$$

$$a_4 = \lambda_m + \lambda_n \quad . \tag{3.29c}$$

In Figure 3.11, the solutions represented by equations (3.27) and equations (3.29) are compared to the solution generated by the finite element method. It is clear that the perturbation method can offer a quick and, in this case, very accurate solution. In fact, the method still produces good results even when ε_f is not "small" (ε_f exceeds one).

This is best illustrated by considering the consolidation of a semi-infinite layer where an analytical solution [equations (3.6)] is available. Following the same procedure as above, the following solution is obtained:

$$\varepsilon_1 = 1 - \text{erf}\,(x) \tag{3.30a}$$

$$\varepsilon_2 = \left[\frac{1}{2} - \frac{2}{\pi} - \frac{2}{\sqrt{\pi}}\, x \exp(-x^2) + \text{erf}\,(x)\right]\text{erf}(x) + \frac{2x}{\sqrt{\pi}} \exp\,(-x^2) + \frac{2}{\pi}\left[1 - \exp\,(-2x^2)\right] - \frac{6}{\sqrt{\pi}} \int_0^x \text{erf}\,(u) \exp\,(-u^2)\,du \tag{3.30b}$$

where $x = (a/2\sqrt{c_v t})$ For $\varepsilon = \varepsilon_1 \varepsilon_f + 0(\varepsilon_f^2)$

$$s(t) = \frac{2\varepsilon_f}{\sqrt{c_v t}} \tag{3.30c}$$

and for $\varepsilon = \varepsilon_1 \varepsilon_f + \varepsilon_2 \varepsilon_f^2 + 0(\varepsilon_f^3)$,

$$s(t) = \left[\frac{2}{\sqrt{\pi}} + \varepsilon_f \cdot \frac{2}{\sqrt{\pi}}\left(\frac{2}{\pi} - \frac{1}{2}\right)\right]\varepsilon_f\sqrt{c_v t} \quad . \qquad (3.30d)$$

The comparison of equations (3.30) with equations (3.6) is shown in Figure 3.12. For $\varepsilon_f = 1.2$, the difference between the analytical solution and the second-order perturbation solution is only 3 percent. The excellence of this method clearly cannot be explained by the perturbation technique alone since for ε_f greater than one, the arguments on which the perturbation technique is based are invalid. The physical reason postulated earlier, that errors caused by the linearization process using the perturbation technique tend to cancel each other out, must play a part.

3.2.4 Finite Difference Method: Accounting for the Convective Effect in an Eulerian Formulation

In the Eulerian formulation with the natural strain as the dependent variable [see equation (2.34)], the material derivative is given by:

$$\frac{D\varepsilon}{Dt} = \frac{\partial\varepsilon}{\partial t} + v_s \frac{\partial\varepsilon}{\partial\xi} \quad . \qquad (3.31)$$

It can be seen that in this definition the velocity of convection is the velocity of the solid phase. From this observation, a method that can be incorporated in a numerical scheme to account for the convective term is now introduced.

In all the consolidation theories considered thus far, the solid phase has been assumed to be incompressible. This makes it possible to

introduce the concept of the "equivalent height" of solid content (the solid phase) z within a Lagrangian formulation [see equation (2.35)]. To extend this idea to the Eulerian formulation, an "equivalent control volume" of solid content is introduced. For example, in the one-dimensional case, consider an equivalent control volume V_s which has a uniform void ratio of e_o initially. The volume of soil that contains such a control volume is $V_s(1+e_o)$. On consolidation, the soil layer is deformed and the soil volume is reduced. Though the control volume will also move correspondingly with the soil, its volume will remain unchanged.

The velocity of this control volume will be the velocity of the solid phase. Thus if a point in this control volume is followed, then the time derivative of the dependent variable at this point is equivalent to the material derivative of the said dependent variable in an Eulerian formulation by virtue of the definition given in equation (3.31). This idea is conceptually similar to following a pathline or material-line in fluid mechanics (Currie, 1974).

To illustrate the procedure, this idea will now be incorporated into a finite difference scheme that was suggested, on an intuitive basis, by R. F. Scott. The consolidation of a finite layer is considered, with an impervious base, uniform initial condition, constant coefficient of consolidation and absence of self-weight. These constraints are not necessary but they are used here for ease in illustrating the concept. The governing equation is obtained from equation (2.34) and is as follows:

$$c_v \frac{\partial^2 \varepsilon}{\partial \xi^2} = \frac{D\varepsilon}{Dt} \qquad (3.32a)$$

and the initial and boundary conditions are:

at the top surface $\xi = s(t)$

$$\varepsilon = \varepsilon_f \ ; \qquad (3.32b)$$

at $\xi = H$

$$\frac{\partial \varepsilon}{\partial \xi} = 0 \ ; \qquad (3.32c)$$

at $t = 0$

$$\varepsilon = 0.0 \ . \qquad (3.32d)$$

Suppose at time $t = 0$, the layer of thickness H is divided into m equal sections each of length $\Delta\xi_o = \frac{H}{m}$ (see Figure 3.13). To predict the value at time $t = \Delta t$, the following finite difference scheme is introduced:

$$\varepsilon(i,1) = \varepsilon(i,0) + c_v \frac{\Delta t}{\Delta \xi_o^2} \left[\varepsilon(i+1,0) - 2\varepsilon(i,0) + \varepsilon(i-1,0)\right] \ . \qquad (3.33)^*$$

After the value of ε has been determined for time $t = \Delta t$, it is used to determine the nodal coordinates for the new grid to be used to predict the value at the next time step. This is achieved by keeping the volume of solid content between two nodal points constant at all time. So the new spacing between nodes i-1 and i to be used for the

* $\varepsilon(i,j)$ denotes the value of node i at time $t = j\Delta t$.

next time step, $\Delta\xi_i(\Delta t)$, is obtained from:

$$\Delta\xi_i(\Delta t) = \left(\exp\left[-\frac{1}{2}\left(\varepsilon(i-1,1) + \varepsilon(i,1)\right)\right]\right)\Delta\xi_o \quad . \tag{3.34}$$

If the bottom boundary is assumed to be fixed, the new coordinate of the nodal point i (see Figure 15 for the numbering sequence) is given by:

$$\xi(i\Delta\xi_o,\Delta\tau) = H - \sum_{n=i+1}^{m} \Delta\xi_n(\Delta t) \tag{3.35}$$

and the settlement of the top surface is given by:

$$s(\Delta t) = 1 - \sum_{n=1}^{m} \Delta\xi_n(\Delta t) \quad . \tag{3.36}$$

Thus, after consolidation has begun, the nodal coordinates of the grid at each subsequent time step are determined solely from the computed values of ε. Obviously, the spacings between nodal points are unequal after time t = 0. Since we are following the "equivalent control volume," the material derivative of the nodal values is the same as the time derivative of these values. The explicit forward difference scheme can thus be used to discretize the material derivative. The finite difference scheme that was used was derived by using Taylor's expansion and allowing for uneven nodal spacing. The scheme is presented below.

Let Δt be the time step and $\Delta\xi_o$ the nodal spacing at time t = 0. If the spacing between node i-1 and node i at time $t = \Delta t$ is defined as:

$$\Delta\xi_i(j\Delta t) = n(i,j)\Delta\xi_o \tag{3.37}$$

then the finite difference scheme is as follows:

$$\varepsilon(i,j+1) = \varepsilon_{ij} + c_v \frac{\Delta t}{\Delta \xi_o^2} \left[\frac{\varepsilon(i+1,j)-\varepsilon(i,j)}{n(i+1,j)} - \frac{\varepsilon(i,j)-\varepsilon(i-1,j)}{n(i,j)} \right] \cdot$$

$$\frac{2}{n(i+1)+n(i,j)} \qquad (3.38a)$$

and the nodal spacing is given by

$$n(i,j) = \exp\left[-\frac{1}{2} (\varepsilon(i-1,j) + \varepsilon(i,j) \right] . \qquad (3.38b)$$

A method has thus been introduced that can be incorporated in a finite difference scheme to account for the convective term.

The method as described above differs from those introduced by Crank and Gupta for moving boundary diffusion problems (see Crank, 1975) and used by Lee and Sills (1979) to solve a specially formulated moving boundary consolidation problem. Since the moving boundary diffusion problem (or Lee and Sills's formulation) does not involve a material derivative, in their method no special procedure is needed to account for the convective effect. Only the moving boundary has to be tracked in their method.

The consolidation of a finite layer (neglecting self-weight) with an impervious base is now solved by the finite difference scheme as stated in equations (3.38) and the results compared to those generated by the finite element method (see Figure 3-14). The very good agreement between the two set of results indicates the validity of the concept introduced. In the next section, this concept will be extended to a three-dimensional case.

3.3 CONSOLIDATION OF SOILS BY VERTICAL DRAINS

As explained earlier in Chapter II, this case has practical importance, since vertical drains are often used to accelerate the consolidation process. However, thus far, this problem has not been considered within the context of finite strain. The problem dealt with here is subjected to the realistic restriction of no lateral strain since generally large numbers of vertical drains are used so that the consolidation of each region dependent on a drain is identical. It is recognized that the governing equation as given by equation (2.37) is not strictly correct since the Cryer-Mandel effect has been neglected. However, the infinitesimal strain form of this equation has been used extensively (Barron, 1948; Richart; 1959; and Yoshikuni and Nakanodo, 1974). Thus it is worth investigating the finite strain effect with this assumption (neglecting Cryer-Mandel effect).

In practice, vertical drains are arranged in a hexagonal pattern. However, for ease of mathematical modeling, this has been approximated by a circle. Furthermore, the symmetry boundary condition at the exterior boundary [equation (3.39c)] requires this boundary to be impervious.

The problem to be solved is shown in Figure 2.2. The governing equation is (2.37) and for a symmetric problem is of the following forms:

$$\frac{c_v}{m_v}\frac{\partial}{\partial r}\left(m_v\frac{\partial u}{\partial r}\right) + c_v \cdot \frac{1}{r}\cdot\frac{\partial u}{\partial r} + \frac{c_v}{m_v}\frac{\partial}{\partial \xi}\left(m_v\frac{\partial u}{\partial \xi}\right) = \frac{Du}{Dt} \qquad (3.39a)$$

where u is the excess pore pressure and the boundary and initial conditions are:

at $r = r_w$

$$u = 0 \tag{3.39b}$$

at $r = r_e$

$$\frac{\partial u}{\partial r} = 0 \; ; \tag{3.39c}$$

at $\xi = H$

$$\frac{\partial u}{\partial \chi} = 0 \; ; \tag{3.39d}$$

at $\chi = s(r,t)$

$$u = 0 \; ; \tag{3.39e}$$

and assuming a homogeneous initial condition, at $t = 0$

$$u = u_o \; . \tag{3.39f}$$

Finite Element Method - Inclusion of Convective Effect

To solve equations (3.39) requires a numerical method. The "equivalent control volume" concept suggested earlier will now be incorporated into a finite element scheme that allows for variable properties.

The finite element method involves discretizing the entire region into elements (this time rectangular elements are used) and assuming that the dependent variable behaves in a specified manner within each

element. The formulation will make use of the fact that the problem is axisymmetric. Using the Galerkin method and following standard procedure (Zienkiewicz, 1977), the following matrix equation is again obtained:

$$\underset{\sim}{C}\,\frac{D\underset{\sim}{\phi}}{Dt} + \underset{\sim}{K}\,\underset{\sim}{\phi} = \underset{\sim}{F} \tag{3.40a}$$

where $\underset{\sim}{C}$ and $\underset{\sim}{K}$ are assembled from element matrices defined as follows:

for $\underset{\sim}{C}$

$$C_{ij}^{e\ell} = \int_{v}^{e\ell} N_i^{e\ell}\, N_j^{e\ell}\, r\,dr\,d\xi \tag{3.40b}$$

and for $\underset{\sim}{k}$

$$k_{ij}^{e\ell} = \int_{v^e} m_v \frac{\partial}{\partial r}\left(\frac{c_v}{m_v} N_i^{e\ell}\right)\frac{\partial N_j^{e\ell}}{\partial r}\, r\, dr\, d\xi + \int_{v^e} m_v \frac{\partial}{\partial \xi}\left(\frac{c_v}{m_v} N_i^{e\ell}\right)\frac{\partial N_j^{e\ell}}{\partial \xi}\, r\, dr\, d\xi \quad . \tag{3.40c}$$

For the boundary conditions as specified in this case [see equations 3.39]; $\underset{\sim}{F}$, the vector on the right hand side of (3.40a) is identically zero. If other boundary conditions are specified, they can be easily included in $\underset{\sim}{F}$ by following standard procedure in finite element analysis (see Section 3.2.2 for example).

To account for the convective term on the right-hand side, the concept of "equivalent control volume" is employed. Because of the assumption of no lateral strain, this concept is easier to apply since there will not be any convective effect due to motion in the lateral direction. In essence, this technique requires that, after each time step, the mesh is updated to follow the "equivalent control volume." The actual process is described below.

Consider an element (see Figure 3.15) that has an initial void ratio of e_o (assume constant in this study). The "equivalent control volume" of solid content of this element is:

$$V_s = \frac{\pi \Delta \xi_o}{1+e_o} \left[2\Delta r + (\Delta r)^2\right] \quad . \tag{3.41a}$$

Now suppose that the nodal values of this element are known at time $t = k\Delta t$. Since we are following the "equivalent control volume," the coordinates of the element at time $t = k\Delta t$ must be such that the volume of solid content is equal to V_s implying that:

$$2\pi \int_{V^{e\ell}} \frac{r \, dr \, d\xi}{1+e^{e\ell}} = V_s \quad . \tag{3.41b}$$

If the coordinates of the bottom two nodes (nodes 3 and 4 in Figure 3.15) are known, then we have two unknowns to determine with only one equation (3.41b). A simple but approximate solution to this problem is to assume that, for the element closest to the exterior boundary, the lengths of the two vertical sides are proportional to their (1+e) values calculated from the nodal excess pore pressure values as follows:

$$\frac{\ell_{14}}{1+\frac{1}{2}(e_1+e_4)} = \frac{\ell_{23}}{1+\frac{1}{2}(e_2+e_3)} \qquad (3.41c)$$

where e_1 to e_4 are the nodal void ratio values (see Figure 3.15) for nodal number). This is chosen because the displacement is expected to be smallest at points furthest away from the well and thus the error induced by this assumption is expected to be small.

With this setting and assuming that the bottom boundary is fixed, calculation of the new mesh size will proceed from the bottom left hand corner element (see Figure 3.15) and the lengths of its vertical sides computed using equations (3.41b) and (3.41c). With this, the size of the element on the right will be calculated next. Since the length of the left vertical side is already known, we can use equation (3.41b) to calculate the other side. The procedure is now repeated.

As can be seen, equation (3.41b) is an integral equation with the region of integration the unknown. This is a difficult problem. For this study, a simple approximation is made, that the value of (1+e) in an element is constant and equal to the average of the nodal values. For elements away from the drainage surface, this assumption is realistic, for the variation of (1+e) within each element is expected to be small. But for elements next to the drained boundary, this assumption is unrealistic at small time where the value of (1+e) is expected to vary like an error function. Since the error function is difficult to fit and integrate, a hyperbolic function is assumed. Some simple calculations suggest that the errors induced in this assumption are small. Nevertheless, it is reorganized that this is only an approximation.

In the above, a method to incorporate the convective effect in a finite element scheme using the concept of "equivalent control volume" is introduced. As is clear from the formulation, the above method can incorporate nonlinear material properties. Note too that the self-weight effect can be included in a manner similar to the procedure used in Section 3.2.2 by adding its contribution to $\underset{\sim}{K}$ (the governing equation is similar to equation (3.39a) but with body forces included).

Since there is a dearth of data with respect to this problem for nonlinear properties, the above method will be illustrated for the finite strain condition by solving the problem with m_v and c_v constant (same assumptions as in infinitesimal theories like Barron's and, Yoshikuni and Nakanodo's). The settlement of the top surface with time is shown in Figure 3.16. It is clear from this analysis (see Figure 3.16) that arching will occur. In practice, this will cause some redistribution of the load depending on the stiffness of the loading platform. This effect was recognized by Barron (1948), but he considered a case where arching would not redistribute the load; that is, the platform is very flexible. This is the case considered here. But in general, the method introduced here can be adapted to study the case where a redistribution of load is allowed. It is very difficult to compare the results obtained here to any existing studies since, in all the studies cited in this section, the quantity by which these authors chose to present their results is the average consolidation degree (the average over the entire region of the ratio of amount of pore pressure dissipated at each point to the initial pore pressure). This has very

little physical significance.

In this chapter, a number of interesting points have been made and methods of solution to the problem of consolidation presented. These will be summarized in the next chapter.

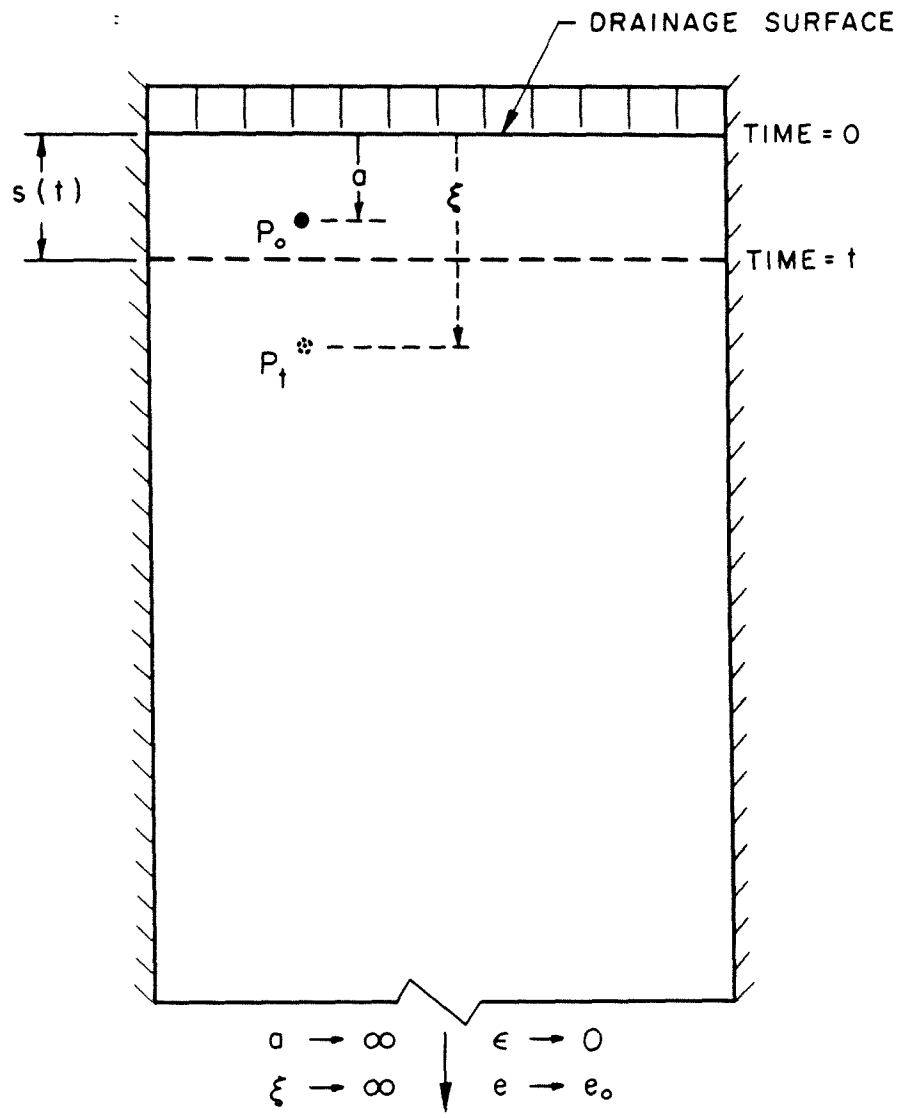

Figure 3.1 One-dimensional consolidation of a semi-infinite layer
a ... Lagrangian coordinate
ξ ... Eulerian coordinate

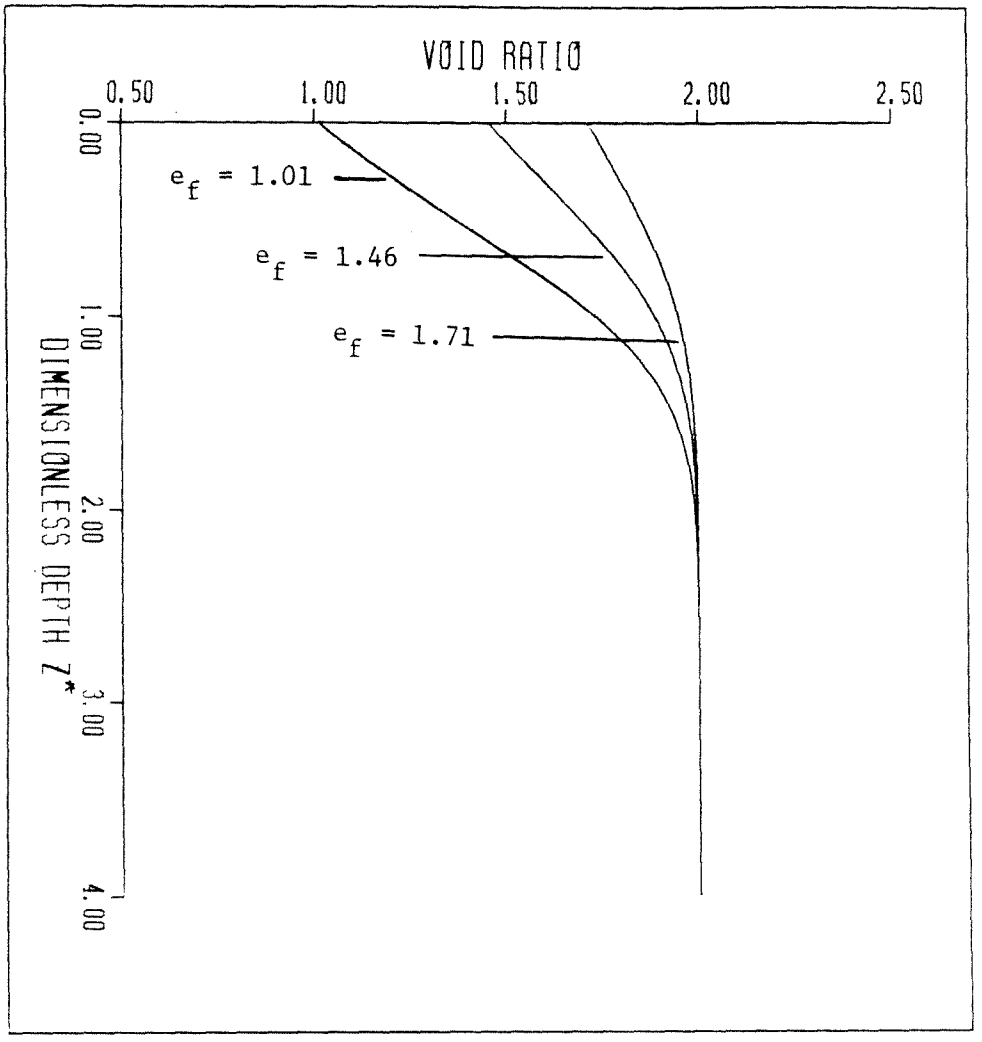

Figure 3.2 Analytical solutions to one-dimensional finite strain consolidation of a semi-infinite layer Dimensionless depth z^* is defined in equation (3.2d). Initial void ratio = 2.0

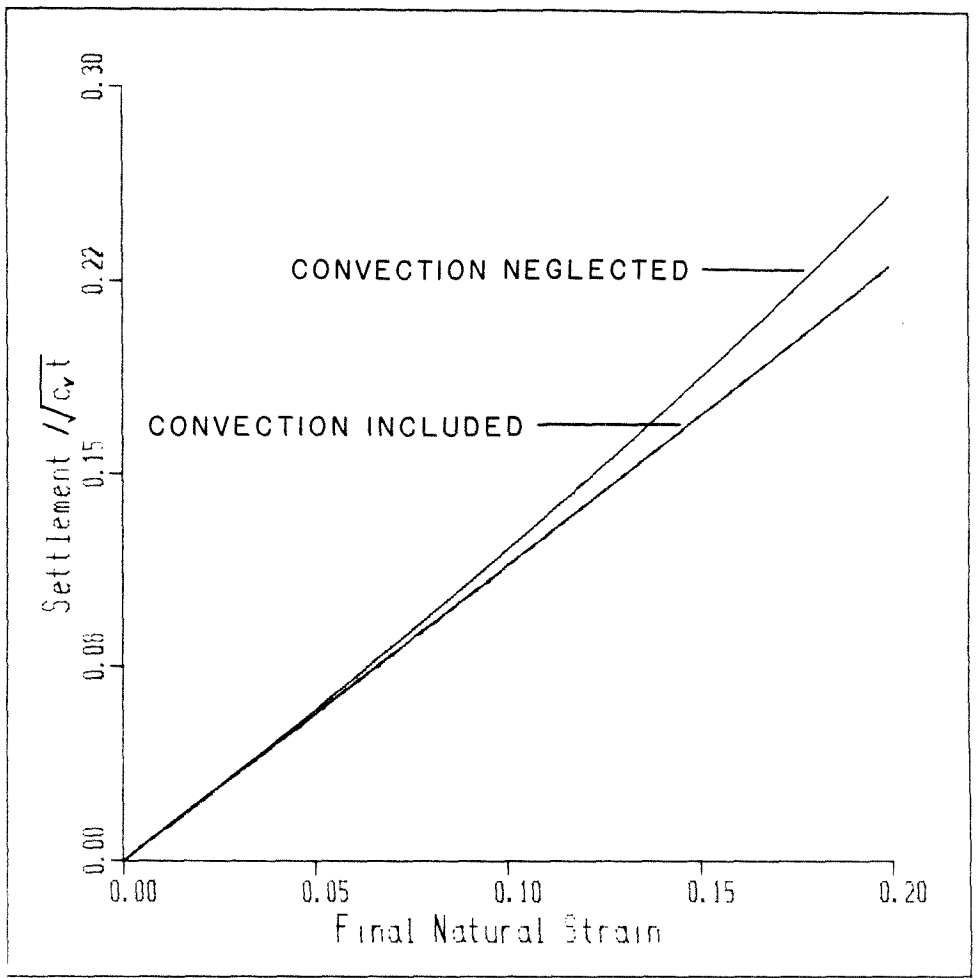

Figure 3.3a One-dimensional finite strain consolidation: Effect of neglect of convection in terms of settlement $/\sqrt{c_v t}$

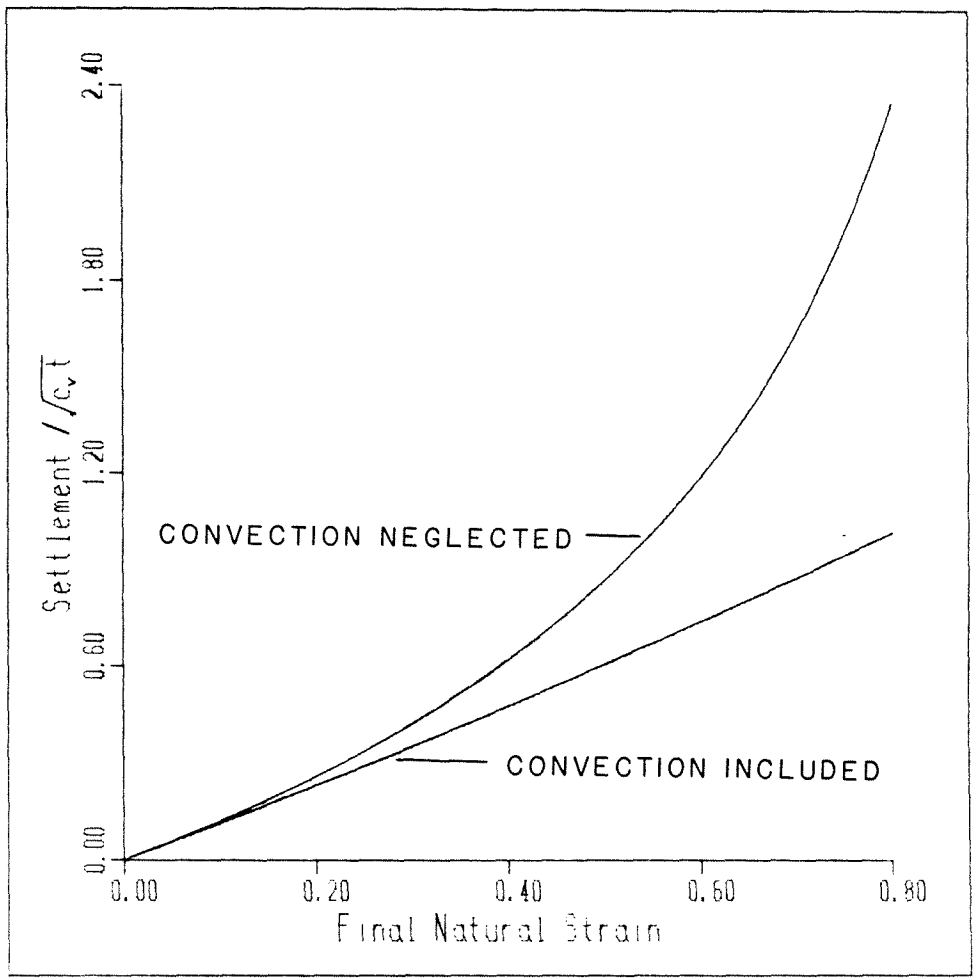

Figure 3.3b One-dimensional finite strain consolidation: Effect of neglect of convection in terms of settlement $/\sqrt{c_v t}$

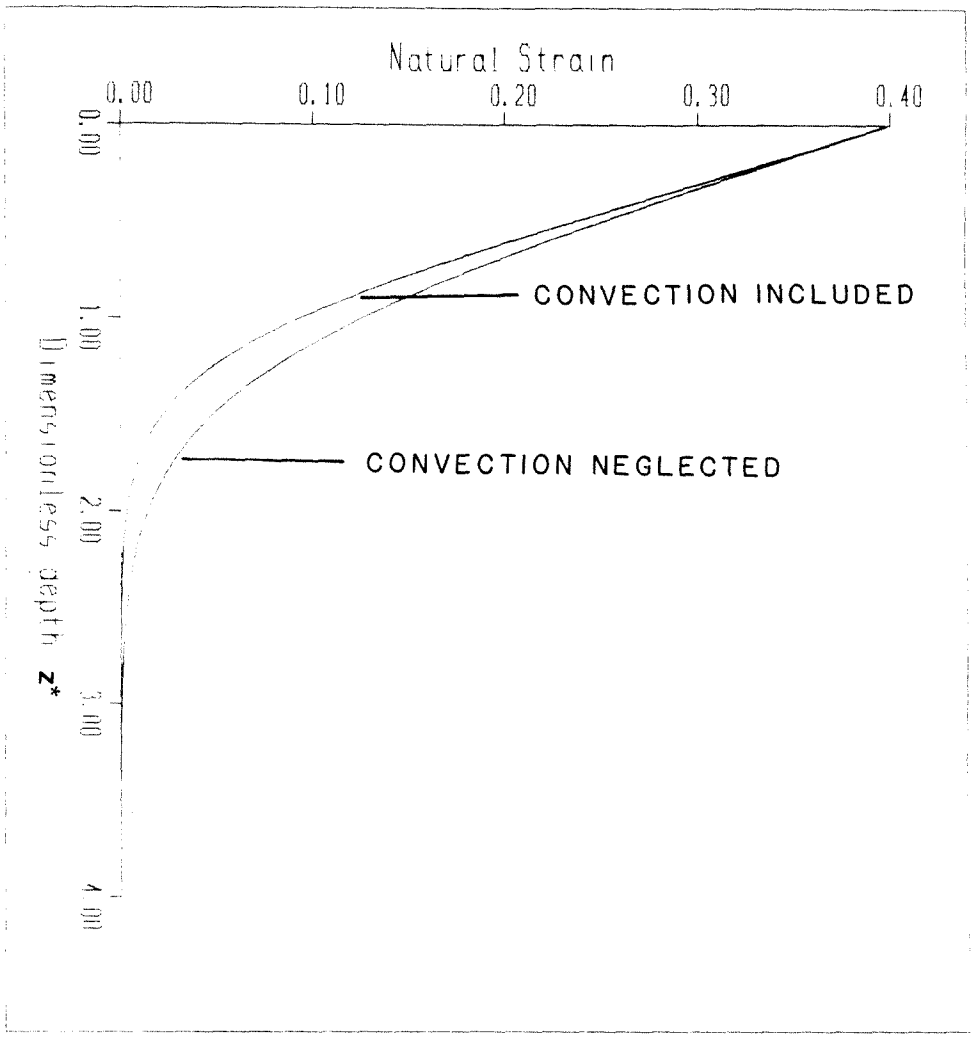

Figure 3.4 1-D finite strain consolidation: Effect of neglect of convection in terms of natural strain distribution. z^* defined in equation (3.2d) Final natural strain = 0.4

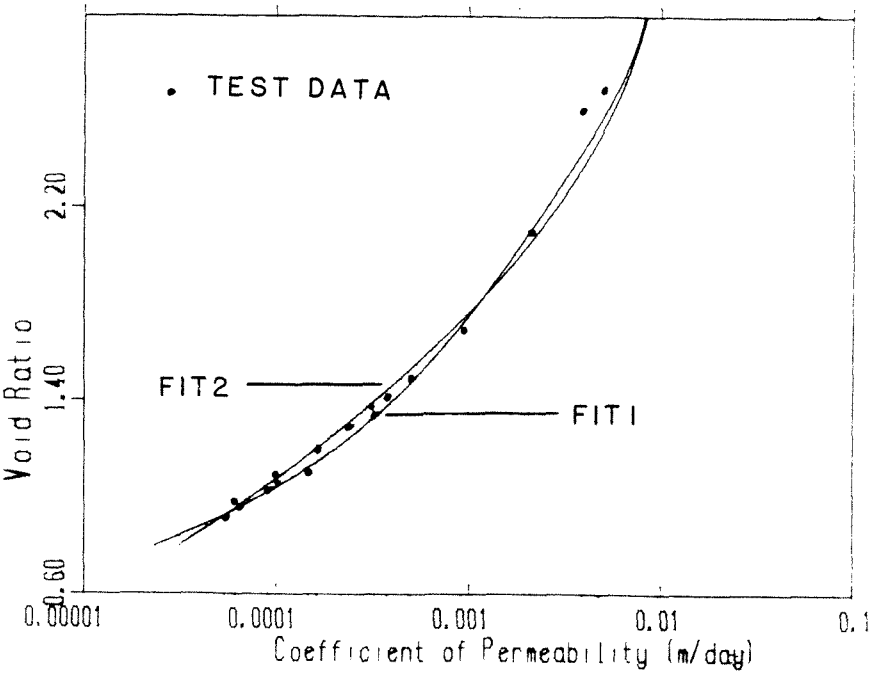

(a)

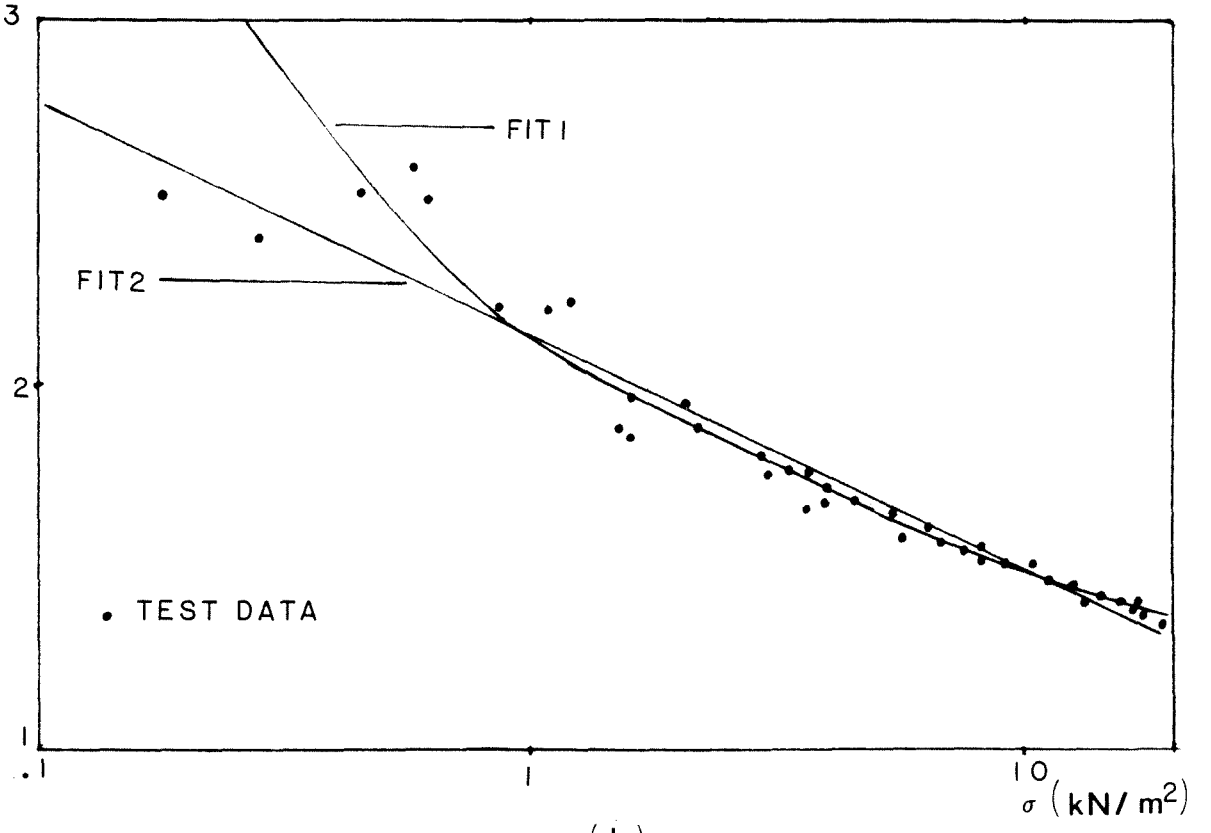

(b)

Figure 3.5 Input data and fitting curves for Croce et al.
a. e versus k
b. e versus σ'

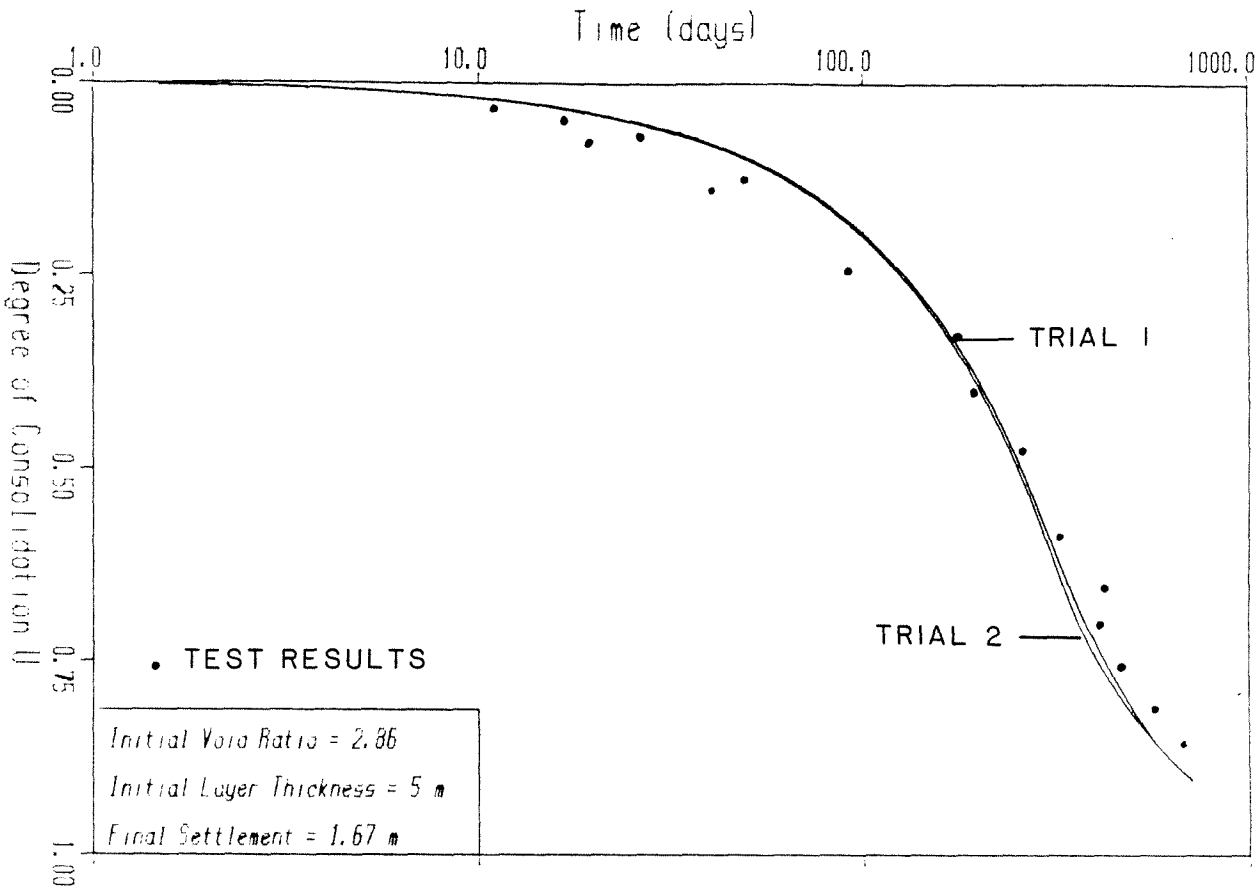

Figure 3.6 One-dimensional self-weight consolidation (singly drained) : Comparison of theoretical and experimental results (Croce et el. tests)

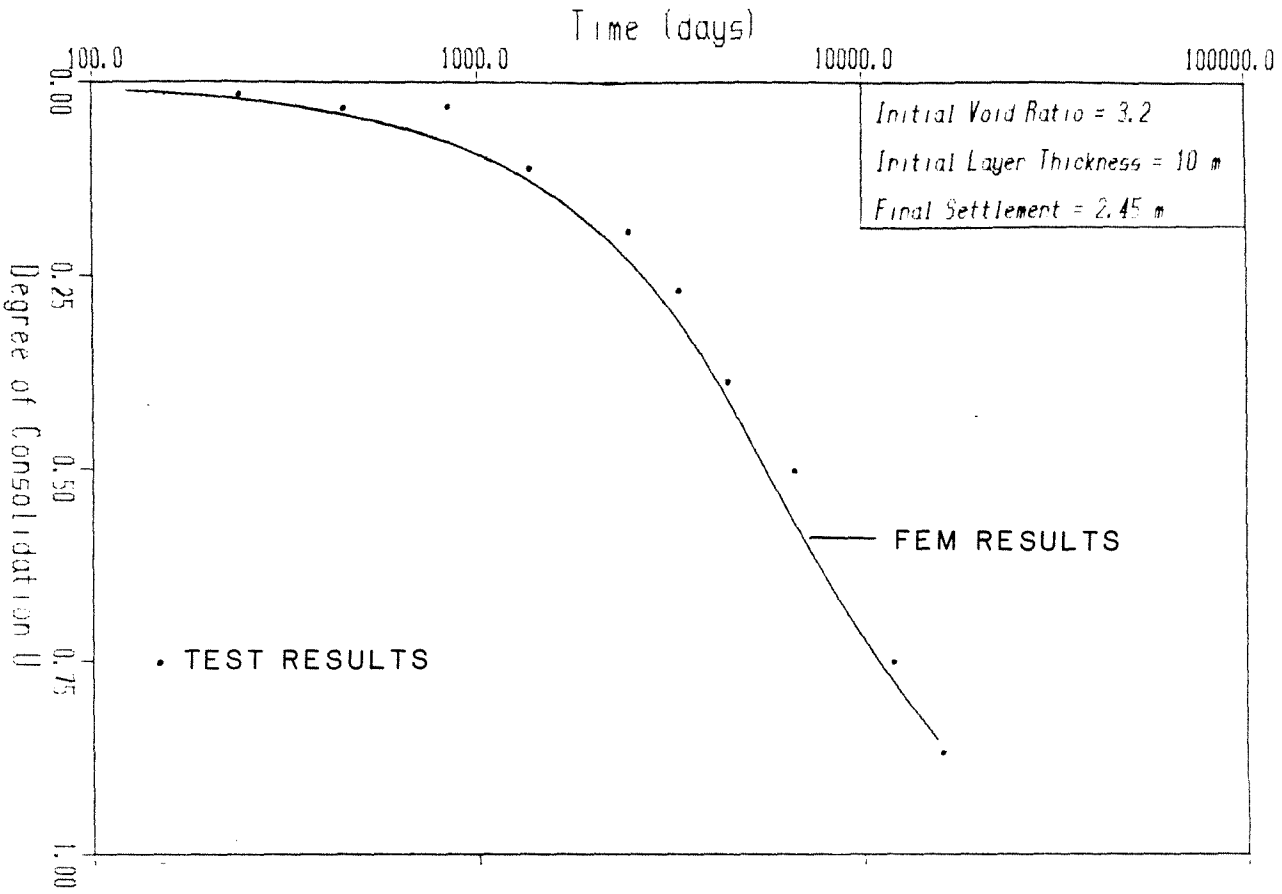

Figure 3.7 One-dimensional self-weight consolidation (singly drained) : Comparison of theoretical and experimental results (Mikasa and Takada tests)

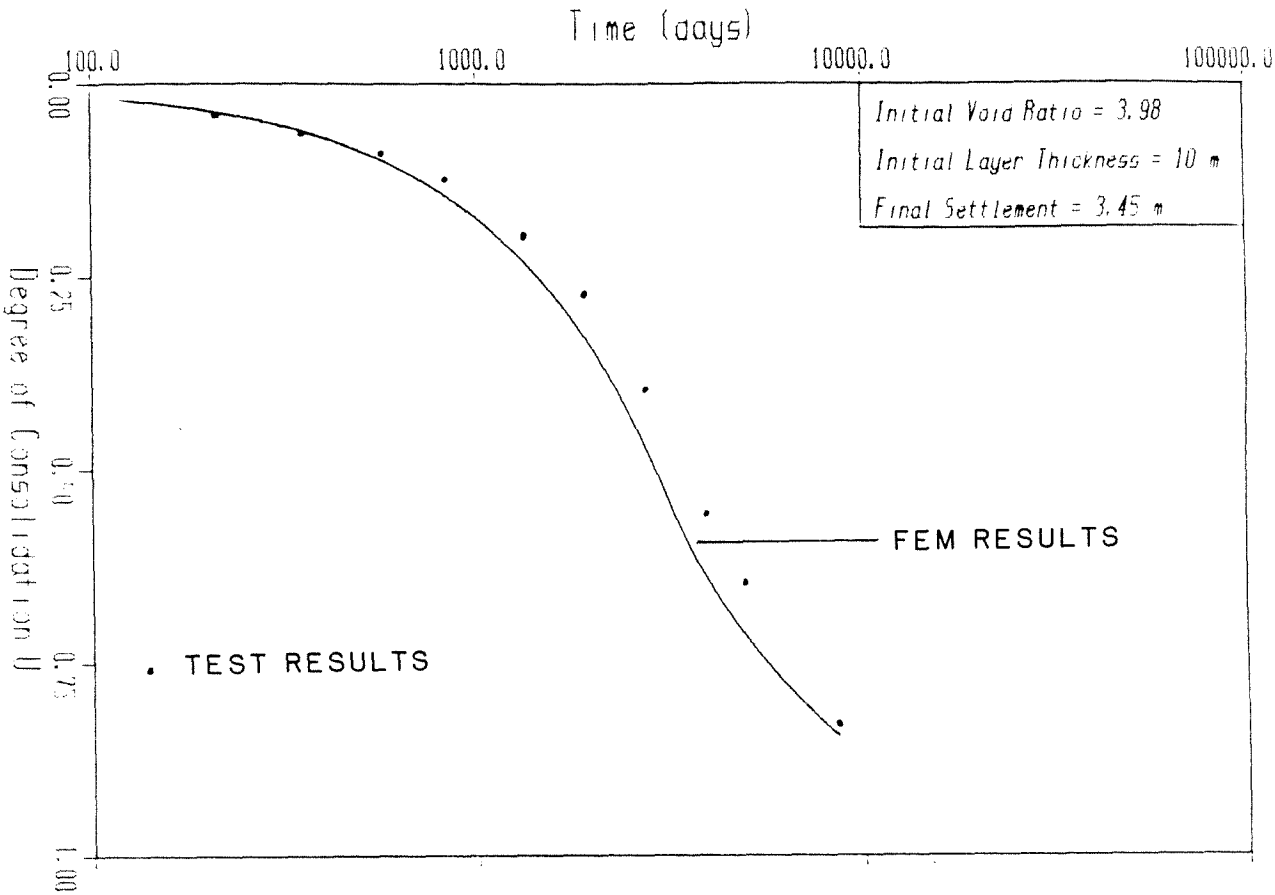

Figure 3.8 One-dimensional self-weight consolidation (singly drained) : Comparison of theoretical and experimental results (Mikasa and Takada tests)

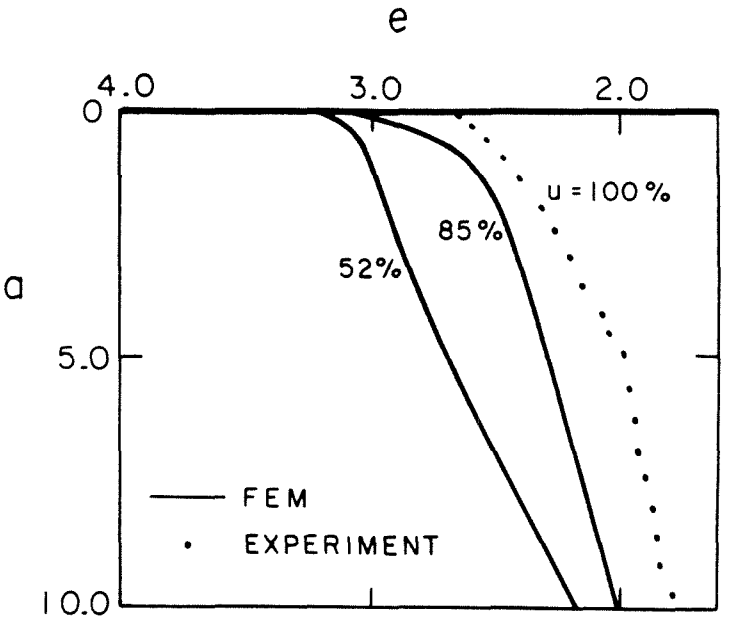

(a) $e_o = 3.20$

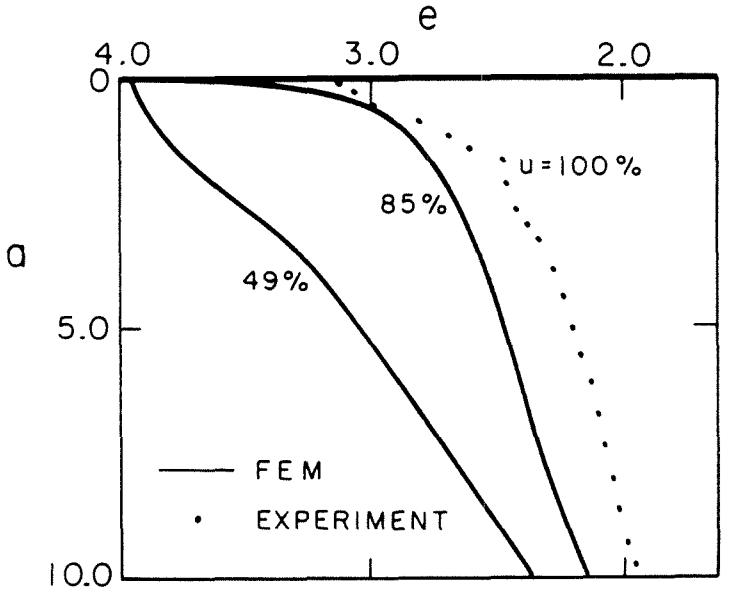

(b) $e_o = 3.98$

Figure 3.9 1-d self-weight consolidation (singly drained) Typical void ratio distribution with Lagrangian depth (in m). Experimental data shown are for 100% consolidation.
a. Initial void ratio = 3.2
b. Initial void ratio = 3.98

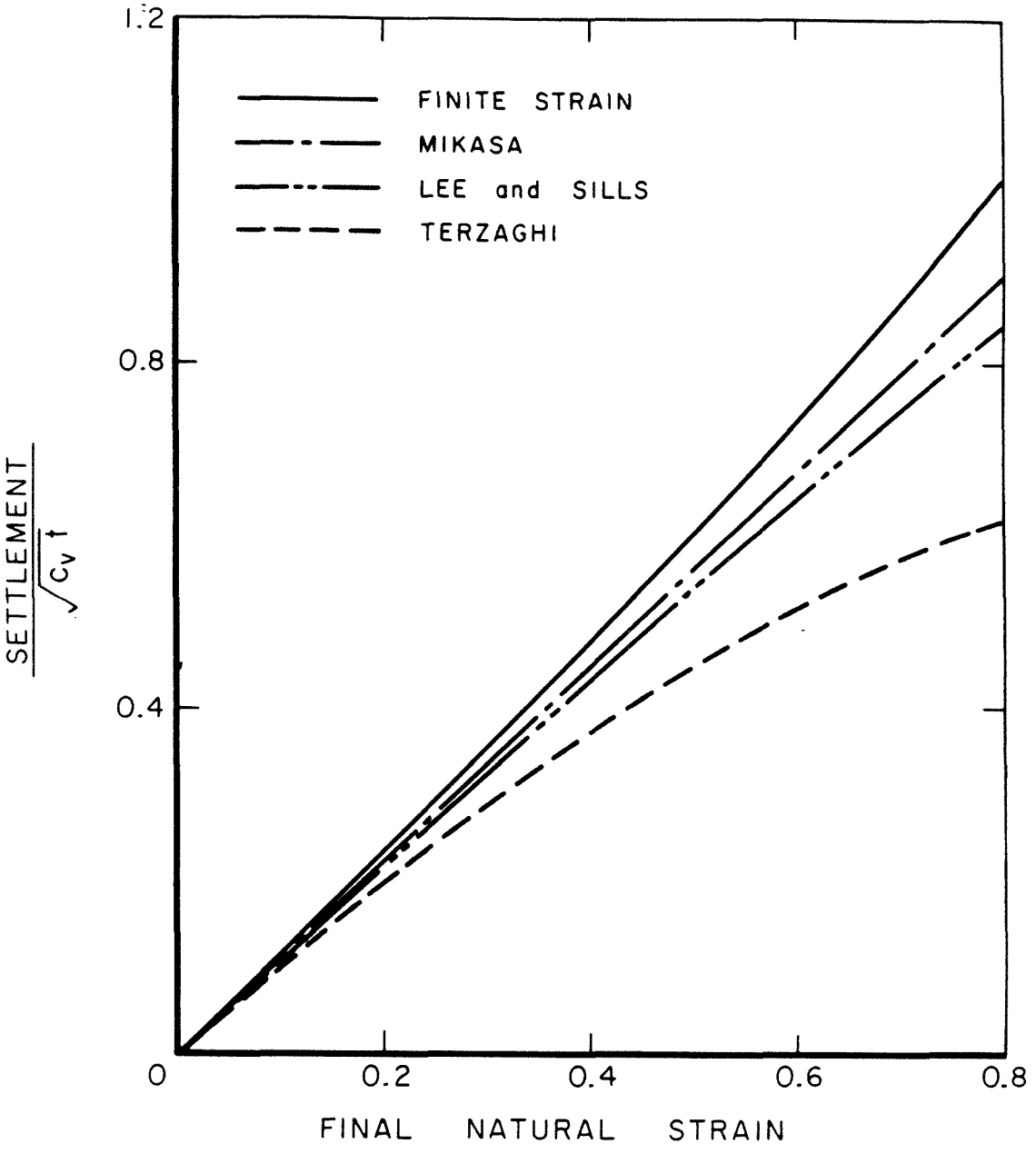

Figure 3.10 Comparison of Infinitesimal theories with exact finite strain solution for one-dimensional consolidation of a semi-infinite layer

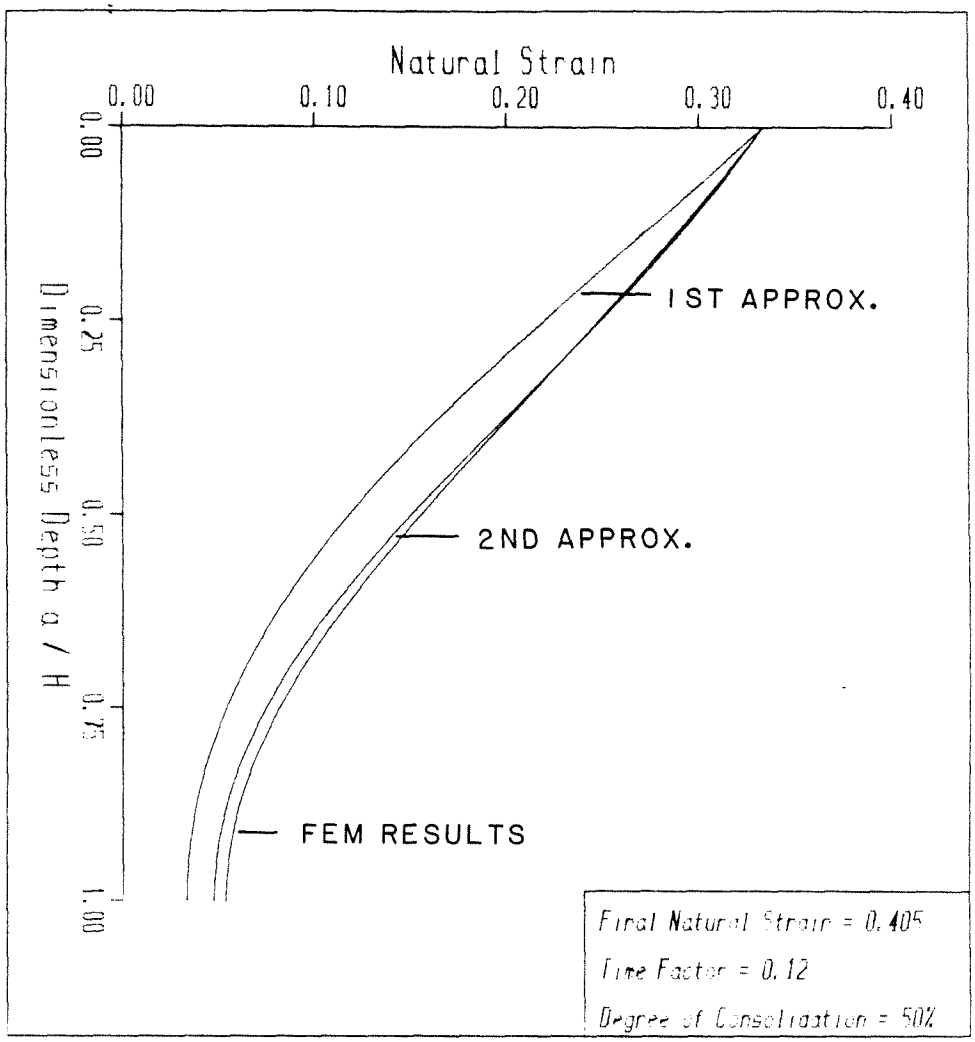

Figure 3.11 One-dimensional finite strain consolidation of a finite layer of initial thickness H : Comparison of results by perturbation method with FEM

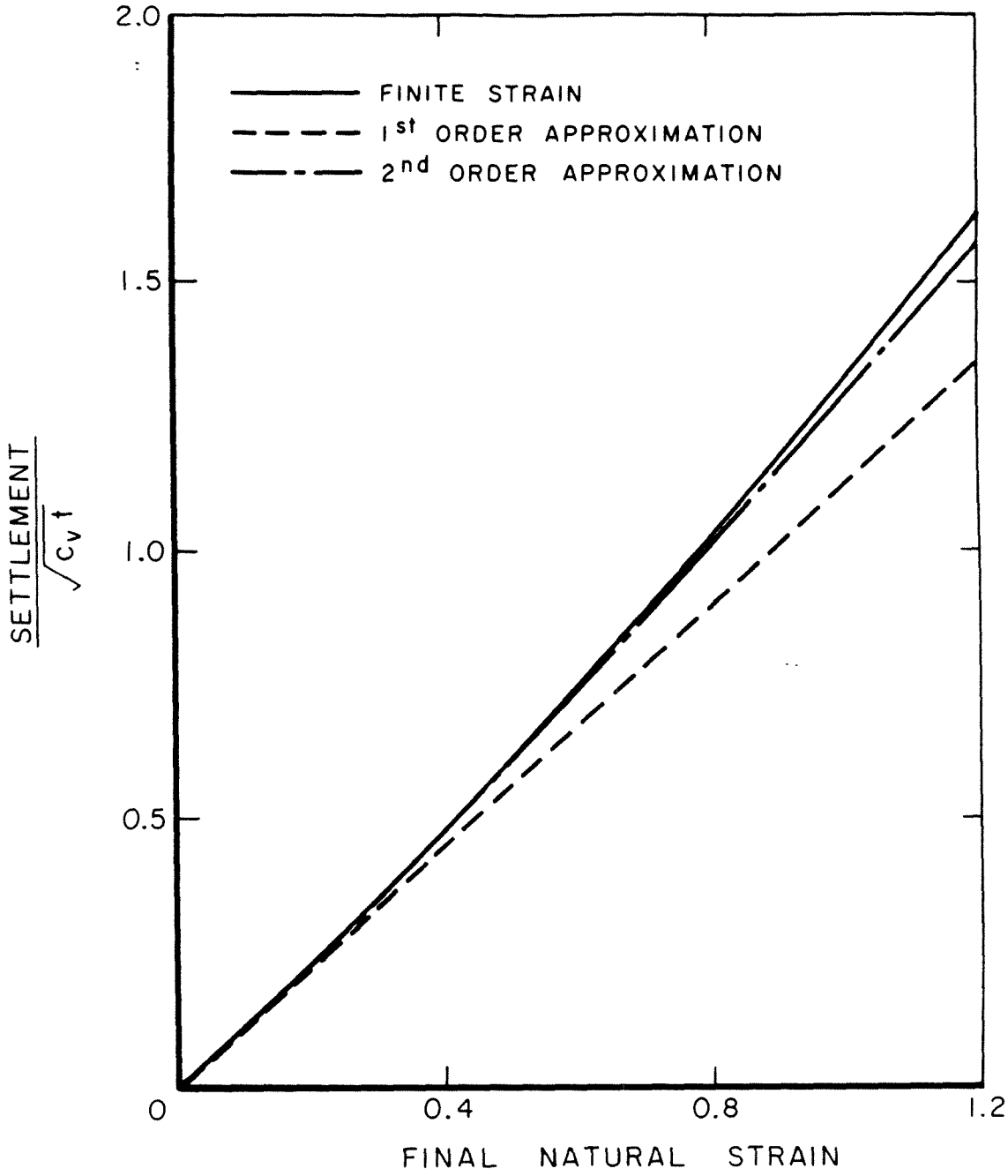

Figure 3.12 One-dimensional finite strain consolidation of a semi-infinite layer : Comparison of results of perturbation method with analytical results

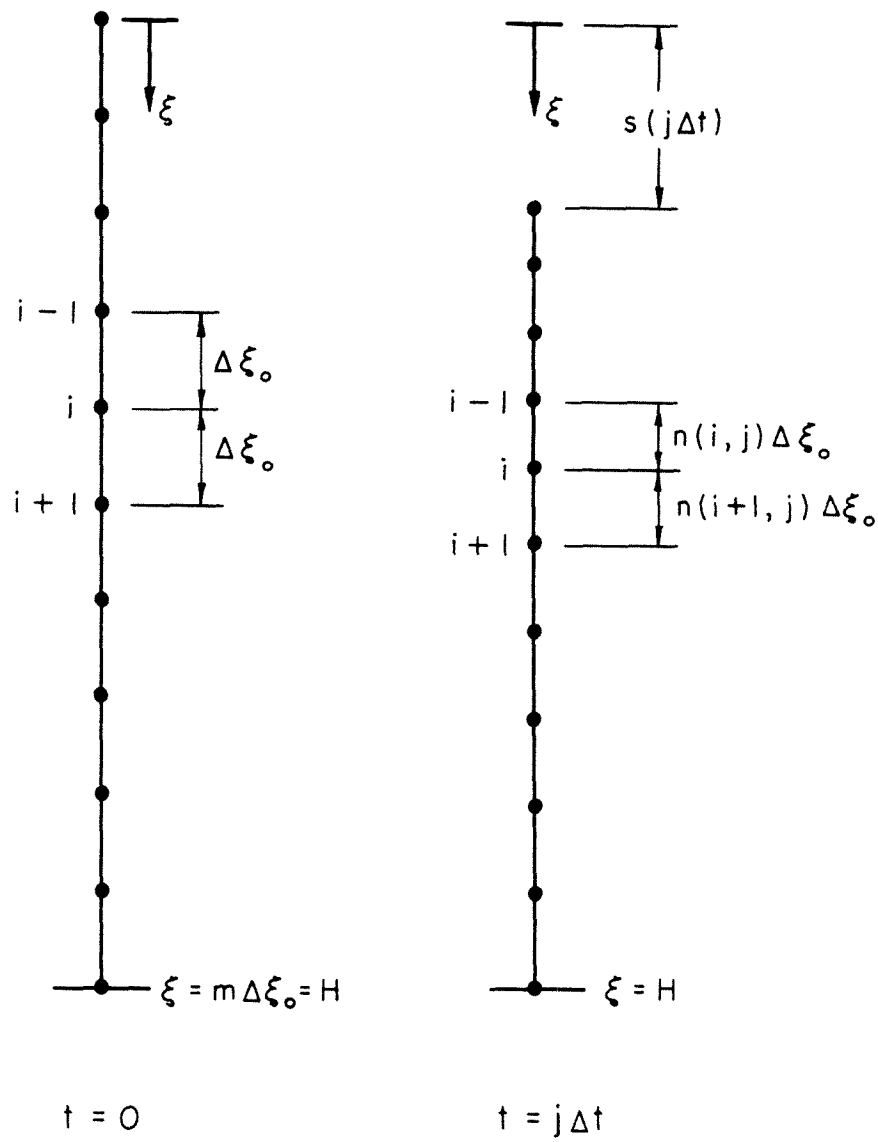

Figure 3.13 Schematic representation of mesh used for finite difference method at time = 0 and time = $j(\Delta t)$ 1-D finite strain consolidation of a finite layer

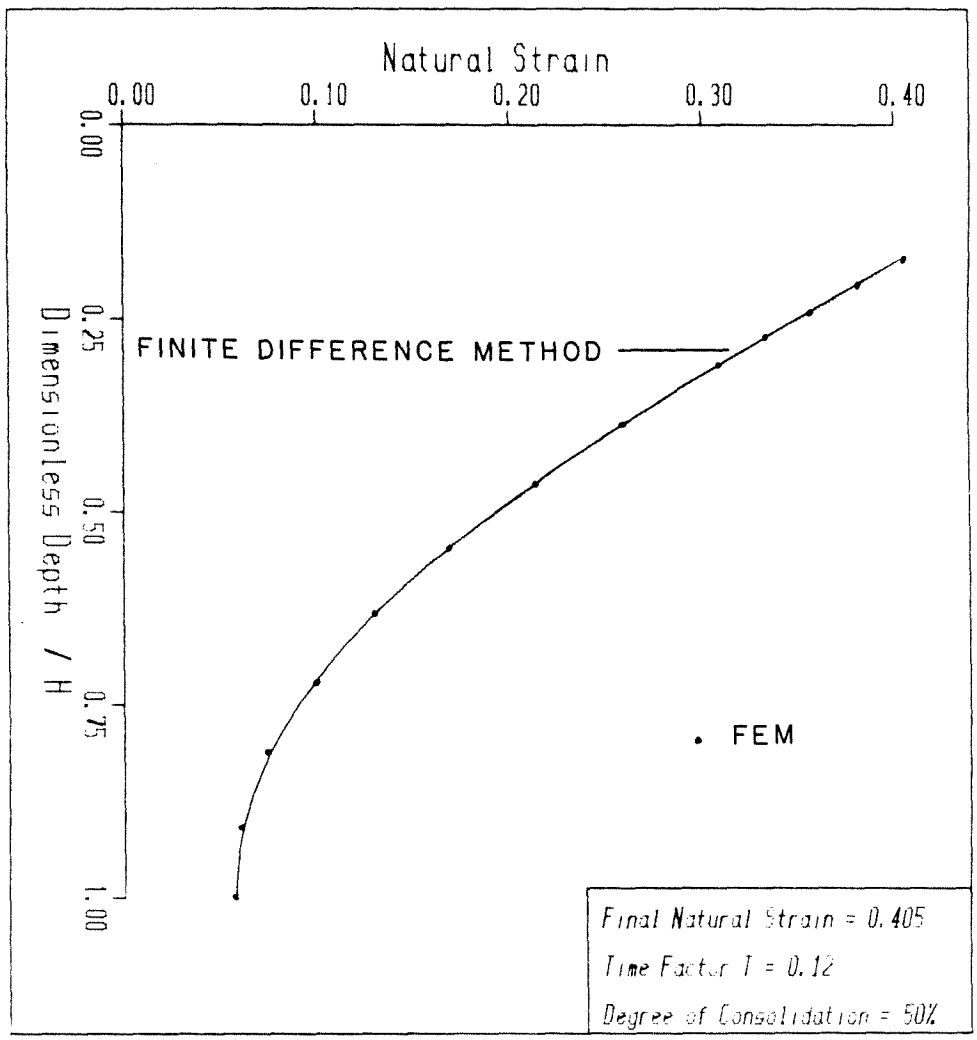

Figure 3.14 1-D finite strain consolidation of a finite layer : Comparison of results of finite difference method for an Eulerian formulation with FEM for a Lagrangian formulation

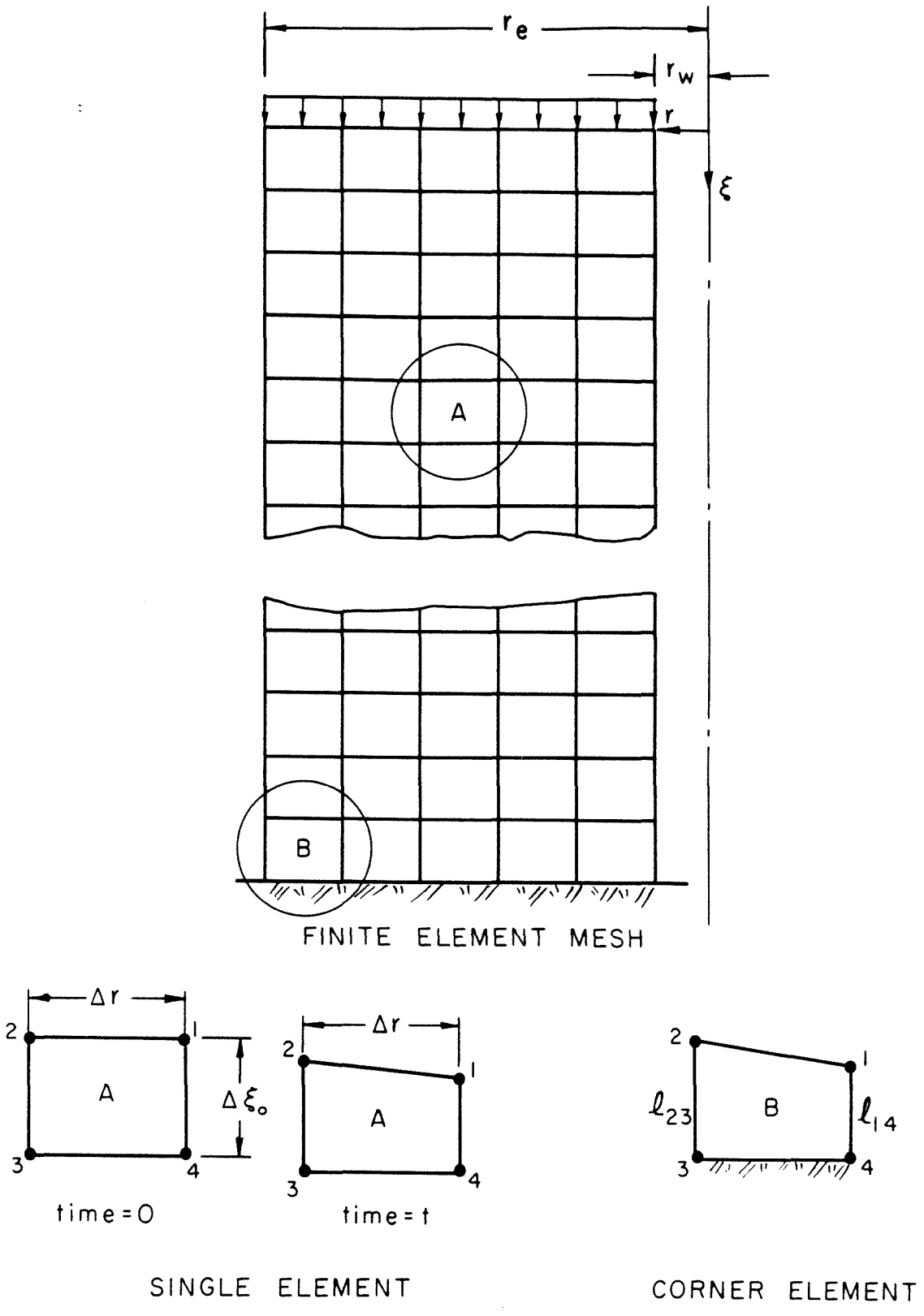

Figure 3.15 FEM mesh used for the axisymmetric problem of finite strain consolidation by a vertical drain (Eulerian formulation)

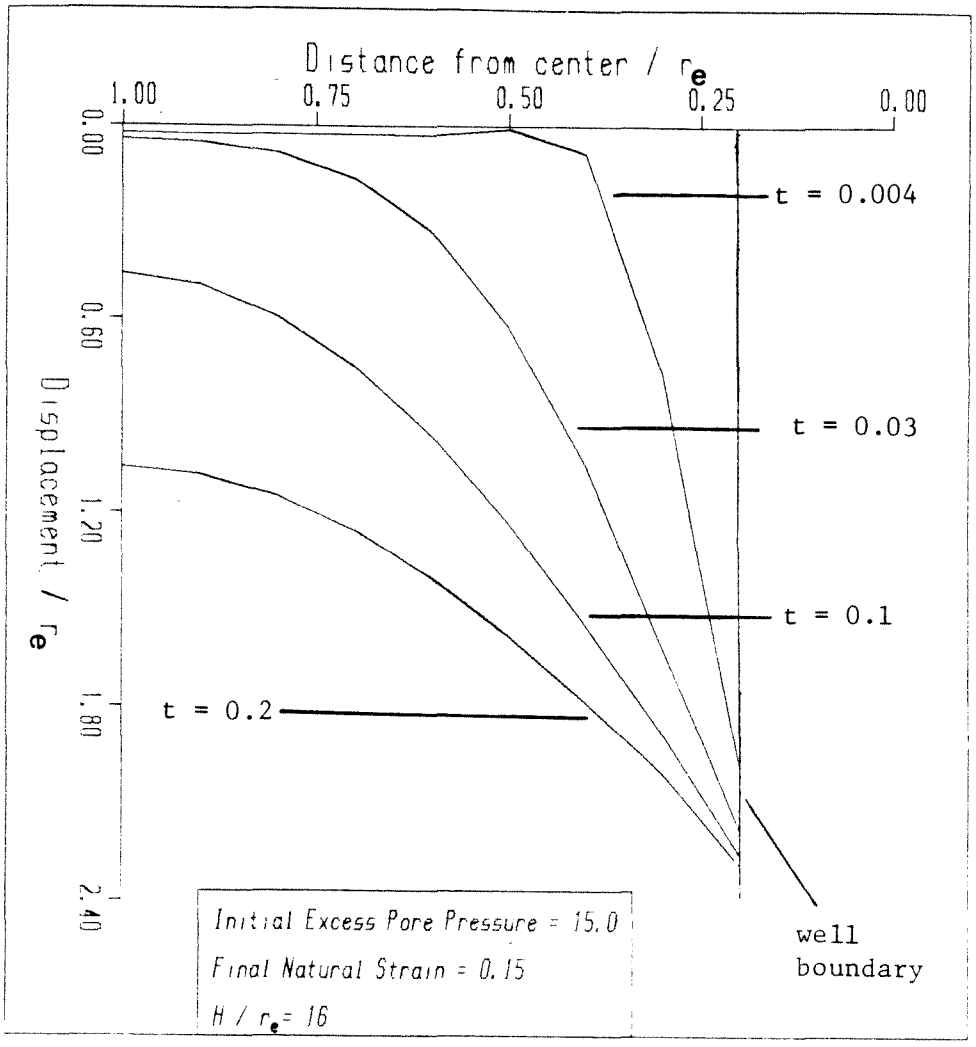

Figure 3.16 Finite strain consolidation by a vertical drain : Displacement of top surface with time

CHAPTER IV

SUMMARY AND CONCLUSIONS

4.1 SUMMARY

The problem of finite strain consolidation of soil, a two-phase medium, is investigated in this study. In the study, a consistent approach is presented that unifies all the current theories of consolidation of soil. In the process, the assumptions these theories are based on are pointed out. In particular, it is pointed out that in the Eulerian formulation of the finite strain problem, the material derivative includes a convective term. This has been neglected in many of the studies.

The question of whether the convective term is negligible is then addressed. An analytical study of the consolidation of a semi-infinite layer neglecting self-weight and assuming uniform initial conditions and constant coefficient of consolidation is carried out. Two cases (one includes convection and the other neglects it) are studied and their results compared to determine the significance of the convective effect.

Next, for the one-dimensional case, a Lagrangian finite element approach is presented that can include all non-linear geometric and material properties. This formulation is used to compute the results of self-weight consolidation tests done at University of Colorado and Osaka City University.

To make this study viable to geotechnical engineers, a regular perturbation technique applied to the formulation where the dependent variable is the natural strain is introduced.

A method that can be incorporated in a numerical scheme to account for the convection in an Eulerian formulation is next introduced. This method is demonstrated by incorporating it in a finite difference scheme to solve the one-dimensional consolidation of a finite layer and the results compared to that of a Lagrangian finite element formulation.

The method is then used in a finite element scheme to solve the consolidation of a layer accelerated by the use of vertical drains.

A number of interesting conclusions can be made from this study and these are given in the next section.

4.2 CONCLUSIONS

The finite strain consolidation theory has to be used when the settlement involved is large and self-weight effect included. This is demonstrated for the one-dimensional case where the Lagrangian finite element formulation of this theory is used to predict the results of three tests done by other researchers. The very good agreement in these cases demonstrate that the theory is a viable one. The finite element formulation allows for both material and geometric non-linearities.

In the three cases studied, it is found that the linear void ratio versus the logarithm of effective stress relation gives results that correlate with the test data very well. This is another evidence in support of this long suggested relation.

For geotechnical engineers who need a quick and reasonably accurate answer to one-dimensional consolidation, the regular perturbation technique applied to the formulation using the natural strain as the dependent variable can be used. This formulation is chosen because the errors induced in the linearization process cancel each other out. This fact is apparent for the perturbation results still agree very well with the exact solution for the consolidation of a semi-infinite layer even when the final natural strain, the variable used to form the asymptotic sequence, exceeds one.

In the analytical study of the consolidation of the semi- infinite layer, it is found that for small deformation (natural strain of order of ten percent or smaller), the convective effect is negligible. However, for larger strain, the neglect of this effect will produce a rate of settlement significantly higher than if the convective effect is not neglected. For example, when the natural strain is 80 percent, the rate of settlement when convection is neglected is 130 percent higher than if it is accounted for. Clearly, for finite strain, convection has to be accounted for.

Introduced in this study, a method based on the concept of an "equivalent control volume", is shown to be able to account for the convective effect. This method can be incorporated into both the finite difference and finite element methods. In the context of a numerical scheme, the essence of this concept is to keep the volume of solid content in an element termed the "equivalent control volume" a constant as the soil deforms.

By following this element, in actual fact, the solid phase is being tracked. Thus, the material derivative of any dependent variable in this element is the same as the time derivative since the "material path" is followed. The attractiveness of this method is that it can be used for three-dimensional problems.

Consolidation of a layer accelerated by the use of vertical drains is studied for the first time within the context of finite strain using the above method. Significant arching of the top surface is found. In practice, this will cause a redistribution of load and has to be accounted for. Also, this suggests that the significance of the Cryer-Mandel effect ought to be investigated.

REFERENCES

Ames, W.F. (1972), Nonlinear Partial Differential Equations in Engineering, Volume II, Academic Press, New York.

Atkinson, M.S. and Eldred, P.J.L. (1981), "Consolidation of Soil using Vertical Drains," Géotechnique, Vol. 31 (Proc., Third Géotechnique Symposium - Vertical Drains), pp. 33-43.

Barden, L. and Berry, P.L. (1965), "Consolidation of Normally Consolidated Clay," Proc. ASCE, SM5, pp. 15-35.

Bardet, J.P. (1983), "Application of Plasticity Theory to Soil Behavior," Soil Mechanics Laboratory Report No. SML 83-01, California Institute of Technology.

Barron, R.A. (1948), "Consolidation of Fine-Grained Soils by Drain Wells," Trans. ASCE, Vol. 113, pp. 718-742.

Bathe, K. (1982), Finite Element Procedures in Engineering Analysis, Prentice-Hall, Inglewood Cliffs.

Biot, M.A. (1941a), "General Theory of Three-Dimensional Consolidation," Journal of Applied Physics, Vol 12, February, pp. 155-164.

Biot, M.A. (1941b), "Consolidation Settlement Under a Rectangular Load Distribution," Journal of Applied Physics, Vol.12, May, pp. 426-430.

Biot, M.A. (1955), "Theory of Elasticity and Consolidation for a Porous Anisotropic Solid," Journal of Applied Physics, Vol. 26, February, pp. 182-185.

Biot, M.A. and Clingan, F.M. (1941), "Consolidation Settlement of a Soil with an Impervious Top Surface," Journal of Applied Physics, July, pp. 578-581.

Bowles, J.E. (1982), Foundation Analysis and Design, Third Edition, McGraw-Hill Book Co., New York.

Carrillo, N. (1942), "Simple Two and Three Dimensional Cases in the Theory of Consolidation of Soils," Journal of Mathematics and Physics, Vol. 21, No. 1, pp.1-5.

Carslaw, H.S. and Jaeger, J.C. (1959), Conduction of Heat in Solids, Second Edition, Oxford University Press, New York.

Carter, J.P., Booker, J.R. and Davis, E.H. (1977), "Finite Deformation of an Elasto-Plastic Soil," Int. Journal for Numerical and Analytical Methods in Geomechanics, Vol. 1, pp. 25-43.

Carter, J.P., Booker, J.R. and Small, J.C. (1979), "The Analysis of Finite Elasto-Plastic Consolidation," International Journal for Numerical and Analytical Methods in Geomechanics, Vol. 3, pp. 107-129.

Crank, J. (1975), The Mathematics of Diffusion, Second Edition, Clarendon Press, Oxford.

Croce, P., Pane, V., Znidarcic, D., Ko, H.-Y., Olsen, H.W., Schiffman, R.L. (1984), "Evaluation of Consolidation Theories by Centrifuge Modeling," Proc., Symp. on The Application of Centrifuge Modeling to Geotechnical Design, Manchester 16-18 April 1984, pp. 380-401.

Cryer, C.W. (1963), "A Comparison of the Three-Dimensional Consolidation Theories of Biot and Terzaghi," Quart. Journ. Mech. and Applied Math., Vol. XVI, Pt. 4, pp. 401-412.

Currie, I.G. (1974), Fundamental Mechanics of Fluids, McGraw-Hill Book Co., New York.

Davis, E.H. and Raymond, G.P. (1965), "A Non-linear Theory of Consolidation," Géotechnique, Vol. 15, No. 2, pp. 161-173.

Elnaggar, H.A., Krizek, R.J. and Karadi, G.M. (1973), "Effect of Non-Darcian Flow on Time Rate of Consolidation," Journal of Franklin Institute, Vol. 296, No. 5, pp. 323-337.

Fung, Y.C. (1965), Foundations of Solid Mechanics, Prentice-Hall, Inc., Englewood Cliffs, New Jersey.

Garg, S.K. and Nur, A. (1973), "Effective Stress Laws for Fluid-Saturated Porous Rocks," Journal of Geophysical Research, Vol.78, No. 26, pp. 5911-5921.

Gibson, R.E., England, G.L. and Hussey, M.J.L. (1967), "The Theory of One-Dimensional Consolidation of Saturated Clays," Géotechnique, Vol. 17, pp. 261-273.

Gibson, R.E., Schiffman, R.L. and Cargill, K.W. (1981), "The Theory of One-dimensional Consolidation of Saturated Clays. II. Finite Nonlinear Consolidation of Thick Homogeneous Layers," Can. Geotech. J., Vol. 18, pp. 280-293.

Hildebrand, F.B. (1976), Advanced Calculus for Applications, Second Edition, Prentice-Hall, Inc., Englewood Cliffs, New Jersey.

Lambe, T.W. and Whitman, R.V. (1969), Soil Mechanics, John Wiley and Sons, New York.

Lee, K-S. and Sills, G.C. (1979), "A Moving Boundary Approach to Large Strain Consolidation of a Thin Layer," Proc. Third International Conference on Numerical Methods in Geomechanics, Aachen, 2-6 April 1979, pp. 163-173.

Lee, K-S. and Sills, G.C. (1981), "The Consolidation of a Soil Stratum, Including Self-Weight Effects and Large Strains; Int. Journal for Numerical and Analytical Methods in Geomechanics, Vol. 5, pp. 405-428.

Mandel, J, (1953), "Consolidation Des Sols (Etude Mathématique)," Géotechnique, Vol. 3, No.7, pp. 287-299.

Mikasa, M. (1965), "The Consolidation of Soft Clay - A New Consolidation Theory and Its Application," Civil Engineering in Japan, pp. 21-26.

Mikasa, M. and Ohnishi, H. (1981), "Soil Improvement by Dewatering in Osaka South Port," Proc. Sixth International Conference on Soils Mechanics and Found. Engrng., Case History Volume, 1981, pp. 639-664.

Mikasa, M. and Takada, N. (1984), "Selfweight Consolidation of very Soft Clay by Centrifuge," Proc., ASCE Sponsored Symposium on Sedimentation Consolidation Models, 1984 ASCE Convention in San Francisco, California.

Mitchell, J.M. (1976), Fundamentals of Soil Behaviour, John Wiley and Sons, Inc., New York, pp. 121-140.

Monte, J.L. and Krizek, R.J. (1976), "One-Dimensional Mathematical Model for Large-Strain Consolidation," Géotechnique, Vol. 26, No. 3, pp. 495-510.

Pane, V., Croce, P., Znidarcic, D., Ko, H.Y., Olsen, H.W. and R.L. Schiffman (1983), "Effects of Consolidation on Permeability Measurements for Soft Clay," Géotechnique, Vol. 33, pp. 67-72.

Pane, V. and Schiffman, R.L. (1981), "A Comparison between Two Theories of Finite Strain Consolidation," Soils and Foundations, Jap. Soc. of Soil Mech. and Found. Engrng., Vol. 21, No. 4, pp. 81-84.

Rendulic, L. (1936), "Porenziffer und Porenwasserdruck in Toren," Der Bauingenieur, Vol. 17, pp. 559-564.

Richart, F.E. (1959), "Review of the Theories for Sand Drains," Trans. ASCE, Vol 124, pp. 709-736.

Schiffman, R.L. (1970), "The Stress Components of a Porous Medium," Journal of Geophysical Research, Vol. 75, No. 20, pp. 4035-4038.

Schiffman, R.L., Pane, V. and Gibson, R.E. (1984), "An Overview of Nonlinear Finite Strain Sedimentation and Consolidation," ASCE Convention in San Francisco, California, pp. 1-29.

Schofield, A.N. and Wroth, C.P. (1968), Critical State Soil Mechanics, McGraw-Hill.

Scott, R.F. (1963), Principles of Soil Mechanics, Addison-Wesley Publishing Co., Reading, Massachusetts.

Taylor, D.W. (1948), Fundamentals of Soil Mechanics, John Wiley and Sons, Inc., New York.

Terzaghi, K. (1923), "Die Berechnung der Durchlassigkeitsziffer des Tones aus dem Verlauf der Hydrodynamischen Spannungserscheinungen, Akademie der Wissenschaften in Wien, Sitzungsberichte, Math. Naturw. Klasse, Part IIa, Vol. 132, No. 3-4, pp. 125-138.

Terzaghi, K. (1925), Erdbaumechanik auf bodenphysikalischer Grundlage, Leipzig, Deuticke.

Terzaghi, K. (1943), Theoretical Soil Mechanics, John Wiley and Sons, Inc., New York.

Wallis, B.G. (1969), One-dimensional Two-phase Flow, McGraw-Hill Book Company, New York.

Yoshikuni, H. and Nakanodo (1974), H., "Consolidation of Soils by Vertical Drain Wells with Finite Permeability," Soils and Foundations, Jap. Soc. of Soil Mech. and Found. Engrng., Vol. 14, No. 2, pp. 35-46.

Zienkiewicz, O.C. (1977), The Finite Element Method, Third Edition, McGraw-Hill Book Co. (UK) Ltd., London.

APPENDIX A

NOTATION

a	Lagrangian coordinates
c_v	Coefficient of consolidation
e	Void ratio
e_o	Initial void ratio
e_f	Final void ratio
H	Thickness of layer
k	Coefficient of permeability
m_v	Coefficient of compressibility
n	Porosity
N_i	Shape functions
p	Pore pressure
r	Radial polar coordinate
s	Settlement of top surface
T	Time factor = $\frac{c_v t}{H^2}$
t	Time
u	Excess pore pressure
u_s	Hydrostatic pore pressure
v	Approach velocity
v_f	Fluid velocity
v_s	Velocity of solid phase
V_s	Equivalent control volume of solid content

APPENDIX A

NOTATION (CONT'D)

z	Equivalent length of solid content (a coordinate in Lagrangian frame)
γ_f	Unit weight of fluid
γ_s	Unit weight of solid
ε	Natural strain
ε_f	Final natural strain
ζ	Compression ratio
ξ	Eulerian coordinate
θ	Volumetric strain
ρ_s	Density of solid
ρ_f	Density of fluid
σ	Total stress
σ'	Effective stress

CHAPTER I

INTRODUCTION

Testing of reduced scale models of soil structures in a centrifuge has gained wide acceptance in recent years. Just in the last year, three international symposiums* on geotechnical centrifuge modeling were held. Researchers have used the centrifuge to study a wide variety of soil problems; an idea of the problems studied can be found in the survey done by Cheney (1984)**

Many of the studies were on static or quasi-static problems. Scaling relations for such problems have been established (see Appendix A) based on the assumption that the centrifuge produces an acceleration field equivalent to that of an ng planet where n is the linear dimension scaling factor (Rocha, 1957; Roscoe, 1968; Pokrovsky, 1975). Since centrifugal acceleration is perpendicular to the axis of rotation and proportional to the distance from the axis, the acceleration field in the centrifuge diverges from that of an ng planet. However, if the size of the test model is sufficiently small with respect to the centrifuge dimension, such divergence is not significant for most soil tests (Pokrovsky, 1975; Schofield, 1980).

Dynamic tests of soil models in the centrifuge where the soil is considered as a single phase material have also been performed (Liu, et al., 1978; Ortiz, 1982 and Hushmand, 1983). These comprise mostly

---

* : The symposiums were held in Tokyo, Japan; Manchester, UK and Davis, USA in 1984.

** : References given at the end of thesis.

dynamic shaking of structures in dry soil. In these tests, dynamic effects dominate the mechanisms involved. For this class of problems, the deviation from an ng planet due to Coriolis acceleration has to be considered. For most of these dynamic tests, the soil does not move much and it has been shown that such deviation has a small effect (Pokrovsky, 1975 and Schofield, 1980) and is in fact negligible. For tests where the soil may have significant relative velocity with respect to the bucket such as model tests of landslides, the deviation may not be negligible and needs to be considered. Scaling relations have been established on the basis that Coriolis acceleration is negligible (Pokrovsky, 1975) and are given in Appendix A.

A third class of tests, also dynamic, done in the centrifuge is cratering experiments (Schmidt and Holsapple, 1980, and Holsapple and Schmidt, 1982). A basic assumption in the establishment of scaling relations for these experiments is that the position vector of a soil mass in the model is scaled by a scalar to obtain the position vector of the homogeneous soil mass in the prototype (Schmidt and Holsapple, 1980). This assumption neglects the effects due to Coriolis acceleration. Since Coriolis acceleration is important in the model whereas there is no Coriolis acceleration in the prototype except for very large craters, the trajectories of homologous soil masses will be different and the associated position vectors will be vectorially different. Thus the above assumption is invalid.

The centrifuge has also been used to study the behavior of soil when its response as a two-phase medium is important (Goodings, 1984; and Mikasa and Takada, 1984). A significant aspect of such tests is the flow of water through the soil. Here, it is assumed that Darcy's law is obeyed in both the model and prototype. Based on this assumption, scaling relations have been established for consolidation tests (Mikasa and Takada, 1984) and seepage flow through dams (Goodings, 1984; and Cargill and Ko, 1983).

In recent years, many researchers have also used the centrifuge to study the phenomenon of dynamically induced (earthquake induced) liquefaction (reduction of effective stresses to zero) in soils (Lambe and Whitman, 1982; Dean and Schofield, 1983; Schofield and Venter, 1984; and Lee and Schofield, 1984). This is a very difficult problem at full scale and the actual mechanism of liquefaction is still a much-debated topic. When a soil structure is subjected to an earthquake, cyclic shear stress is generated. For sand, this will cause the pore pressure to increase. Simultaneously, diffusion will occur and this will cause a decrease in pore pressure. For sufficiently fine sand, this decrease will be less than the dynamically induced pore pressure. A net build-up in pore pressure results. If the build-up is large enough to bring the effective stresses to zero, liquefaction ensues. After liquefaction has occurred, a sedimentation process dominates since the soil has fluidized. This is demonstrated by experimental data which show that pore pressure is constant with time immediately after liquefaction has occurred (Dean and Schofield, 1983).

According to current understanding of centrifuge scaling relations (see Appendix A), if a model is subjected to an acceleration ng, dynamically induced generation of pore pressure occurs n times slower than the dissipation due to diffusion. This presents a difficulty for liquefaction experiments where pore pressures are simultaneously generated dynamically and dissipated by diffusion. Since Darcy's law is assumed to be valid which implies that diffusion depends linearly on the viscosity of the fluid, one current practice in such cases is to use a model fluid of viscosity n times that of the prototype. With such a fluid, it is intended that the diffusion process will be slowed down n times. Superficially, this seems to be a reasonable solution provided the scaling relations currently used (Appendix A) are correct. The concept of "modeling of models" sometimes is used to justify these scaling relations (Lambe and Whitman, 1982 and Cargill and Ko, 1983). In this approach, a series of tests on models of different scales is conducted at different accelerations in the centrifuge. The tests are scaled so that each represents the same prototype. Results from each test are then scaled according to the scaling relations adopted. If the scaled values for these tests match, it is deduced that the behavior of the centrifuge model satisfies similarity requirements and the scaling relations adopted are indeed correct. So far, adoption of this concept has not produced any conclusive results on the validity of these scaling relations (Lambe and Whitman, 1982 and Cargill and Ko, 1983). Even if similarity is evident in these tests, it seems that only similarity of behaviors of different models in a centrifuge has been established and

not between the model and uniform g-field prototype behaviors.

Clearly, many questions about similarity requirements for testing of models in a centrifuge still remain unresolved, particularly for tests where the soil is saturated and different dynamic processes are involved such as in liquefaction tests and seepage flows through dams. It is natural then to ask how correct are the current scaling relations (Appendix A)? What errors are generated in extending the results of model tests to the prototype?

It is the purpose of this study to examine these questions in detail, with particular reference to the problem of liquefaction. Conceptually, when a centrifuge is used to test models, two simulations are involved. First, the behavior of the prototype structure at 1g is assumed to be similar to that of the model tested in a uniform ng gravitational field. Then the centrifuge is assumed to produce an acceleration field equivalent to the uniform ng gravitational field. Both assumptions need to be valid before a model can be used with confidence to study prototype behavior. The work to be described subsequently is done within this conceptual framework.

CHAPTER II

MODELING THE POST-LIQUEFACTION PROCESS FOR SCALING STUDIES

2.1 INTRODUCTION

To examine the similarity requirement and to derive the correct scaling relations for the modeling of liquefaction in a centrifuge, the dynamics of liquefaction must be considered. Since the mechanics of liquefaction are not yet well understood, a general formulation cannot be attempted at present; in consequence, an analytical study of a simplified situation is carried out to provide a first level of understanding of this complicated problem.

Complete liquefaction herein is understood to mean that the soil particles have lost contact with each other during the process. Thus, the effective stresses are reduced to zero. Hence, on liquefaction, the particles are suspended in the fluid and thereafter settle. It follows that pore water pressure decay and surface settlement following liquefaction are not represented by a consolidation process but rather by the mechanics of sedimentation. This is the mechanism to be studied here. Even this, sedimentation of a fluidized soil, is complicated to represent. For the purpose of this study which is to examine similarity requirements and check current scaling relations (Appendix A), the dynamics of a single particle moving in a fluid is examined as a first level of understanding.

2.2 FORMULATION OF THE PROBLEM

We will consider the single sphere moving in a fluid under two different conditions. They are:

(i) A sphere settling in a uniform ng field. (If n = 1, it represents the prototype situation.)

(ii) A sphere settling in a bucket subjected to centrifugal motion such that the centrifuge acceleration at the initial position of the sphere is ng ($\omega^2 R = ng$)*.

In both cases, the particle starts from rest with respect to the container surrounding it.

2.2.1 A Sphere Settling in a Fluid in a Uniform ng Field

With no initial velocity of the particle relative to the fluid, there is only one space coordinate, x, and the governing equation of motion for the particle is:

$$v_s(\rho_s-\rho_\ell)ng - C_D \cdot \frac{1}{2}\rho_\ell \pi a^2\left(\frac{dx}{dt}\right)^2 = v_s\left(\frac{\rho_\ell}{2} + \rho_s\right)\frac{d^2x}{dt^2} \quad . \qquad (2.1)$$

The initial conditions are: $x(0) = 0$, $\left.\frac{dx}{dt}\right|_{x=0} = 0$.

A number of assumptions were made to obtain equation (2.1). They are:

(a) The added mass has been taken to be $\frac{1}{2} v_s \rho_\ell$ which is the exact value for rectilinear motion of a sphere in an ideal fluid

* : List of symbols given in Appendix B.

occupying an infinite domain (Yih, 1977). The assumption of an infinite domain is reasonable since this study concerns a sphere of diameter 1mm or less in a container tens of centimeters in dimension. Very difficult to assess is the assumption of an ideal fluid since the fluid used is viscous. Current data on this, the effect of viscosity on the added mass, are limited and contradictory (Brennen, 1982). In this study, the potential flow value is chosen. It is recognized that this may be inaccurate and that pathological behavior might occur in certain ranges of frequency (or typical times of acceleration) and Reynolds number. However, it is the only definite information available.

(b) An approximate fitting of the sphere drag coefficient versus Reynolds number (Re) curve (Schlichting, 1979) was employed. The fit is given for different ranges of Re as follows:

$Re < 1.0$

$$C_D = \frac{24.0}{Re}\ 1.0+0.1875Re) \text{ where } Re = \frac{2\rho_f a}{\mu}\frac{dx}{dt}$$

$1.0 < Re < 2000.0$

$$C_D = 28.5 - 24.0\ \ell n\ Re + 9.176(\ell nRe)^2 \qquad (2.2)$$

$$- 1.828\ (\ell nRe)^3 + 0.1819\ (\ell nRe)^4 - 0.007099\ (\ell nRe)^5$$

$Re > 2000.0$

$C_D = 0.40$.

It is recognized that the above data come from experiments on a sphere in steady rectilinear motion. Because of this, later on in the numerical analysis of equation (2.1), the problem has to be treated as "quasi-steady" between time steps.

2.2.2 Sphere in a Fluid Subjected to Centrifugal Motion

As shown in Figure 2.1, A, the position of a particle at time t_1 will be observed from a frame of reference (the centrifuge model frame) attached to B, a point fixed to the centrifuge bucket. This frame of reference rotates with the same angular velocity as B about the vertical axis of the centrifuge. The origin is at B, the x-axis is taken perpendicular to the bucket base, and the y-axis is perpendicular to the x-axis.

Analysis gives the acceleration of A, $\underset{\sim}{a}_A$, with respect to an inertia frame of reference (Meriam, 1971) as follows:

$$\underset{\sim}{a}_A = \left(\frac{d^2x}{dt^2} - \omega^2 R - \omega^2 x - 2\omega \frac{dy}{dt}\right)\underset{\sim}{i} + \left(\frac{d^2y}{dt^2} - \omega^2 y + 2\omega \frac{dx}{dt}\right)\underset{\sim}{j} \quad . \tag{2.3}$$

The equation of motion is now given by:

$$\begin{aligned} m_s \underset{\sim}{a}_A + m_a\left(\frac{d^2x}{dt^2}\underset{\sim}{i} + \frac{d^2y}{dt^2}\right)\underset{\sim}{j} &= -\omega^2 \rho_\ell v_s \left[(R+x)\underset{\sim}{i} + y\underset{\sim}{j}\right] \\ - C_D \cdot \frac{1}{2}\rho_\ell \pi a^2 &\left[\left(\frac{dx}{dt}\right)^2 + \left(\frac{dy}{dt}\right)^2\right]^{1/2} \left[\frac{dx}{dt}\underset{\sim}{i} + \frac{dy}{dt}\underset{\sim}{j}\right] \quad . \end{aligned} \tag{2.4}$$

The assumptions discussed with reference to equation (2.1) were also used here. A number of other assumptions have also been made as follows to obtain equation (2.4).

(a) It is assumed that the radius of the sphere is very small compared to the length of the centrifuge arm. This is usually valid for soil tests as the centrifuge arm generally is 1m or longer compared to particle sizes of 1mm or less. Thus, we can consider the mass and the viscous reaction force to be concentrated at the center of the sphere.

(b) In general, there will be some rotation of the sphere, but it is not expected to be appreciable. Thus, any effect due to rotation of the sphere is assumed to be negligible.

(c) In computing the drag force, it is assumed that the form obtained for rectilinear motion is still applicable. At each instant, the velocity of the particle relative to the moving frame is used to compute the Reynolds number and the associated drag coefficient. The drag force is then computed and is assumed to act in a direction opposite to the velocity.

Using equation (2.3) for $\underset{\sim}{a}_A$ in equation (2.4), we have:

in the x-direction,

$$v_s\left(\rho_s + \frac{\rho_\ell}{2}\right)\frac{d^2x}{dt^2} + C_D \cdot \frac{1}{2}\rho_\ell \pi a^2\left(\left(\frac{dx}{dt}\right)^2 + \left(\frac{dy}{dt}\right)^2\right)^{1/2}\frac{dx}{dt}$$
$$- \omega^2 v_s(\rho_s-\rho_\ell)x = v_s(\rho_s-\rho_\ell)\omega^2 R + v_s\rho_s \cdot 2\omega\frac{dy}{dt} \qquad (2.5)$$

and in the y-direction,

$$v_s\left(\rho_s + \frac{\rho_\ell}{2}\right)\frac{d^2y}{dt^2} + C_D \cdot \frac{1}{2}\rho_\ell \pi a^2\left(\left(\frac{dx}{dt}\right)^2 + \left(\frac{dy}{dt}\right)^2\right)^{1/2}\frac{dy}{dt}$$
$$- \omega^2 v_s(\rho_s-\rho_\ell)y = -v_s\rho_s \cdot 2\omega\frac{dx}{dt} \quad . \qquad (2.6)$$

The drag coefficient functions given in equation (2.2) are again used for C_D.

2.3 NUMERICAL METHODS

To solve equations (2.1), and (2.5) and (2.6), the Kutta-Simpson's method (Hildebrand, 1976) for a system of first-order differential equations is used. Here, for equations (2.5) and (2.6)

$$\frac{dx}{dt} = x_1 \qquad (2.7)$$

$$\frac{dy}{dt} = y_1 \qquad (2.8)$$

so that equations (2.5) and (2.6) become, respectively,

$$\frac{dx_1}{dt} = \left(\frac{\rho_s-\rho_\ell}{(\rho_s+\rho_\ell/2)}\right)\omega^2(R+x) + \left(\frac{2\rho_s}{(\rho_s+\rho_\ell/2)}\right)\omega y_1 - C_D \cdot \left(\frac{\frac{1}{2}\rho_\ell \pi a^2}{V_s(\rho_s+\rho_\ell/2)}\right)(x_1^2 + y_1^2)^{1/2} x_1 \tag{2.9}$$

$$\frac{dy_1}{dt} = \left(\frac{\rho_s-\rho_\ell}{\rho_s+\rho_\ell/2}\right)\omega^2 y - \left(\frac{2\rho_s}{(\rho_s+\rho_\ell/2)}\right)\omega x_1 - C_D\left(\frac{\frac{1}{2}\rho_\ell \pi a^2}{V_s(\rho_s+\rho_\ell/2)}\right)(x_1^2 + y_1^2)^{1/2} y_1 \quad . \tag{2.10}$$

Equations (2.7) to (2.10) constitute a system of first-order equations to be solved by the Kutta-Simpson's method. Equation (2.1) can be rewritten as a system of two first-order equations in a similar manner.

2.4 VERIFICATION OF NUMERICAL ALGORITHM

The only case where equations (2.5) and (2.6) can be solved analytically is when the "fluid" is a vacuum. For this problem, $\rho_\ell = 0$. Using the Laplace Transform Method in this case, the solutions to equations (2.5) and (2.6) are:

$$x = R(\cos \omega t + \omega t \sin \omega t - 1) \tag{2.11}$$

and

$$y = R(\omega t \cos \omega t - \sin \omega t) \quad . \tag{2.12}$$

However (see Fig. 2.1), from the flight path of the released particle (a straight line perpendicular to the radius of the initial particle position since the "fluid" is a vacuum) and the trajectory of the bucket

(hence that of the moving reference frame), the motion of the released particle with respect to the moving frame can be found geometrically. It is described by equations (2.11) and (2.12) without recourse to equations (2.5) and (2.6). Thus, the correctness of equation (2.3) for the acceleration term is assured.

Equations (2.5) and (2.6) are solved using the Kutta-Simpson's method and the results compared to that from equations (2.11) and (2.12) (see Figure 2.2). It appears that the numerical algorithm used is indeed correct.

As a rough check on the validity of the solutions when the fluid is not a vacuum, one displacement solution (an x versus y plot) is compared with an actual particle flight path photographed (see Plate 1) at the Tokyo Institute of Technology (Kimura et al., 1982) for the case where the fluid is air. The researchers at Tokyo Institute of Technology were trying to construct a dry sand embankment while the bucket was in flight. The photograph was taken during the construction and it showed the flight path of a stream of particles. If there were no particle interaction and the air were still, then this flight path would be the same as the trajectory of a single particle. Figure 2.3 compares the calculated flight path with the actual flight path. It is seen that the expected interactions do not seem to play a substantial part in modifying the single particle trajectory. The numerical solutions obtained above can thus be used in the placement of soil structures in flight, which, as the researchers at Tokyo Institute of Technology have found, is a difficult problem.

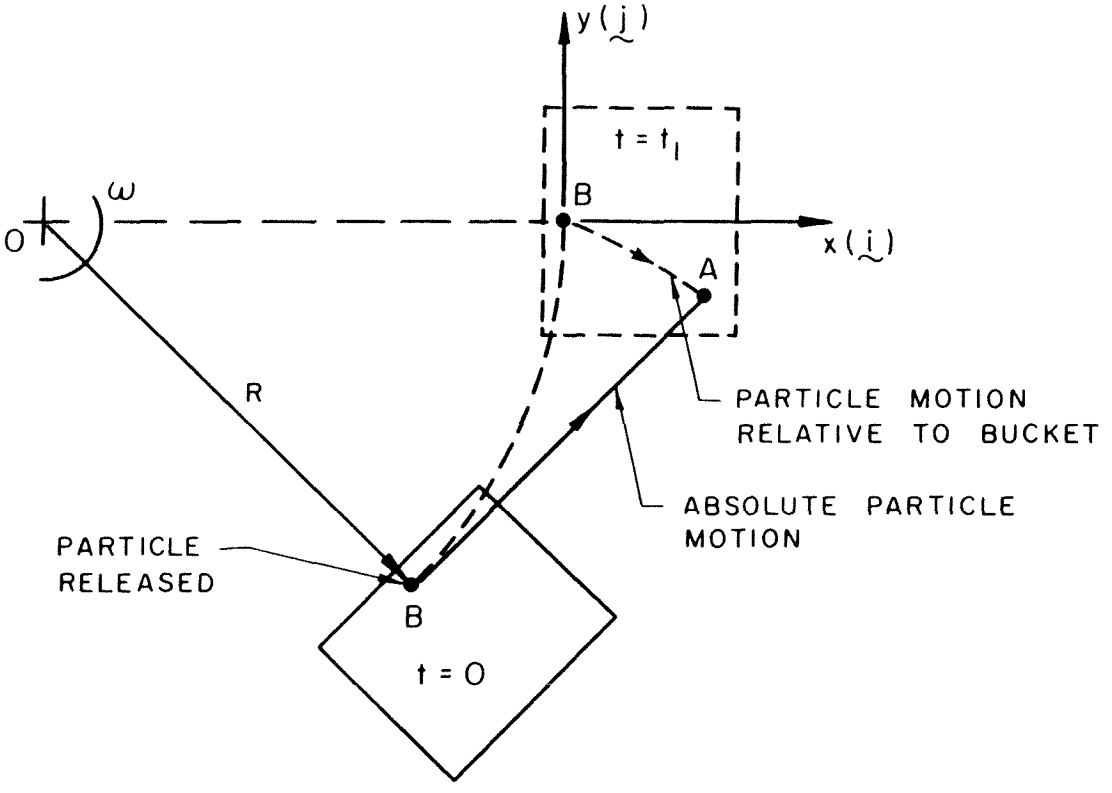

Figure 2.1 Reference frame for a particle's motion in a centrifuge

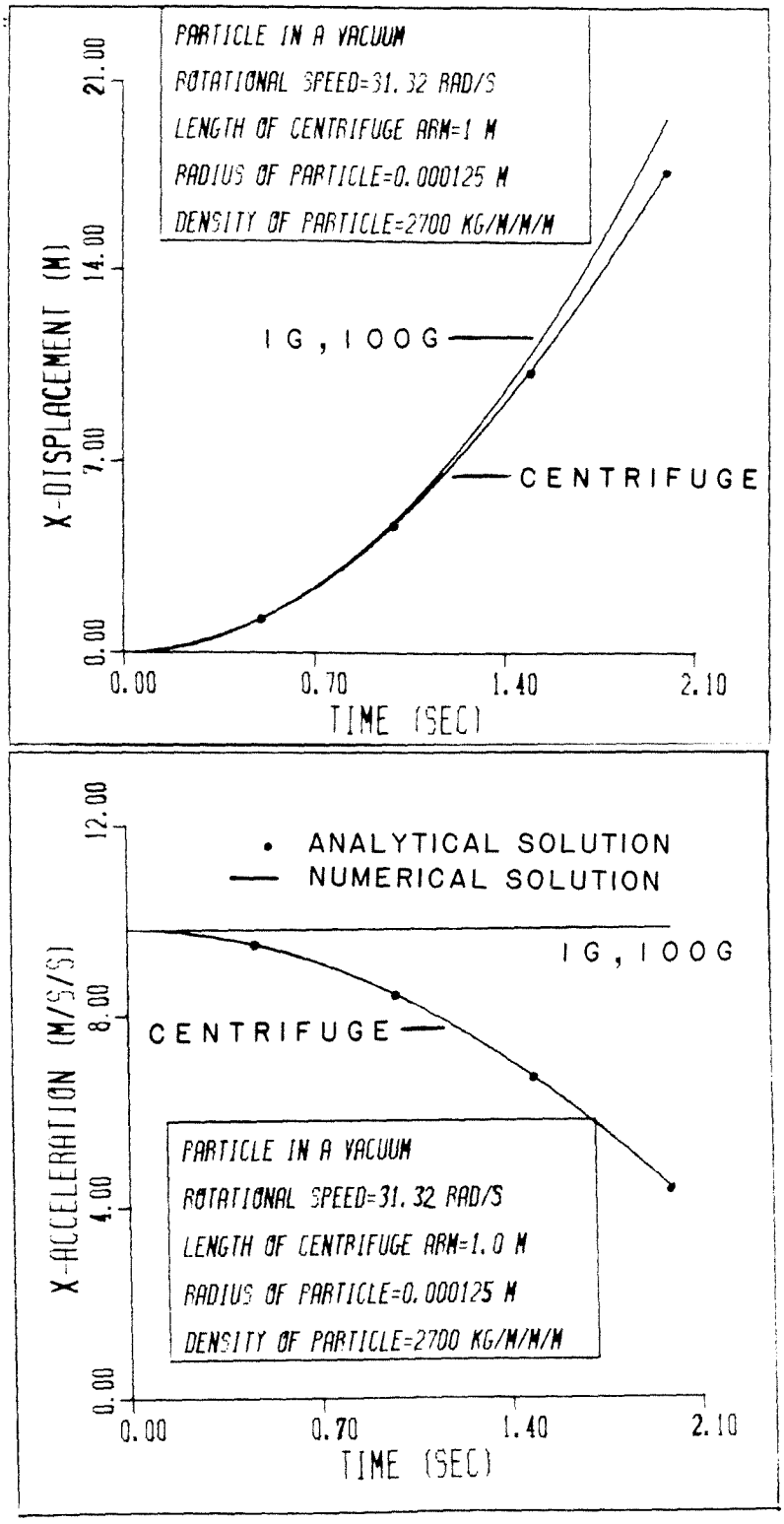

Figure 2.2 Particle in a vacuum in an ng planet (n=1, 100) versus centrifuge ($\omega^2 R$ = 100g). Scales: time = t .n, acceln = (acceln) /n, displ = (displ) .n
Analytical solution for centrifuge only.

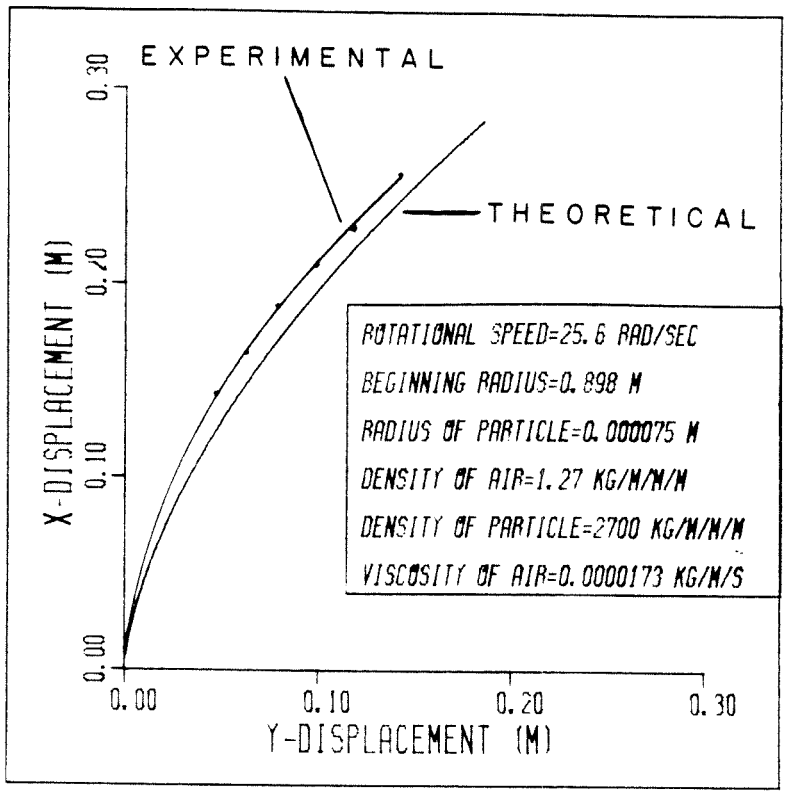

Figure 2.3 Particle in air. Comparison of experimental flight path and calculated flight path. (Refer to figure 1 for definitions of x and y

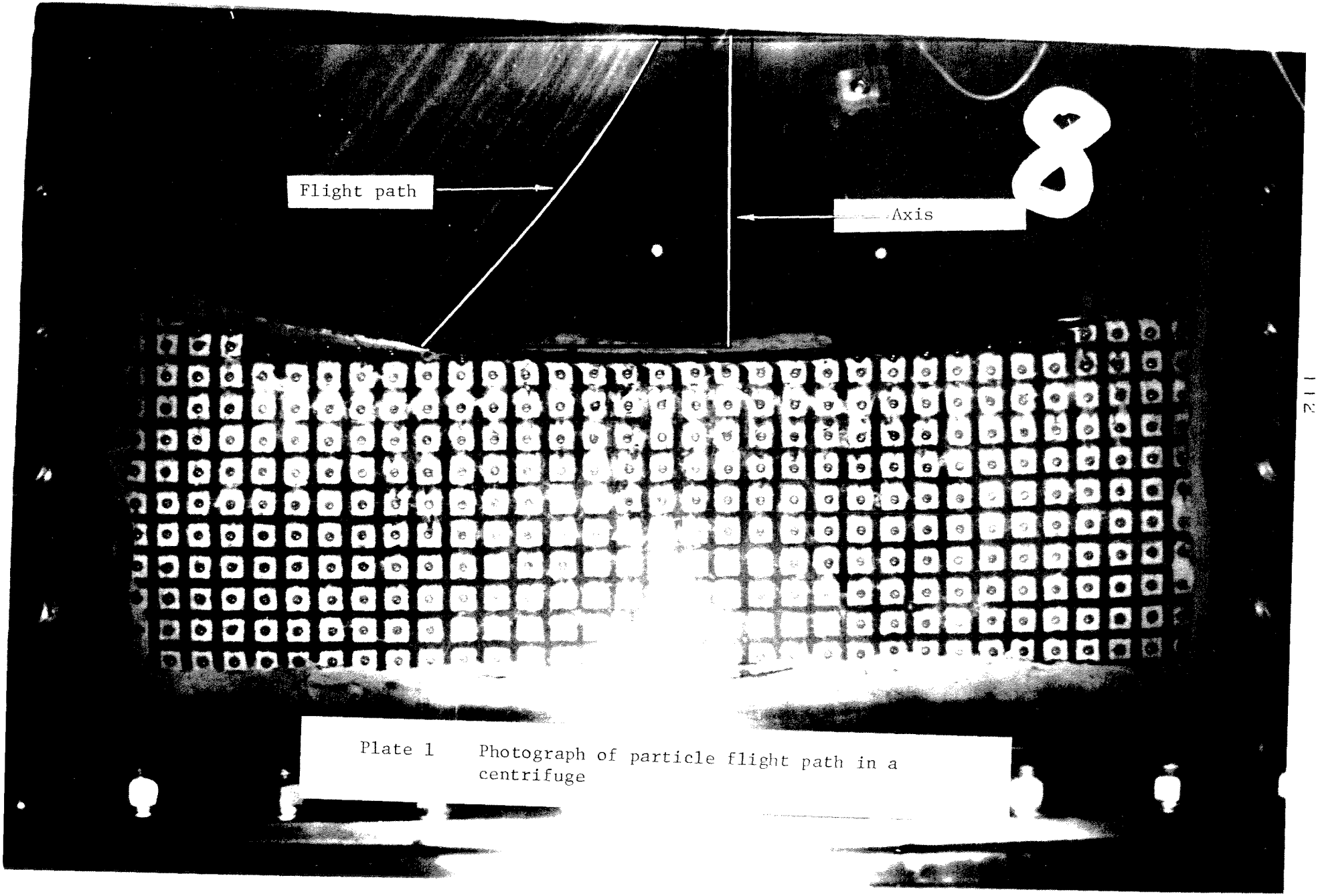

Plate 1 Photograph of particle flight path in a centrifuge

CHAPTER III

RESULTS AND CONCLUSIONS

3.1 INTRODUCTION

In modeling, there are two ways to examine the similarity requirements, namely, similarity analysis and dimensional analysis. There is some overlap between the two analyses but, whenever possible, the similarity approach is preferred (Yih, 1977) and will be employed here. This preference comes from the fact that in similarity analysis, actual governing equations are used and this offers a better understanding of the scaling requirements. Another reason for this choice is that, as will be shown shortly, Reynolds numbers of the particle in the model and prototype can differ by as much as two orders of magnitude (100 times). The use of dimensional analysis will give Reynolds number as one of the dimensionless groups. Since viscous effect is not negligible, Reynolds number has to be considered. But as the Reynolds numbers in the model and prototype are different, therefore, dimensional analysis is not feasible.

The ensuing analysis is done within the concept, as outlined in Chapter I, that two simulations are involved in using a scaled model in a centrifuge to study a prototype structure. Also, the particle size is assumed to remain the same in model and prototype; this follows the general practice in centrifuge testing of using the same soil for both model and prototype. The particle is considered to be attached to the bucket and released.

3.2 BEHAVIOR OF A SPHERE IN A UNIFORM ng FIELD

3.2.1 Problems with Current Scaling Relations

Current practice in centrifuge modeling involving liquefaction uses the same soil in model and in prototype, but a model fluid n times more viscous than that in the prototype. Assuming that the fluid densities remain the same and using Appendix A, the following is obtained for a single particle:

$$\frac{(Re)_m}{(Re)_p} = \frac{a_m}{a_p} \cdot \frac{\left(\frac{dx}{dt}\right)_m}{\left(\frac{dx}{dt}\right)_p} \cdot \frac{\rho_m}{\rho_p} \cdot \frac{\mu_p}{\mu_m} \quad ; \qquad (3.1)^*$$

that is,

$$\frac{(Re)_m}{(Re)_p} = 1 \cdot 1 \cdot 1 \cdot \frac{1}{n} = \frac{1}{n} \quad . \qquad (3.2)$$

Thus Reynolds number in the model is smaller than that in the prototype. In soil mechanics, Darcy's law is usually considered to be valid if the Reynolds number (based on an average diameter of particles and the superficial velocity) is less than one (Muskat, 1946). This is linked to the fact that for a single particle (microscopic level) Stokes's flow is valid for Reynolds number less than one. Thus, prior to liquefaction, if Darcy's law is considered to be valid in the prototype, then it is generally accepted to be valid in the model because of equation (3.2) (Lee and Schofield, 1984, and Goodings, 1984). Despite the difference in the Reynolds number, the coefficient of permeability

* subscripts m and p refer to model and prototype, respectively.

is assumed to scale as follows:

$$\frac{k_m}{k_p} = \frac{\gamma_m}{\gamma_p} \cdot \frac{K_m}{K_p} \cdot \frac{\mu_p}{\mu_m} = n \cdot 1 \cdot \frac{1}{n} = 1 \quad . \tag{3.3}$$

Even for this scaling, there is some confusion in the literature (Tan and Scott, 1985). It has to be realized that flow through soil as described by Darcy's law is a linearly viscous phenomenon (Scheidegger, 1974 and Scott, 1963) and this, the assumption that the flow is linearly viscous, is only an approximation. Furthermore, Darcy's law, as is understood in soil mechanics, links an averaged flow quantity (the seepage velocity) with an averaged hydraulic gradient (Scott, 1963). On liquefaction, Darcy's law may or may not be valid in both model and prototype since the mechanics of sedimentation governs the behavior. Even if the averaged variables obey Darcy's law, the dynamics of a single particle (microscopic level) may be very different in model and prototype. Since the averaged variables are an integration of the microscopic values, similarity may no longer be achieved. This is examined subsequently.

3.2.2 Similarity Analyses

For the model, equation (2.1) gives:

$$A \cdot ng + \left(C_D\right)_m \cdot B\left(\frac{dx_m}{dt_m}\right)^2 = C \cdot \frac{d^2x_m}{dt_m^2} \tag{3.4}$$

where $A = V_s(\rho_s - \rho_f)$, $B = -\frac{1}{2}\rho_f \pi a^2$, $C = V_s(\rho_s + \rho_f/2)$, and A, B and C have the same values in both model and prototype provided the particle radius, and particle and fluid densities in the model and prototype are the same. Assuming this is the case at present, then for the prototype, n = 1 and equation (2.1) becomes

$$A \cdot g + (C_D)_p \cdot B\left(\frac{dx_p}{dt_p}\right)^2 = C \cdot \frac{d^2x_p}{dt_p^2} \tag{3.5}$$

If C_D or B = 0 in both model and prototype, as is the case, for example when the particle moves in a vacuum, then it is observed that, if the linear dimension is scaled as $x_p/x_m = n$, equation (3.5) is similar to equation (3.4), if t_p/t_m scales as n. This is the so-called "dynamic time" scaling.

However, if $C_D \neq 0$ and $B \neq 0$, then for equations (3.4) and (3.5) to be equivalent, both the following conditions must be met:

$$t_m = \frac{1}{n} t_p \tag{3.6}$$

$$(C_D)_m = n(C_D)_p \quad . \tag{3.7}$$

Equation (3.7) is a very difficult condition to achieve exactly since the drag coefficient, C_D, is a nonlinear function of Reynolds number in general (see equation 2.2). Experimenters in fluid mechanics recognize this difficulty and avoid it by scaling the object size and fluid viscosity so that they only need to satisfy $(C_D)_m = (C_D)_p$. This is the dynamic similarity requirement which is achieved if $(Re)_m = (Re)_p$

(Batchelor, 1967). In soil mechanics, a similar approach is not feasible, since using soils of a different size will affect the constitutive behavior which is normally required to be unchanged and which is important for material behavior before liquefaction. Also, it is very difficult to find soils that scale in grain dimension appropriately.

From equation (3.6) and $x_p/x_m = n$, velocity of the particle has to be the same at homologous points in model and prototype. If the same fluid is used in both model and prototype, Reynolds number is thus unchanged and equation (3.7) is not satisfied. The consequence of this violation in terms of acceleration is shown in Figure 3.1 where the same fluid is used in all five cases (for n = 1, 5,10,50,100). All the results for n greater than 1 have been scaled to correspond to the prototype situation. If exact similarity were achieved, all these curves would lie on top of the n = 1 curve.

If for very low Reynolds number (Re << 1.0), we assume that Stokes's law is valid (Yih, 1977), we have:

$$C_D = \frac{24}{Re} = \frac{24\mu}{2\rho_f a \frac{dx}{dt}} . \qquad (3.8)$$

Noting that if equation (3.6) holds, $\frac{dx_p}{dt_p} = \frac{dx_m}{dt_m}$, and inserting equation (3.8) in equations (3.4) and (3.5), respectively, the following equa-

tions result:

$$\text{(equation(3.4))} \qquad A \cdot g + \frac{\mu_m}{n} \cdot \frac{12B}{\rho_f a} \frac{dx_p}{dt_p} = C \frac{d^2x_p}{dt_p^2} \tag{3.9}$$

$$\text{(equation(3.5))} \qquad A \cdot g + \mu_p \cdot \frac{12B}{\rho_f a} \frac{dx_p}{dt_p} = C \frac{d^2x_p}{dt_p^2} \quad . \tag{3.10}$$

Clearly equations (3.9) and (3.10) are identical if $\mu_m = n \cdot \mu_p$; i.e., the model fluid has higher viscosity than the prototype fluid. Here exact similarity is possible because drag force is linear with respect to velocity (second term on LHS of equations (3.9) and 3.10)). This situation would occur for Re << 1 only, that is, for particles of size much less than 0.1 mm when the prototype fluid is water.

As the particle moves, its velocity and the associated Reynolds number change continuously. Thus, for the usual case where the size of the particle is greater than 0.1 mm, even if the model fluid viscosity is n times that of the prototype, similarity is achieved only briefly when the drag force is linear with respect to velocity (Re << 1). Since Reynolds number in the prototype is n times that in the model, the drag force in the prototype will become nonlinear with respect to velocity at a time when the drag force in the model is still linear with respect to velocity. Thus, exact similarity cannot be achieved.

For example, consider the case where n = 100, the particle size is 0.25mm and the fluid is 100 times as viscous as water (Figure 3.4). In this case, the Reynolds number of the particle in the model is much less

than one over the entire range of velocities, reaching a terminal velocity of 0.056 m/s and a Reynolds number of 0.14. But in the prototype (1g), Reynolds number is less than 1 for less than a millisecond and reaches a terminal value of 8.4 at a velocity of 0.034 m/s. If there were similarity in behaviors in model and prototype, then the velocities shown in Figure 3.4 should be identical.

Figures 3.2, 3.3, 3.4 and 3.5 portray the effects of changing particle size, with resulting variation in Reynolds number and drag coefficient. These effects are illustrated in terms of different velocities as a function of g-level and time. In the calculations, μ_m is set equal to $n\mu_p$ (n=1,10,100) and the fluid densities are assumed to remain the same. The particle diameters in the figures range from 1mm to 0.15mm. Note that the curves come closer together as the particle size decreases. Complete similarity would require all curves to coincide. This observation is supported by experimental evidence which shows that similarity is better achieved with finer-grained samples (Cargill, 1983).

It must be emphasized that these conclusions are derived from relations describing the motion of a single particle in fluid only. The more general case of interest, of course, involves relative movement between fluid and a mass of particles, in contact with each other or not. This is the condition where Darcy's law is expected to apply. In soil mechanics, Darcy's law, which represents a linear viscous phenomenon is accepted to be valid for Re < 1.0 (Reynold's number is based on any suitable average diameter of the sand grains (d_{50} in this study)

and the superficial velocity of the fluid) (Muskat, 1946 and Scheidegger, 1974). For a single particle moving in a fluid, Stokes's law which represents a linear viscous flow is considered to be valid for Re < 1.0 (Batchelor, 1967). Thus, Darcy's law is valid if flow at the microscopic level, that is flow about a particle, is linearly viscous. Generally, this is true for flow through a stationary soil matrix (seepage problem) (Goodings, 1984). However, as illustrated above, for most soils on liquefaction, Reynolds number is less than 1 for less than a millisecond. Typical experimental data indicate that the soil particles are suspended for tens of milliseconds (Dean and Schofield, 1983). Clearly, Darcy's law may not be valid in these experiments. Even if Darcy's law is approximately valid in both prototype and model, the flows are not similar and the coefficient of permeability may not scale as equation (3.3).

As pointed out, the above analysis assumes that the densities of fluids in the model and prototype are the same. But for the model fluid to be n times more viscous than the prototype fluid, a different fluid such as a glycerine-water mixture has to be used. In such a case, the model fluid density is also different from that in the prototype. Other model fluids such as silicone oil (Dean and Schofield, 1983) may be more acceptable in terms of density equivalence. A difference in densities can be significant and has to be accounted for.

Assuming that the fluid in the prototype is water (density = ρ_w), then if Stokes's law is considered valid as in current practice instead of scaling relations given in Appendix A, the following should be used:

Defining
$$\lambda = \left[\frac{(\rho_\ell+2\rho_s)(\rho_s-\rho_w)}{(\rho w+2\rho_s)(\rho_s-\rho_\ell)}\right]^{1/2} , \tag{3.11}$$

then
$$\frac{t_m}{t_p} = \lambda \cdot \frac{1}{n} \tag{3.12}$$

$$\frac{dx_m}{dt_m} = \frac{1}{\lambda}\frac{dx_p}{dt_p} \tag{3.13}$$

$$\frac{d^2x_m}{dt_m^2} = \frac{1}{\lambda^2} \cdot n \cdot \frac{d^2x_p}{dt_p^2} \tag{3.14}$$

$$\frac{\mu_m}{\mu_p} = \lambda \cdot \left(\frac{\rho_s-\rho_\ell}{\rho_s-\rho_w}\right) \cdot \frac{1}{n} . \tag{3.15}$$

Figure 3.6 illustrates the discrepancy if the difference is not accounted for. Figure 3.7 shows the improved results when equations (3.12) through (3.15) are used.

3.3 BEHAVIOR OF A SPHERE IN A CENTRIFUGE

3.3.1 Similarity Analysis: Particle in Air

We observe from equation (2.5) that if $\frac{dy}{dt} \simeq 0$ and x is small compared to R, then since $\omega^2 R = ng$, equation (2.5) is the same as equation (2.1). However, when this is not the case, Coriolis acceleration becomes significant and equation (2.5) is very different from equation (2.1). Thus, the centrifuge will not correctly simulate the ng field. Figure 2 where the "fluid" is a vacuum clearly illustrates this.

If the sand grains are moving in air, again the Coriolis acceleration is significant and, as shown in Figure 2.3, the particle path is curved. Thus, in cratering experiments in a centrifuge, Coriolis acceleration must be accounted for. This is a three-dimensional problem. But for the purpose of illustrating the effects of Coriolis acceleration on soil deposition in cratering experiments, the special case of a two-dimensional problem, neglecting earth's gravitational field in comparison with the centrifugal acceleration, will be considered.

The problem considered is that of two particles, one of which is given an initial velocity relative to the bucket of 100 m/s at an angle of 150 degrees with respect to the x-axis, the other 100 m/s at an angle 210 degrees with respect to the x-axis (see Figure 3.8). The centrifuge will simulate an acceleration field of 450 g's. These are typical values for cratering experiments (Schmidt and Holsapple, 1978). In a uniform ng field, the flight trajectories of the two particles will be symmetrical. Clearly, this is not the case in the centrifuge as can be seen from the flight trajectories in Figure 3.8. Also, for typical bucket dimensions (0.4 m diameter for Schmidt's experiments (Schmidt and Holsapple, 1978)), it is clear that the particles will not be deposited in the bucket. This is evident from the experimental data which show that the lip volume (volume of soil deposition) is only a small fraction of the crater volume (Schmidt and Holsapple, 1978). This is in marked contrast with the prototype (earth) situation where the soil is deposited around the crater and modifies the final shape of the crater.

It seems clear that the crater created in the centrifuge simulates that of the crater in the prototype immediately after the explosion and prior to the deposition of the soil, and not that of the final crater.

3.3.2 Similarity Analysis: Particle in Fluid

In general, in a liquid as opposed to a gas, grains with the usual density of soil solids move in almost a straight line to the bottom of the container in a centrifuge test. This is observed for a particle in water at a nominal 100g in Figure 3.9. That is to say, the y-component of motion is not very important.

For sand particles with sizes in the range considered here in a fluid n times more viscous than the prototype, calculations show that the centrifuge is an excellent simulation of the ng field. Figure 3.10 (100g/centrifuge curve) shows that the solutions to equation (2.11) for n = 100, and equations (2.5) and (2.6) for $\omega^2 R$ = 100g are almost identical. However, this does not mean that the centrifuge model is correctly modeling the prototype behavior since it has been shown also in Figure 3.10 that the behavior in an ng field may not be similar to that of the 1g field.

A more pertinent question is whether the concept of modeling of models as employed by Lambe and Whitman (1982), Cargill and Ko (1983), and others is correct. That is, if the models simulate each other, do they also simulate the 1g field prototype correctly? Is modeling of models an adequate proof of the centrifuge results vis a vis the prototype? To investigate this problem, a particle of size 0.11 mm is chosen

as in the soil used by Lambe and Whitman. The particle is then subjected to a centrifugal acceleration of 35g to represent the so-called "model" test. A centrifugal acceleration of 80g is used for the "model-of-the-model" test, as Lambe employed. As Figure 3.11 illustrates, they are very close. However, both behaviors deviate from the prototype 1g situation for the reasons given above and because 35g is not much different from 80g whereas 1g is. Clearly, the concept of modeling of models does not automatically assure similarity between model and prototype.

3.4 CONCLUSIONS

The analysis presented is a simplistic one. In the real case, one has to contend with the fact that there are many particles, some in contact and some not. The development of pore pressure and its subsequent dissipation is a very complicated process. However, for the purpose of examining similarity requirements, it is clear from the arguments given that conclusions drawn from this simple study can be extended to the complicated real case. The conclusions are:

(i) Conceptually, there are two simulations involved in the modeling process. The first is the simulation of a 1g prototype using a model in a uniform ng field and the second is the simulation of the uniform ng field by the use of a centrifuge to produce similar behaviors. Scaling relations (Appendix A) have been established for centrifuge tests. They have been tested in this study. The analysis presented here has demonstrated that, for soil particles larger than

0.1mm in water, the centrifuge model does not simulate the prototype situation well. But, perhaps contrary to expectations, the breakdown is due to the fact that the behavior in a uniform ng field is not similar to that in a 1g field. The difficulty in achieving similarity in the two situations arises because, for centrifuge experiments in soil mechanics as they are currently done, the drag coefficient must be n times larger than that in the prototype. Owing to the complicated nature of fluid behavior and the nonlinearity of the drag force with velocity, this requirement at best is only approximately achieved. In most cases, the centrifuge is actually an excellent simulation of the ng field but neither represents the prototype situation.

(ii) The value of experiments in a centrifuge is important but universal advocacy of the use of centrifuge models to study "site-specific" prototypes (Goodings, 1979 and Craig, 1984) is questionable in cases involving water flow and dynamic testing when the important feature of the soil is that it is a two-phase medium.

(iii) The concept of modeling-of-models does not always assure correct modeling between the model and <u>prototype</u>.

(iv) In using a model fluid n times more viscous than water, the density of the fluid may change and this change needs to be accounted for using equations (3.12) through (3.15) for scaling dynamics quantities.

(v) The paper by Kimura et al. (1982) demonstrates the difficulty of constructing a dry soil structure while in flight. The difficulty arises mainly because of the effect of the Coriolis force. The solution

generated and illustrated in Figure 2.3 can be used to design systems for building a desired shape of soil structure in flight.

(vi) In general, if a structure (either single grain or a section of failing slope, for example) has a significant velocity (of order of 10 m/s) relative to the bucket, the dynamics must include Coriolis effects, and the scaling relations must take this into account (Pokrovsky, 1975).

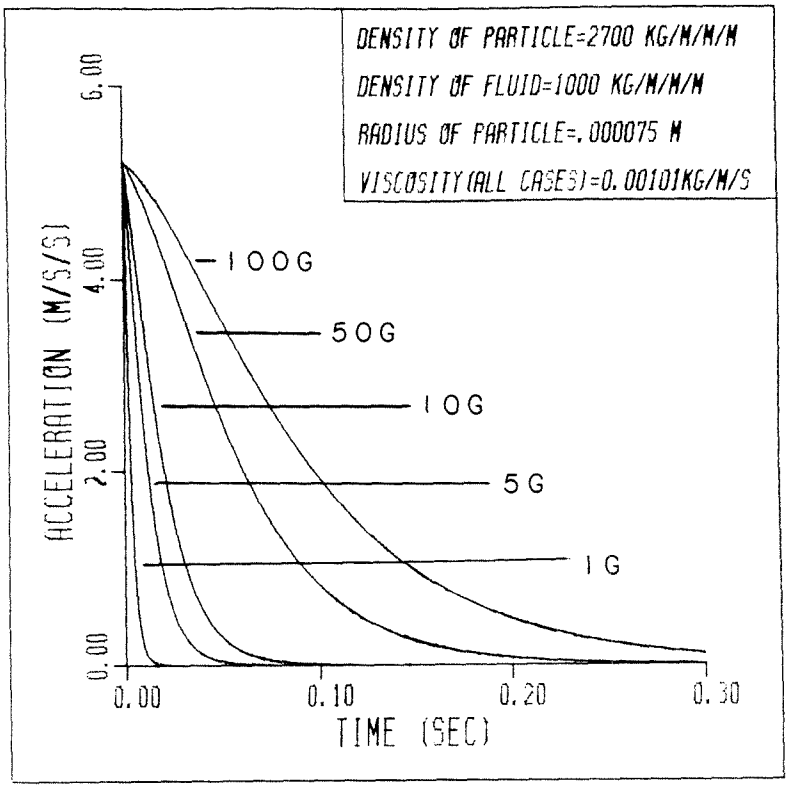

Figure 3.1 Behaviour in a uniform ng field (n=1,5,10,50,100)
$\mu_m = \mu_p$. Scales : time = (time in model).n
acceln = (acceln in model)/n

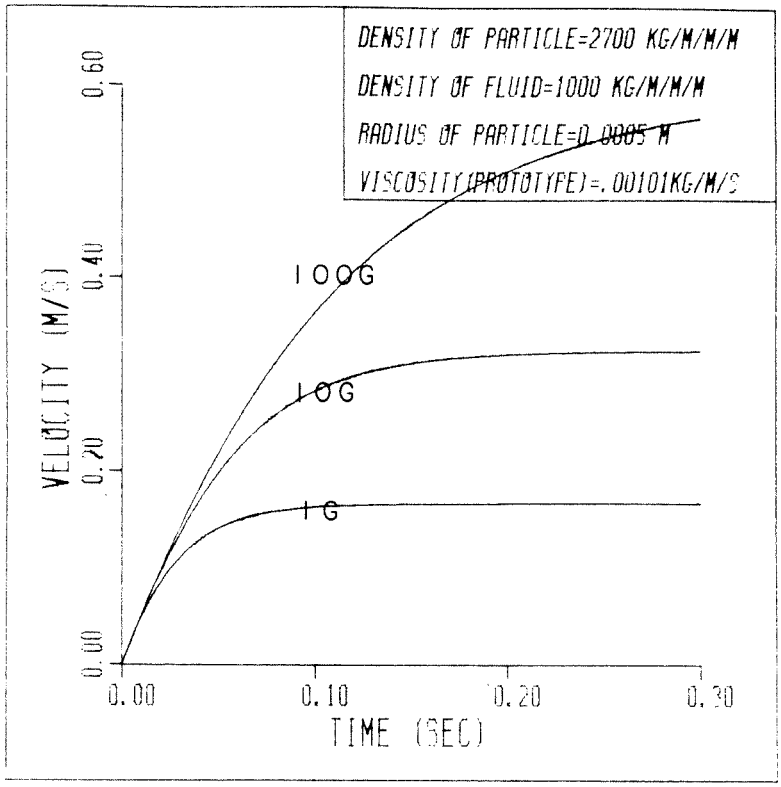

Figure 3.2 A 1.0 mm particle in a uniform ng field (n=1,10, 100). $\mu_m = n.\mu_p$. Scales : time = (time in model).n , velocity = velocity in model

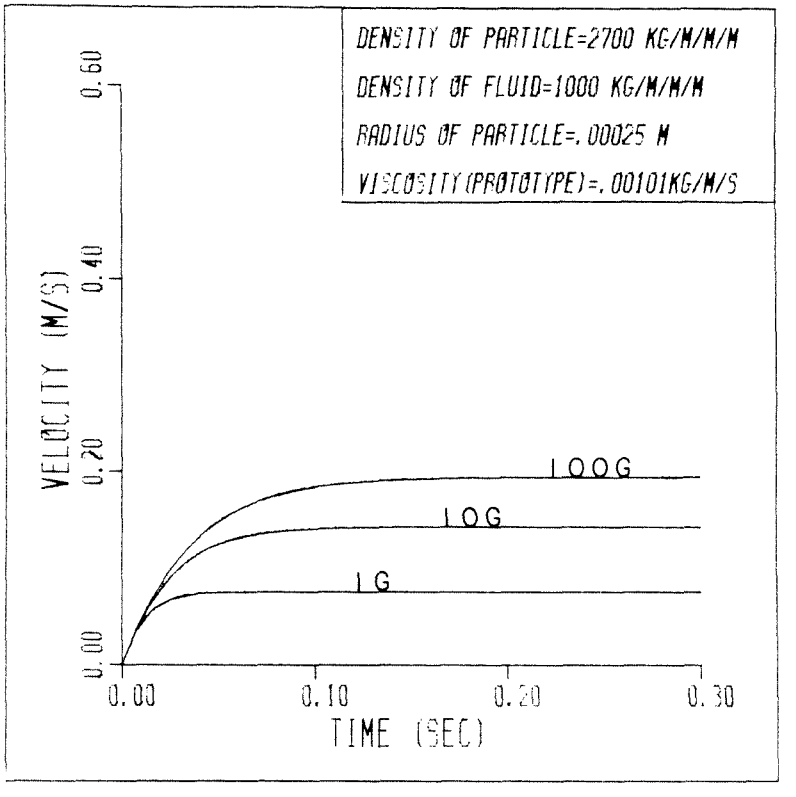

Figure 3.3 A 0.5 mm particle in a uniform ng field (n=1,10, 100). $\mu_m = n.\mu_p$. Scales same as in Figure 3.2

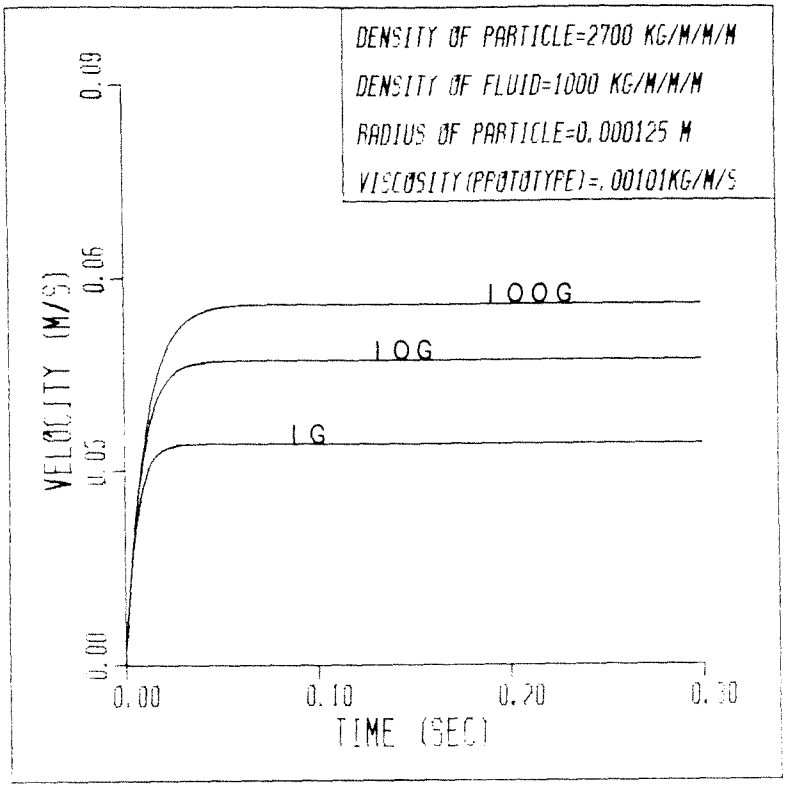

Figure 3.4 A 0.25 mm particle in a uniform ng field (n=1,10, 100). $\mu_m = n.\mu_p$. Scales same as in Figure 3.2

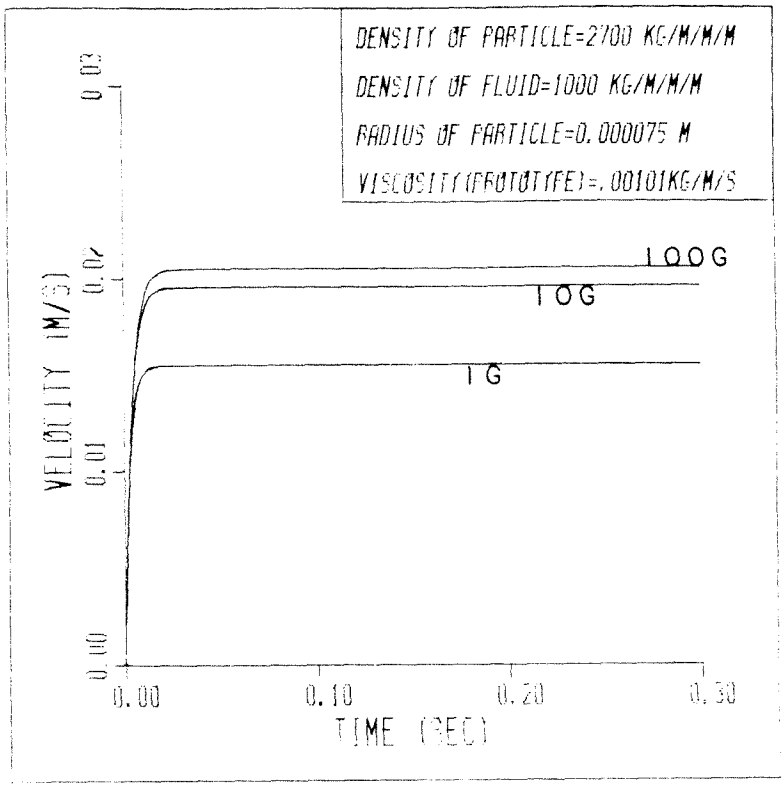

Figure 3.5 A 0.15 mm particle in a uniform ng field (n=1,10, 100). $\mu_m = n.\mu_p$. Scales same as in Figure 3.2

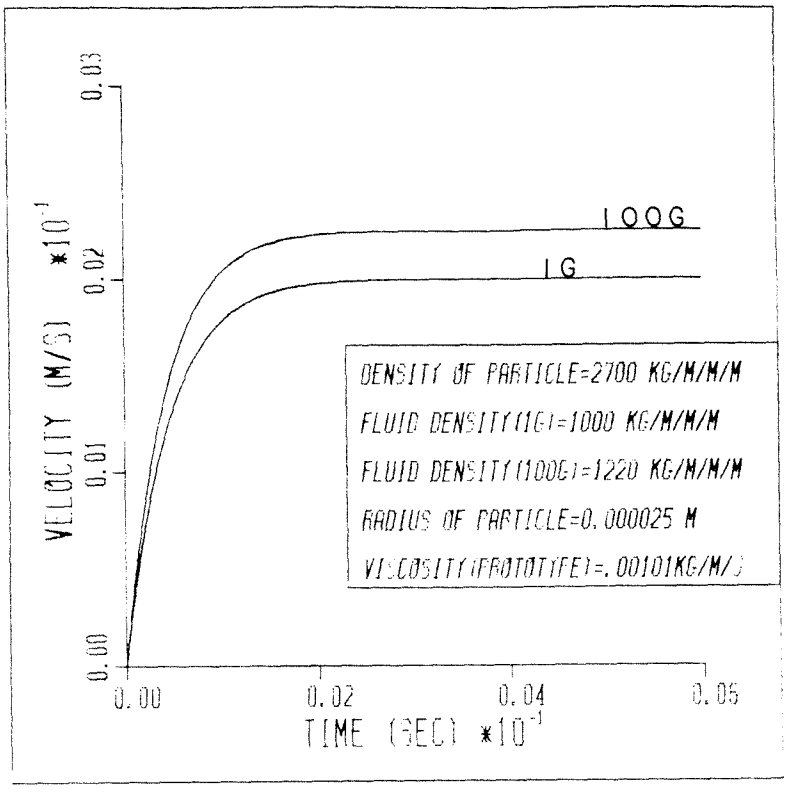

Figure 3.6 A 0.05 mm particle in a uniform ng field (n=1,100) Difference in densities of fluid not accounted. Scales same as in Figure 3.2

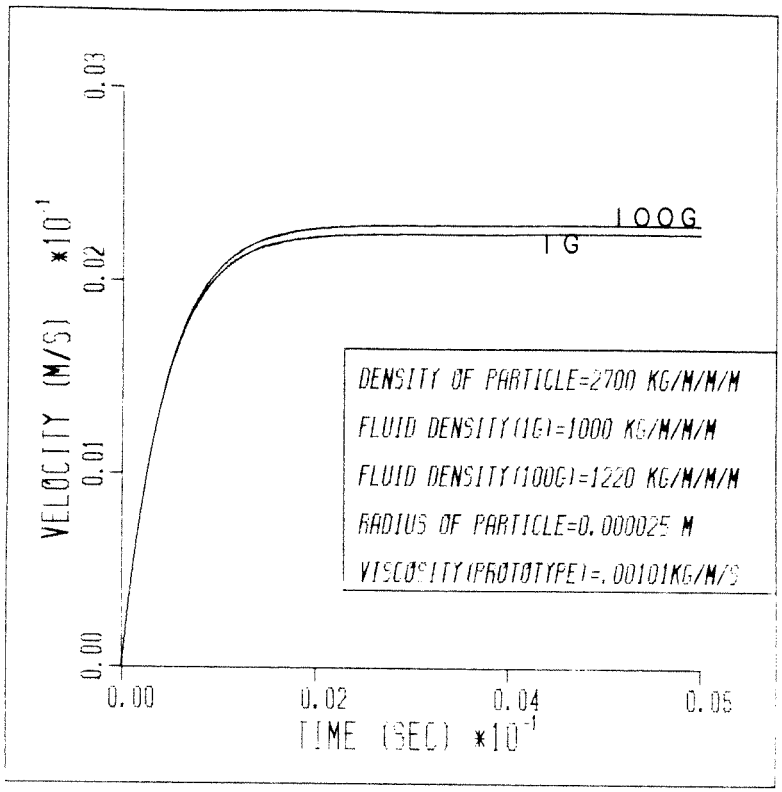

Figure 3.7 A 0.05 mm particle in a uniform ng field (n=1, 100). Difference in densities of fluid accounted. Scales as given by equations (3.11) - (3.15)

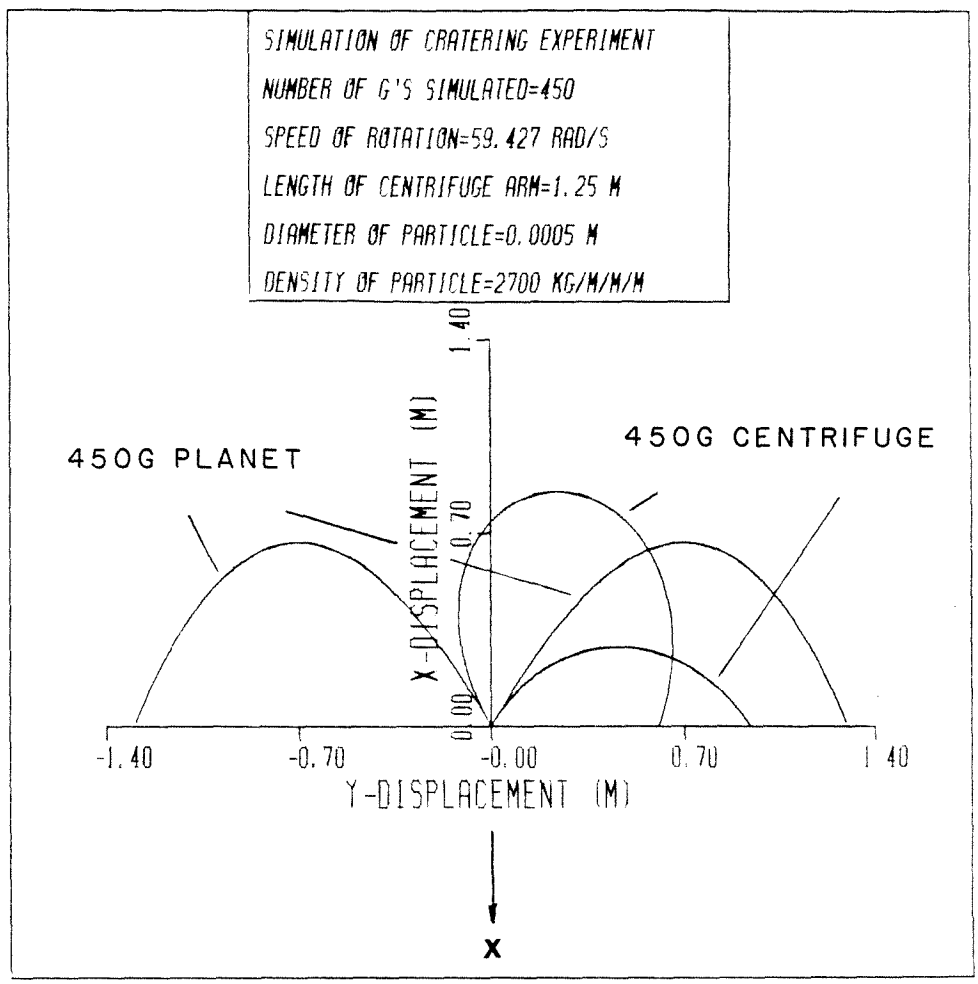

Figure 3.8 Behaviors of a 0.5 mm particle in air in a centrifuge and an ng planet (n = 450). Displacements are actual displacements in model

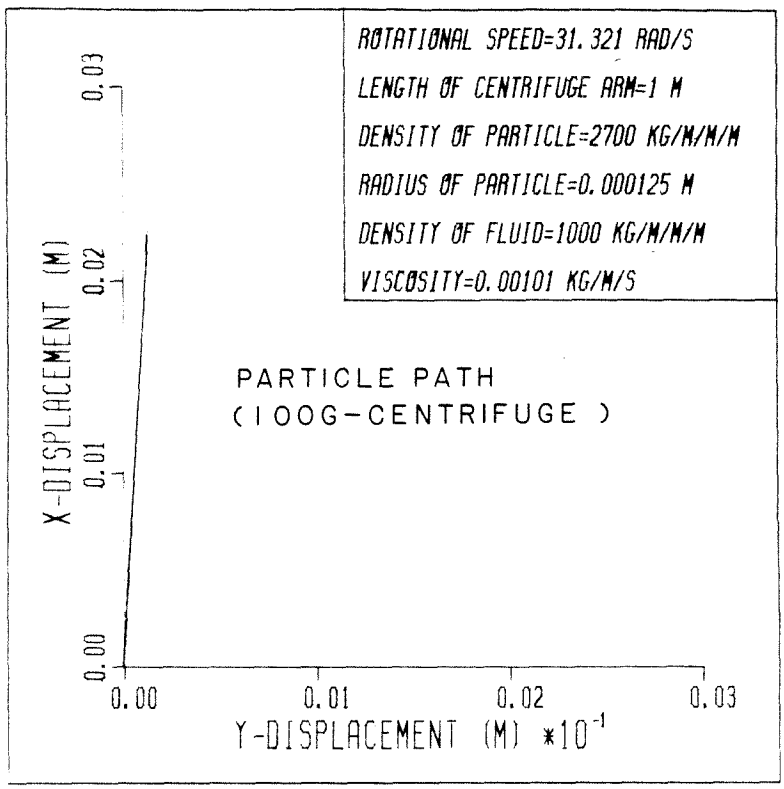

Figure 3.9 Trajectory of a 0.25 mm particle in water in a centrifuge ($\omega^2 R$ = 100g). Displacements are actual displacements in model

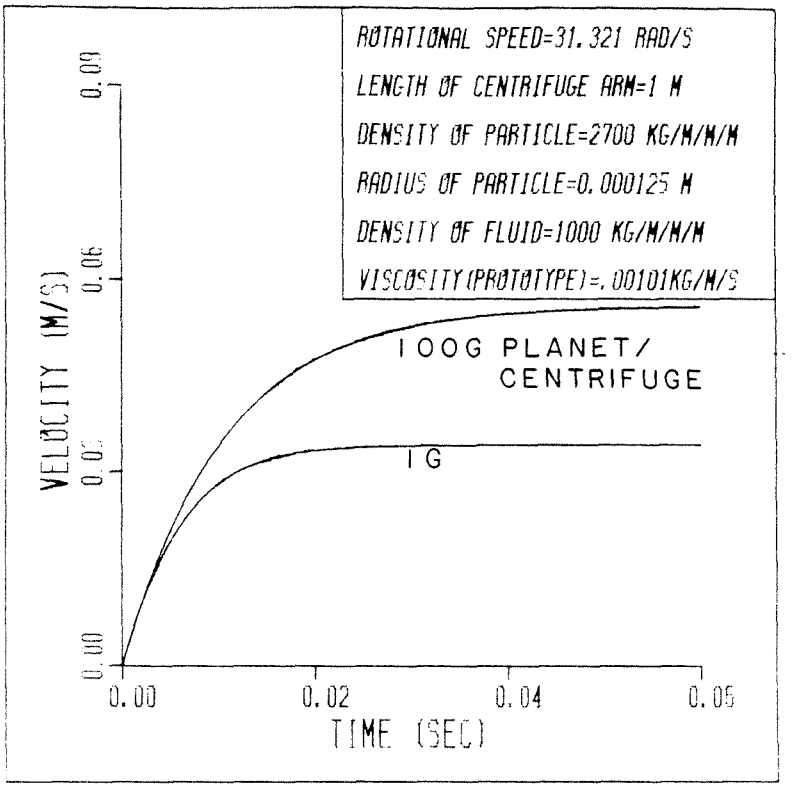

Figure 3.10 Behaviours of a 0.25 mm particle in a 1g planet, a 100g planet and a loog centrifuge. Scales same as in Figure 3.2

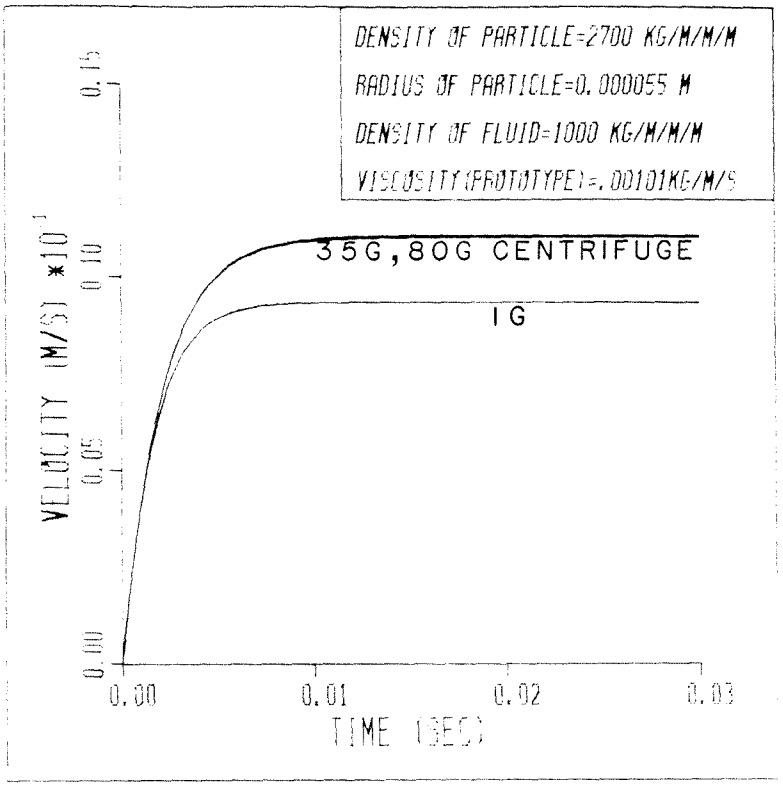

Figure 3.11 A 0.11 mm particle in a 35g centrifuge, a 80g centrifuge and a 1g planet.
Scales same as in Figure 3.2

REFERENCES

Batchelor, G.K. (1967), An Introduction to Fluid Dynamics, At the University Press, Cambridge.

Brennen, C.E. (1982), "A Review of Added Mass and Fluid Inertial Forces," Report No. CR 82.010, Naval Civil Engineering Laboratory, Port Hueneme, California.

Cargill, K.W. and Ko, H-Y. (1983), "Centrifugal Modeling of Transient Water Flow," Jour. of Geotechnical Engineering, ASCE, 109, No. 4, pp. 536-555.

Cheney, J.A. (1984), "American Literature on Geotechnical Centrifuge Modeling 1931-1984," Proc. Symposium on Recent Advances in Geotechnical Centrifuge Modeling, U.C. Davis, July 1984, pp. 1-25.

Craig, W.H. (1984), "The Centrifuge As an Aid to Designer," Proc. of a Symposium on the Application of Centrifuge Modeling to Geotechnical Design, Manchester, April 1984.

Dean, E.T.R. and Schofield, A.N. (1983), "Two Centrifuge Model Tests: Earthquakes on Submerged Embankments," Report No. CUED/D-Soils/TR 134, Cambridge University Engineering Department, pp. 473-489.

Goodings, D.J. (1979), "Centrifugal Modeling of Slope Failures," Ph.D. Thesis, Cambridge University.

Goodings, D.J. (1984), "Relationship for Modeling Water Effects in Geotechnical Centrifuge Models," Proceedings of a Symposium on the Application of Centrifuge Modeling to Geotechnical Design, Manchester, 16-18 April 1984, pp. 1-24.

Hildebrand, F.B. (1976), Advanced Calculus for Applications, (Second Edition), Prentice-Hall, Inc., Englewood Cliffs.

Holsapple, K.A. and Schmidt, R.M. (1982), "On the Scaling of Crater Dimensions 2, Impact Processes," Jour. Geophys. Res., 87(83), pp. 1849-1870.

Hushmand, B. (1983), "Experimental Studies of Dynamic Response of Foundations," Soil Mechanics Laboratory Report No. 83-02, California Institute of Technology, 1983.

Kimura, T., Nakase, A., Kusakabe, O., Saitoh, L. and A. Ohta (1982), "Geotechnical Centrifuge Model Tests at the Tokyo Institute of Technology," Technical Report No. 30, Tokyo Institute of Technology.

Lambe, P.C. and Whitman, R.V. (1982), "Scaling for Earthquake Shaking Tests on a Centrifuge," Proc. of Conf. on Soil Dynamics and Earthquake Engineering, Southampton, July, pp. 367-380.

Lee, F.H. and Schofield, A.N. (1984), "Centrifuge Modeling of Artificial Sand Islands in Earthquakes," Proc. of the Symposium on Recent Advances in Geotechnical Centrifuge Modeling, UC Davis, July 18-20, 1984, pp. 198-234.

Liu, H.P., Hagman, R.L., and Scott, R.F. (1978), "Centrifuge Modeling of Earthquakes," Geophysical Research Letters, Vol. 5, No. 5, pp. 333-336.

Meriam, J.L. (1971), Dynamics , 2nd Edition, John Wiley & Son, New York.

Mikasa, M. and Takada, N. (1984), "Self-Weight Consolidation of Very Soft Clay by Centrifuge," Proc. of an ASCE Sponsored Symposium on Sedimentation Consolidation Models, Predictions and Validation, ASCE Convention in San Francisco, Oct. 1, 1984, pp. 121-140.

Muskat, M. (1946), The Flow of Homogeneous Fluids through Porous Media, First Edition, Second Printing, J.W. Edwards, Inc., Ann Arbor, Michigan.

Ortiz, L.A. (1982), "Dynamic Centrifuge Testing of Cantilever Retaining Walls," Soil Mechanics Laboratory Report No. 82-02, California Institute of Technology, 1982.

Ovesen, N.K. (1975), "Centrifugal Testing Applied to Bearing Capacity Problems of Footings on Sand," Géotechnique, 25 , No. 2, pp. 394-401.

Pokrovsky, G.I. and Fyodorov, I.S. (1975), Centrifuge Model Testing in the Construction Industry, Vol. 1, Building Research Establishment, U.K.

Rocha, M. (1957), "The Possibility of Solving Soil Mechanics Problems by the Use of Models," Proc. 4th Int. Conf. on Soil Mechanics, London, 1957, 1 , pp. 183-188.

Roscoe, K.H. (1968), "Soils and Model Tests," Journal of Strain Analysis, 3 , pp. 57-64.

Scheidegger, A.E. (1974), The Physics of Flow through Porous Media, 3rd Edition, Univ. of Toronto Press, Toronto.

Schlichting, H. (1979), Boundary Layer Theory, 7th Edition, McGraw-Hill, New York.

Schmidt, R.M. and Holsapple, K.A. (1978), "Centrifuge Cratering Experiments I: Dry Granular Soils," Defense Nuclear Agency Report DNA 4568F, Washington, D.C.

Schmidt, R.M. and Holsapple, K.A. (1980), "Theory and Experiments on Centrifuge Cratering," Jour. of Geophys. Res., 85, No. 1, pp. 235-252.

Schofield, A.N. (1980), "Cambridge Geotechnical Centrifuge Operations," Géotechnique, 30 , No. 3, pp. 227-268.

Schofield, A.N. and Venter, K. (1984), "Earthquake-Induced Pore Pressures in the Foundation of a Sea Dyke," Report No. CUED/D-Soils/ TR 150, Cambridge University Engineering Department.

Scott, R.F. (1963), Principles of Soil Mechanics, Addison-Wesley Publishing Co., Reading, Massachusetts.

Tan, T.-S. and Scott, R.F. (1985), "Centrifuge Scaling Considerations for Fluid-Particle Systems," accepted by Géotechnique, to be published.

Yih, C.S. (1977), Fluid Mechanics, West River Press, Ann Arbor.

APPENDIX A

CURRENT SCALING RELATIONS

As in current practices, the following assumptions are made:

i) Linear dimension scaling is set as

$$\frac{x_p}{x_m} = n \quad . \tag{A.1}$$

ii) The same soil is used in the centrifuge model as in the prototype. Thus

(Density) $$\frac{(\rho_s)p}{(\rho_s)m} = 1 \tag{A.2}$$

(Permeability) $$\frac{K_p}{K_m} = 1 \quad . \tag{A.3}$$

iii) In the model, the soil structure is subjected to a gravitational acceleration of ng giving:

$$\frac{(\text{gravitational acceleration})_p}{(\text{gravitational acceleration})_m} = \frac{1}{n} \quad . \tag{A.4}$$

The general equations of motion are given by:

$$\nabla . \underset{\sim}{\sigma} + \underset{\sim}{b} = \rho \frac{d^2 \underset{\sim}{u}}{dt^2} \tag{A.5}$$

where $\nabla .$ is the divergence operator, $\underset{\sim}{\sigma}$ the stress tensor, $\underset{\sim}{b}$ the body force per unit of volume and $\underset{\sim}{u}$ the displacement vector. If $\underset{\sim}{b}$ is due to

gravitational forces, equation (A.4) gives:

$$\frac{{}^{b}\tilde{}p}{{}^{b}\tilde{}m} = \frac{1}{n} \quad . \tag{A.6}$$

Further, equation (A.1) implies:

$$\frac{(\nabla .)_p}{(\nabla .)_m} = \frac{1}{n} \quad .$$

Clearly, for similarity of equation (A.5) in both model and prototype, the following must hold:

$$\frac{{}^{\sigma}\tilde{}p}{{}^{\sigma}\tilde{}m} = 1 \tag{A.7}$$

which is the main objective of centrifuge experiments. Assumption (ii) implies that the constitutive behavior remains the same in model and prototype. Thus, with equation (A.7), the strain in both model and prototype will also remain the same. As equation (A.1) must hold, this implies:

$$\frac{{}^{u}\tilde{}p}{{}^{u}\tilde{}m} = n \quad . \tag{A.8}$$

The following is now obtained from equation (A.5):

$$\frac{t_p}{t_m} = n \tag{A.9}$$

which is the so-called "dynamic" time scaling.

In soil mechanics, the coefficient of permeability, k, is given by

$$k = \frac{\rho g}{\mu} K . \tag{A.10}$$

If the same fluid is used in model and prototype, equation (A.10) yields:

$$\frac{k_p}{k_m} = \frac{\gamma_p}{\gamma_m} \cdot \frac{K_p}{K_m} \cdot \frac{\mu_m}{\mu_p} . \tag{A.11}$$

Using equations (A.3) and (A.4), the following is obtained:

$$\frac{k_p}{k_m} = \frac{1}{n} \cdot 1 \cdot 1 = \frac{1}{n} . \tag{A.12}$$

Darcy's law implies that:

$$\frac{v_p}{v_m} = \frac{k_p}{k_m} \frac{i_p}{i_m} . \tag{A.13}$$

Since i, the hydraulic gradient, is dimensionless, equation (A.12) gives

$$\frac{v_p}{v_m} = \frac{1}{n} . \tag{A.14}$$

Since v, the seepage velocity, has dimensions of length divided by time (L/T), equations (A.1) and (A.14) will thus give:

$$\frac{t_p}{t_m} = n^2 . \tag{A.15}$$

the so-called "diffusional" time scaling.

However, if a different fluid is used in the model so that $\mu_m = n \cdot \mu_p$, then from equation (A.11), k is scaled as:

$$\frac{k_p}{k_m} = 1 \tag{A.16}$$

and equation (A.13) gives

$$\frac{v_p}{v_m} = 1 \quad . \tag{A.17}$$

Thus,

$$\frac{t_p}{t_m} = n \tag{A.18}$$

which corresponds with equation (A.9).

APPENDIX B

NOTATION

$( )_m$	property in the model	g	acceleration of gravitational field (=9.81 m/s^2)
$( )_p$	property in the prototype	p	pressure
ρ_s	density of sphere, or soil grain	h	total head
ρ_f	density of fluid	i	hydraulic gradient $= \frac{\partial h}{\partial x}$
ρ_w	density of water	k	permeability
a	radius of particle	γ	unit weight = ρg
m_s	mass of particle	K	material permeability constant $k = \frac{\gamma K}{\mu}$
m_a	added mass of fluid	C_D	drag coefficient
v_s	volume of particle	Re	Reynold's number
ω	angular velocity of centrifuge	$\underset{\sim}{i}$	unit vector in x-direction
R	length of arm of centrifuge	$\underset{\sim}{j}$	unit vector in y-direction
n	scaling factor	d_{50}	grain diameter whose size is greater than that of 50% of the particles by weight
		μ	viscosity of fluid